Parallel Session 1B

Actions on Buildings

Leere Seite
Blank page
Page vide

An effective Procedure for Combining Actions

Ulrich QUAST
Univ.-Prof. Dr.-Ing.
Technical University
Hamburg-Harburg
FRG

Ulrich Quast, born 1937, got his
civil engineering degree in 1962.
Research officer during 4 and
consultant engineer during 8 years.
Professor for concrete structures
at Braunschweig Technical
University in 1977 and since
1985 in Hamburg-Harburg.

Summary

The combinations which may be decisive for the dimensioning of cross-sections can
directly be determined by vectorially adding the action effects within the N/M-diagram in
the sequence of decreasing load eccentricity. The simplified combinations which are
allowed for building structures are not easier to be applied. Besides they should be
dropped because they may give more unfavourable as well as more favourable results.
Computer programs should present the results in graphics which can easier be understood.

1. Introduction

A lot of criticism against the Eurocodes arises from the preconceived idea, that the
verification of the general or fundamental combination rule is too complicated. Therefore
simplications of the general rule as given in Eurocode 1 by equation (9.10) are deemed to
be absolutely necessary. For this reason simplified rules for building structures are given
by equations (9.13) and (9.14). These equations are the equations (2.7(a)) and (2.8(a)) and
(2.8(b)) in Eurocode 2, "Design of Concrete Structures". In concrete structures normal
forces may act favourable or unfavourable, especially with respect to the required amount
of reinforcing steel. This fact also complicates the situation as it is.

From Table 1 it can be seen that the total number of possible combinations p really
increases very much with the increasing number q of variable actions which are
independent from each other. It can also be seen that this number p is significantly
reduced by the simplification only in cases with 3 and more variable actions. The
remaining number of possible actions still remains too great. It can be concluded that the
reduction of the number of possible combitions is not yet an effective simplification. To
determine the decisive combination for cross-section design with 3 variable actions from
the totality of 16 simplified combinations is not yet more comfortable than to determine
them from 26 combinations. For practical purposes a more pronounced reduction is

aspected when speaking of a simplification or an effective procedure has to be applied, in order to concentrate on the decisive combinations.

For the dimensioning of reinforced cross-sections an effective procedure is to combine the combination of actions with the determination of the required reinforcement. This can be done with computer programs and in the same way by using design charts or other design tools. In both cases the actions are added as vectors within an N/M-diagram. The boundary with the most unfavourable and decisive combinations is directly obtained by adding the actions in the sequence of decreasing load eccentricity. This is shown and can easily be understood by giving an example and by explaining the results. For this aim the column shown in Fig. 1 with 3 variable actions is analysed.

Combination of actions acc. to EC 1, ch. 9.4		q					
		0	1	2	3	4	5
Ch. 9.4.2, eq. (9.10) $\Sigma\gamma_G \cdot G_k + 1.5\,(Q_{k,1} + \Sigma\psi_{0,i}\, Q_{k,i})$	$p = 2 + q \cdot 2^q$	2	4	10	26	66	162
$i > 1$	$r \le q\,(q{+}3)/2$	–	2	5	9	14	20
Ch. 9.4.5, Simplified Verifications for Building Structures, eq. (9.13) or (9.14) (9.13) $\Sigma\gamma_G \cdot G_k + 1.5\, Q_{k,1}$	$p = 2^{q+1}$	(2)	(4)	8	16	32	64
(9.14) $\Sigma\gamma_G \cdot G_k + 1.35\, \Sigma Q_{k,i}$ $i > 1$	$r \le 3\,q$	–	(2)	6	9	12	15

Table 1. Combination of actions for ultimate limit state design in persistent or transient design situations for q different variable actions, independent from each other. Numbers p of all the possible combinations and number r of the reduced set of combinations which have to be considered for cross section dimensioning. The corresponding equations to the cited ones from Eurocode 1 are in Eurode 2 eq. (2.7(a)) and eq. (2.8(a) and (b)).

2.   An Extension of the Model Column Method from Eurocode 2

The well known effective column length for buckling design purposes of an isolated element is determined from the equivalence of the buckling load of the real system and of the isolated element. This fundamental idea can also be applied for using the model column method for other columns than real cantilever columns or pin ended columns with the corresponding effective buckling length. The equivalent model columns have to be determined with respect to equal effects of structural deformations.

For the chosen example in Fig. 1, consisting of a combination of a pin ended reinforced concrete column and a cantilever steel column, the two different model columns b) and c) in Fig. 2 can be derived for the real column system a). In all the three systems the same structural deflection w at the top has to occur so that the same second order effects result for dimensioning the reinforced cross-section b in span 2 of the concrete column.
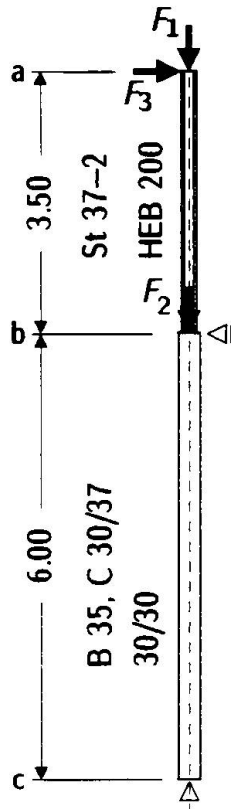
F_i	action	$\psi_{0,i}$	$\gamma_{F,\,inf}$	$\gamma_{F,\,sup}$	$F_{k,i}$ [kN]
G_k	permanent				
1	dead load	–	1.0	1.35	70
2	dead load	–	1.0	1.35	260
Q_k	variable				
1	snow load	0.7	–	1.5	30
2	imposed load	0.8	–	1.5	115
3	wind load	0.6	–	1.5	14.6

Fig. 1. System and dimensions of a column, materials and combination factors ψ_{0i} as given in the german National Application Document, as well as partial safety factors $\gamma_{F,\,inf}$ and $\gamma_{F,\,sup}$ for favourable and unfavourable effects of the characteristic values of the permanent and variable actions G_k and Q_k.

$$w = K \cdot l_1 (l_1 / r_1 + l_2 / r_2) = (4 / 10) \, K_M \cdot l_1^2 / r_2$$
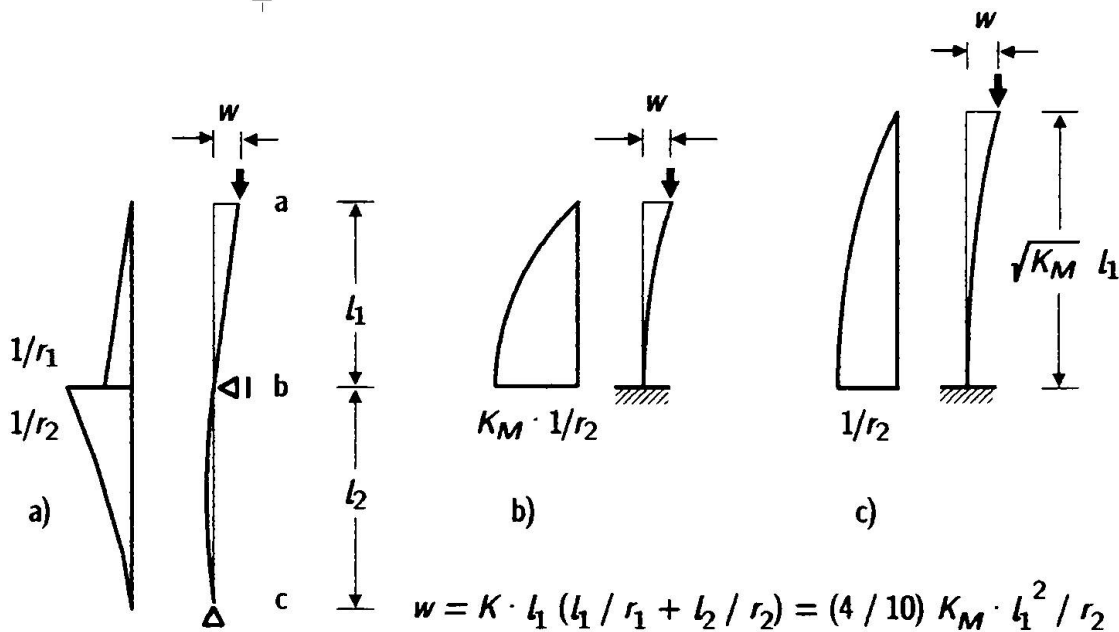
Fig. 2. Equivalent model columns for dimensioning the section b in span 2,

a) column as given,

b) model column with the same length l_1 and modified curvature $K_M \cdot 1/r_2$,

c) model column with the same curvature $1/r_2$ and modified column length $\sqrt{K_M} \, l_1$.

The expression for the top deflection w can be seen from Fig. 2. The model column b) in Fig. 2 with the same column length l_1 and the modified curvature $K_M \cdot 1/r_2$ is taken here for the application of a computer program, the results of which are shown in Fig. 3 to 6. The model column c) with the same curvature $1/r_2$ and the modified column length $\sqrt{K_M} \ l_1$ allows to use standard design charts.

Instability of statically determined slender columns occurs when yielding in the most stressed cross-section happens, which in Fig. 2 is section b. The top deflection w can directly be calculated from the curvatures $1/r_1$ and $1/r_2$ at yielding.

For the steel column the influence of the longitudinal force N is unimportant and by not considering it the overestimation of the curvarture at yielding is very small.

$$r_1 \quad = (h\,/\,2)\,/\,\epsilon_{ay} = 0.5\ h \cdot E_a\,/\,f_{ay}$$
$$= 0.5 \cdot 0.2 \cdot 210\ 000\,/\,240 \qquad\qquad = 87.5\ m.$$

For the reinforced concrete column r_2 can be determined as given by eq. (4.72) in Eurocode 2 with the coefficient $K_2 = f(N_d,\,A_s) = 1$ because of $|\,N_d\,| < N_{bal}$.

$$r_2 \quad = 0.9 \cdot d\,/\,(2 \cdot \epsilon_{yd})$$
$$= 0.45\ d\,/\,(0.0025/1.15)\ = 207\ d$$
$$= 207 \cdot 0.255 \qquad\qquad = 52.8\ m.$$

Assuming triangular diagrams for the curvatures, which in this example is on the safe side for the concrete column because of the limited moment magnification, the top deflection is obtained acc. to the corresponding expression in Fig. 2 with the coefficient $K = 1/3$,

$$w \quad = (1/3) \cdot 3.50\ (3.50/87.5 + 6.00/52.8)$$
$$= 0.179\ m = (4/10) \cdot K_M \cdot 3.50^2/52.8,$$

which then gives the model column coefficient K_M for this example as
$$K_M \quad = 1.93.$$

3. Notes to the Combination of Actions and Dimensioning

For the combination of actions together with the dimensioning of reinforced cross sections the computer code EKoB was written. It allows to consider all the possible combinations acc. to eq. (2.7(a)) and all the simplified combinations acc. to eq. (2.8(a)) and (2.8(b)). The results as given in Fig. 3 can be limited to the most important combinations. The second order analysis of a column is transformed to cross section design acc. to ch. 4.3.5.6.3 (b) of Eurocode 2. The total design moment $M_{Sd,tot}$ is the sum of the first order moment $M_{Sd,0}$ augmented by $M_{Sd,a}$ allowing for the effect of imperfections and by $M_{Sd,2}$ allowing for the effect of structural deformations, the socalled second order effect,

$$M_{Sd,tot} \quad = M_{Sd,0} + M_{Sd,a} + K_2(N_{Sd},\,A_s) \cdot M_{Sd,2}\,.$$

The characteristic values of $M_{Sk,0}$, $M_{Sk,a}$ and $M_{Sk,2}$ for $K_2(N_{Sd},\,A_s) = 1$ can be seen in Fig. 3. With respect to the cross section b there are no effects of imperfections and of structural deformations within the action effects from G_2 , Q_2 and Q_3 .

```
EKoB (C)94 Quast - Einwirkungen, Kombinationen, Bemessung nach EC 2-1-1
                   Actions, Combinations, Dimensioning acc. to
---------- Worked example: Concrete column with steel column ----------
       K.2 G.k,1    G.k,2    Q.k,1    Q.k,2    Q.k,3 cross-section : R2 - 15
------------------------------------------------------------------------------
N    kN  -70.00 -260.00  -30.00 -115.00      0           conrete    : C 30/37
M.0 kNm   0        0        0        0       51.10    reinforcing : BSt 500
x    m    3.50     0        3.50     0        0        model column method
M.a kNm   1.23     0        0.52     0        0          alfa.a    :    1/200
M.2 kNm  12.54     0        5.37     0        0        EC 2-1-1, 4.3.5.6.3 b)
   = 1.930*|N|*x*x / (517.5*d) ; without creep effects.
e.tot/h   -        0.14     0.66     0       >1E6
psi.0     -        -        0.70     0.80     0.60            b    : 0.300 m
gam.F,sup 1.35     1.35     1.50     1.50     1.50            h    : 0.300 m
gam.F,inf 1.00     1.00     -        -        -              d    : 0.255 m
========== Only decisive combinations of all possible ones ============
26 fundamental combinations, EC 2-1-1, Gl.(2.7(a)) N.Sd      M.Sd      A.s
 1  1.000  1.00    1.00     1.05     -        1.50 -361.50    96.61    12.43
 2  1.000  1.00    1.00     -        -        1.50 -330.00    90.42    11.63
 3  1.000  1.35    1.35     1.05     -        1.50 -477.00   101.43    11.60
16 simplified combinations,  EC 2-1-1, Gl.(2.8(a) oder (b))
 1  1.000  1.00    1.00     -        -        1.50 -330.00    90.42    11.63
 2  1.000  1.00    1.00     1.35     -        1.35 -370.50    90.72    10.96
 3  1.000  1.35    1.35     -        -        1.50 -445.50    95.23    10.71
==============================================================================
req A.s = 12.43 cm2,   min A.s (0.3% / 0.15 nue) =    2.70 /    2.24 cm2
M.tot   = 1.232 M.1,   eps.c / eps.s = -3.50 /   5.73 mm/m, x/d = 0.379
```

Fig. 3. Display of the dimensioning of the reinforced concrete column from Fig. 1. According to Fig. 2 the column analysis has been transformed to cross section design by adopting the model column method with the coefficient $K_M = 1.93$.

In this example longitudinal forces N act favourably. The decisive fundamental combination is therefore $1.00 \; G_k + 1.5 \; Q_{k,3} + 1.5 \cdot 0.7 \; Q_{k,1}$. The dominant variable action is Q_3. The variable action Q_2 acts favourably and is therefore not included.

The decisive simplified combination is $1.00 \; G_k + 1.5 \; Q_{k,3}$. It is more unfavourable than the simplified combination $1.00 \; G_k + 1.35 \; Q_{k,1} + 1.35 \; Q_{k,3}$. It requires 11.63 cm^2 reinforcing steel, which are only 94% of the reinforcing steel of 12.43 cm^2, which is required for the fundamental combination.

The results are graphically shown within a detail of the N_d / M_d-diagram. For better clarity all the 26 fundamental combinations are shown in Fig. 4 whereas all the 16 simplified combinations are shown in Fig. 5. The figures show the design values $\gamma_G \; G_k$ and $\gamma_Q \; Q_k$ of the action effects as vectors. On the corresponding vectors of the variable action effects also the design values of the combination values $\gamma_Q \; \psi_{0,i} \; Q_{k,i}$ are marked by smaller quadrats. The starting point of all the vectors of the variable action effects is the value $1.00 \; G_k$ of the permanent action. The part $0.35 \; G_k$, which has to be added in cases when being unfavourable, appears like a variable action.
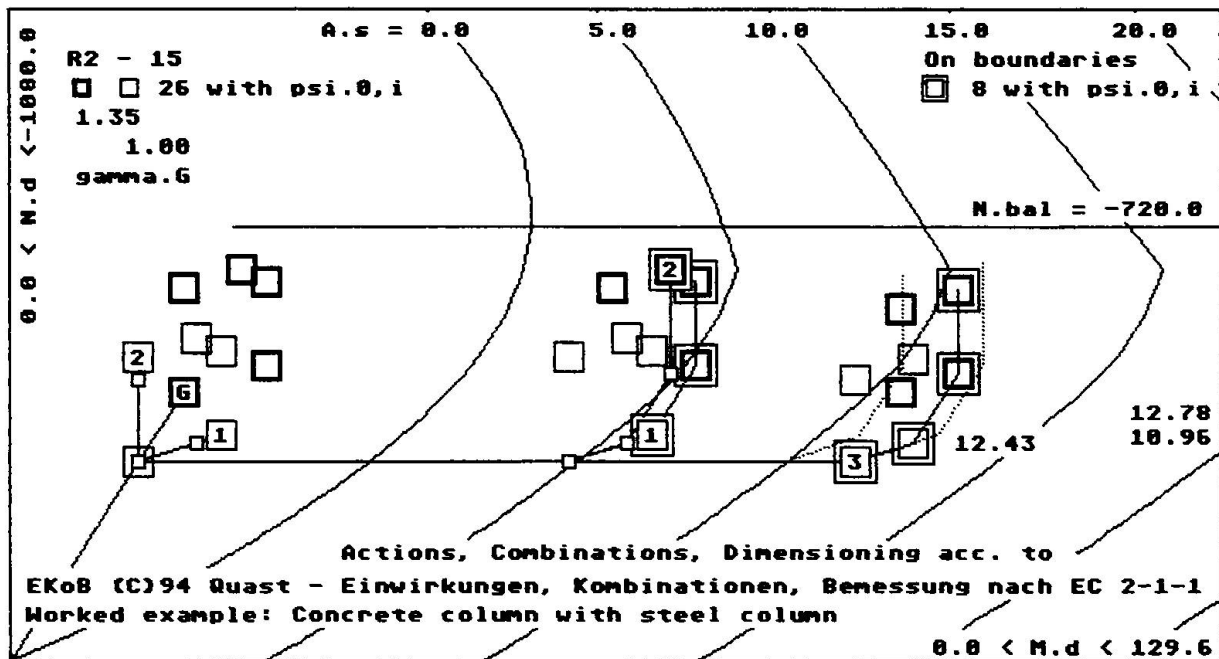
Fig. 4. Representation of the 26 combinations acc. to EC 1, eq. (9.10), within a detail of the N_d / M_d —diagram. For the vectors of the variable actions 1 to 3 the design values $\gamma_Q \cdot Q_{k,i}$ and the design values of the combination values $\gamma_Q \cdot \psi_{0,i} \cdot Q_{k,i}$ are marked. The 8 combinations on the boundaries, which have to be considered for dimensioning the cross section, are marked by double quadrats.
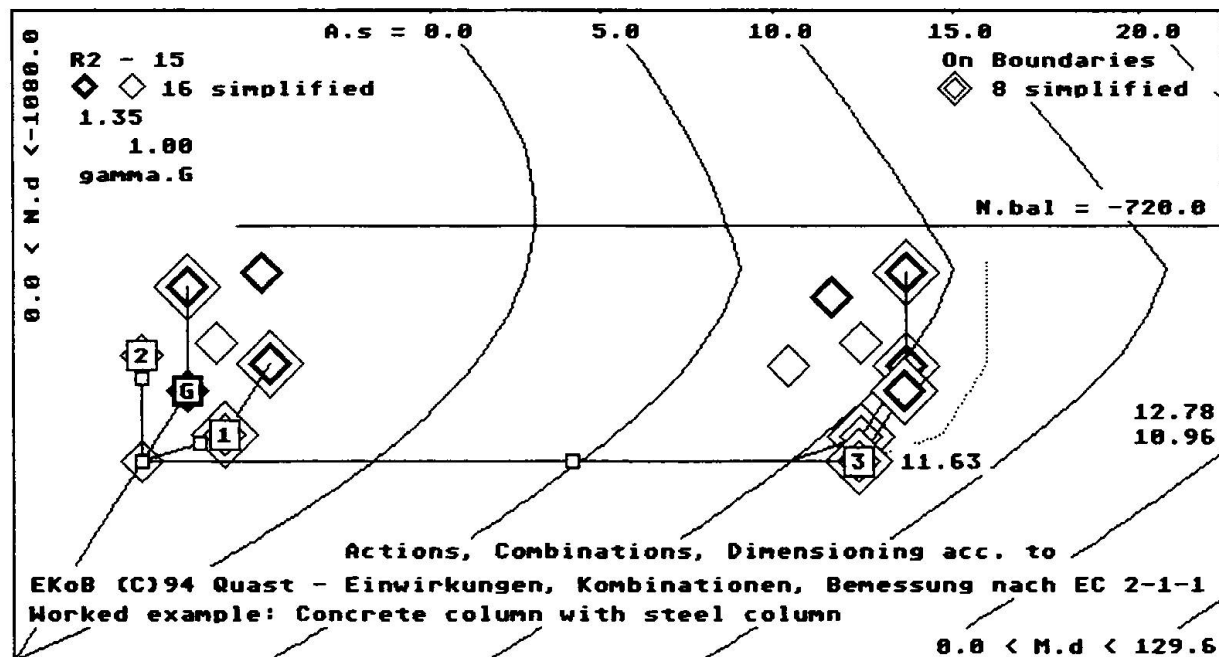

Fig. 5. Representation of the 16 simplified combinations acc. to EC 1, eq. (9.13) and (9.14), within a detail of the N_d / M_d —diagram. The 8 combinations on the boundaries, which have to be considered for dimensioning the cross section, are marked by double diamonds.

The decisive combination in Fig. 4, giving the maximum required reinforcement area, is a point on the boundary which is formed by the polygone

$$1.0\ G_k + 1.5\ Q_{k,3} + 1.5\ \psi_{0,1}\ Q_{k,1} + 0.35\ G_k + 1.5\ \psi_{0,2}\ Q_{k,2}\ .$$

This boundary is formed by the permanent action effect, the dominant variable action effect, the other variable action effects and the 0.35fold permanent action effect in the sequence of decreasing load eccentricity $e_d = M_d\ /\ |N_d|$. Which point on this boundary gives the greatest required reinforcement depends from the greater or smaller inclination of the $N_d\ /\ M_d$-line, as it is the case for different arrangements of the reinforcement in the cross section, for example at four sides instead of only two sides as in Fig. 4 to 6. Especially this point needs not be the point with the greatest axial force, nor the point with the greatest bending moment, nor the point with the greatest load eccentricity, as can be seen from Fig. 4.

Within the two other polygones the corresponding dominant actions are Q_1 and Q_2. Adding the action effects in the sequence of decreasing load eccentricity results in the polygones:

$$1.0\ G_k + 1.5\ \psi_{0,3}\cdot Q_{k,3} + 1.5\ Q_{k,1} + 0.35\ G_k + 1.5\ \psi_{0,2}\ Q_{k,2}$$

and

$$1.0\ G_k + 1.5\ \psi_{0,3}\cdot Q_{k,3} + 1.5\ \psi_{0,1}\ Q_{k,1} + 0.35\ G_k + 1.5\ Q_{k,2}\ .$$

The points which are possible for dimensioning are marked by double quadrats. The first of these points is the point of the corresponding dominant action and then all the following ones. These alltogether 8 points are emphasized in the above given expressions.

In this example Q_3 is not the dominant action because it yields the most unfavourable action effect, as it can clearly be seen from Fig. 4. Q_3 is in this example the dominant action because its reduction $\gamma_Q\,(1 - \psi_{0,i})\ Q_{k,i}$ when not being the dominant action is the most unfavourable one compared with the possible reductions of the other variable actions Q_1 and Q_2. These possible reductions of the variable action effects are the distances between the smaller mark and the end of the vectors of these variable action effects. When graphically adding the action effects the dominant action i can clearly be detected as that action which has the most unfavourable part $\gamma_Q\,(1 - \psi_{0,i})\ Q_{k,i}$.

From the 16 simplified combinations in Fig. 5 the decisive one is within the polygone $1.0\ G_k + 1.5\ Q_{k,3} + 0.35\ G_k$, which is one possible acc. to eq. (2.8(a)). The two remaining polygones for combinations acc. to eq. (2.8(a)) $1.0\ G_k + 1.5\ Q_{k,1} + 0.35\ G_k$ and $1.0\ G_k + 0.35\ G_k + 1.5\ Q_{k,2}$ are not decisive. Also the simplified combination acc. to eq (2.8(b)) $1.0\ G_k + 1.35\ Q_{k,3} + 1.35\ Q_{k,1} + 0.35\ G_k + 1.35\ Q_{k,2}$ does in this example not give the maximum amount of reinforcement. All the 8 possible points are in Fig. 5 marked by double diamonds and emphasized in the expressions in top.

The number r of the reduced set of combinations which form the possible polygones and which are in general sufficient to be considered and which have to be considered only then, if the dominant variable action is not known in before, are given in Table 1. There is

nearly no difference between the fundamental combinations and the simplified ones. Knowing that Q_3 is the dominant variable action in this example, the corresponding polygone in Fig. 4 needs to consider 4 combinations only from the totality of 26, whereas the corresponding polygones in Fig. 5 have to consider 2 plus 3 combinations from the totality of 16. It can be concluded that the simplified verification of the combination of actions for building structures acc. to eq. (9.13) and (9.14) in Eurocode 1, which are the eq. (2.8(a)) and (2.8(b)) in Eurocode 2, is not really simpler. It should therefore be taken away. The advantage would be, that equivocal and contradictory dimensionings are avoided and that it becomes very obvious, that a comprehensible procedure has to be applied.
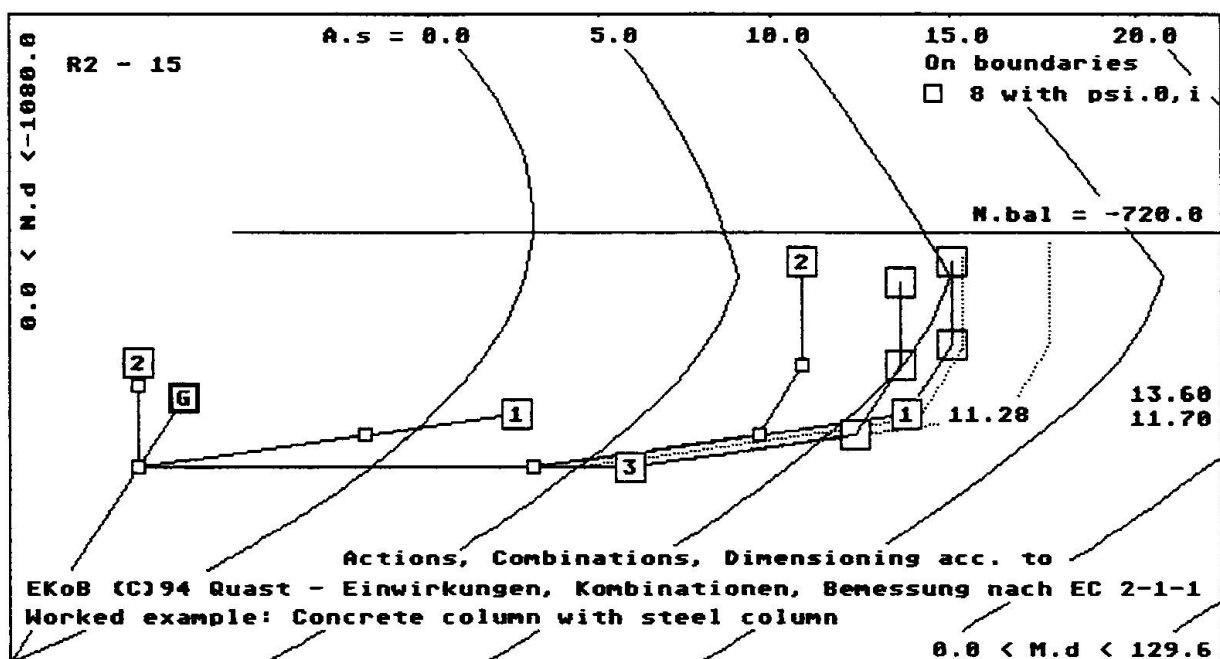

Fig. 6. Representation of the required 8 combinations on boundaries acc. to EC 1, eq. (9.10), within a detail of the N_d / M_d —diagram. Only these combinations have to be considered for dimensioning of the cross section out of a totality of 26. For the vectors of the variable actions 1 to 3 the design values $\gamma_Q \cdot Q_{k,i}$ and the design values of the combination values $\gamma_Q \cdot \psi_{0,i} \cdot Q_{k,i}$ are marked.

The last Fig. 6 deals with a modification of the action effects such that the possible reduction $\gamma_Q (1 - \psi_{0,i}) Q_{k,i}$ when not being the dominant variable action effect is most unfavourable for the variable action Q_1, which is not the first one in the sequence of decreasing load eccentricities. It is obvious that this most unfavourable distance between the smaller mark and the end of the action effect vector belongs to Q_1. In this case only the polygone

$$1.0 \; G_k + 1.5 \; \psi_{0,3} \cdot Q_{k,3} + 1.5 \; Q_{k,1} + 0.35 \; G_k + 1.5 \; \psi_{0,2} \; Q_{k,2}$$

needs to be considered, which give the 3 possible combinations which have to be looked at for determining the required amount of reinforcement out of a totality of 26.

Comparative study of Eurocode 1, ISO and ASCE procedures for calculating wind loads
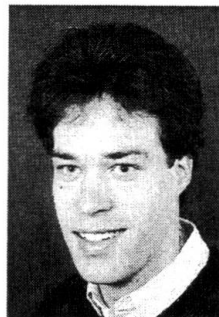
Dan LUNGU
Professor
Technical University of
Civil Engineering
Bucharest
Romania

Dan Lungu, born 1943, got his civil engineering degree in 1967 and his PhD in 1977. He is professor of structural reliability and seismic risk at the Technical University of Civil Engineering, Bucharest.

Pieter VAN GELDER
Researcher
Technical University
Delft,
The Netherlands

Pieter van Gelder, born 1968, got his degree in technical mathematics in 1991. He has been working at the Ministry of Water Management from 1991-1994. Since 1994, he is researcher at the section of Probabilistic Methods at Delft University of Technology.

Romeo TRANDAFIR
Associate Professor
Technical University of
Civil Engineering
Bucharest
Romania

Romeo Trandafir, born 1950 got his mathematical degree In 1974. Since 1978, he joined the Technical University of Civil Engineering, Bucharest.

SUMMARY

This paper contains a comparative study of the basic parameters involved in the prediction of the wind loads with Eurocode 1, ISO DIS 4354 and ASCE 7 standards: reference wind velocity; V_{ref}, exposure factor; C_{exp}, turbulence intensity at height z; $I(z)$, gust factor; C_{gust}, spectral density functions of Davenport, Solari and von Karman for along-wind gustiness and peak factor for calculating the largest extreme value of velocity pressure.

Davenport and Solari spectra. The hierarchy of spectra remains the same for $z=150m$.
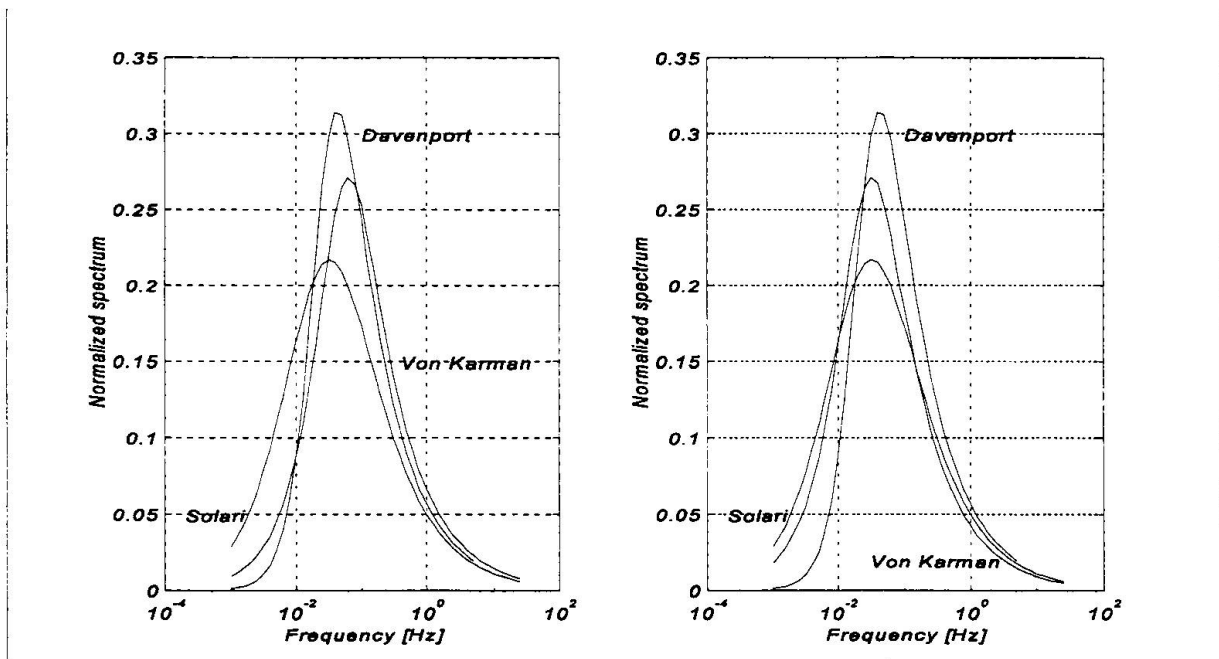
Fig. 4. Davenport, Solari and von Karman spectra at $z=10m$, $z_0=0.05m$, $V_{ref}=30m/s$, with 2 lengths of integral scale of turbelence in the von Karman spectrum; left:ESDU, right:Couniham.

4.   Conclusions

In spite of complexity involved in evaluating the wind effects on buildings there is a clear need for an international harmonization of calculating methods for the building response to strong winds. We hope that the IABSE Colloquium in Delft will give the opportunity for an EC1/ISO/ASCE Liaison Committee on Actions, or at least on wind action to come up with recommendations for an unified calculating format for wind loads.

5.   References

1. ASCE 7-93, "Minimum design loads for buildings and other structures", American Society of Civil Engineers, 1993.
2. Lungu, D., Demetriu, S., Aldea A., "Basic code parameters for environmental actions in Romania harmonised with EC1", ICASP7, Vol.2, p.881-887, Paris, 1995.
3. Solari, G., "Gust buffeting. I: Peak wind velocity and equivalent pressure", Journal of Structural Engineering, Vol.119, No.2, February, 1993.
4. CIB-Report W81, "Actions on structures, Windloads", 6th Draft, May, 1994.
5. JCSS Probabilistic Model Code, Part 2: Loads, Section 2.13: Wind, Second draft, 1995.
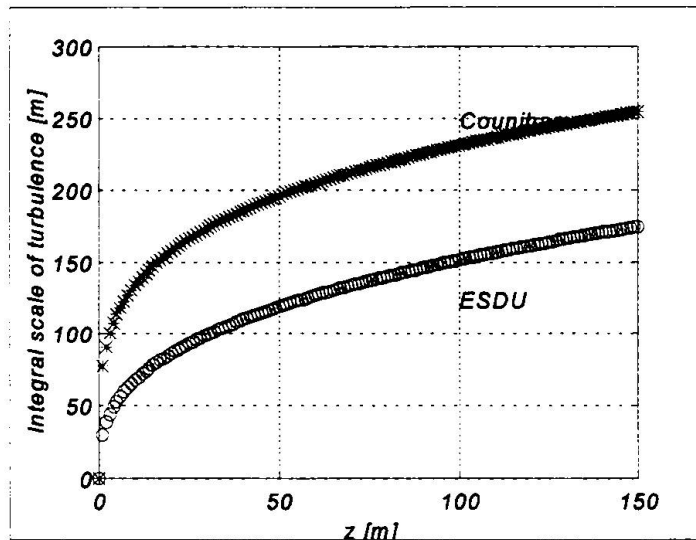
i) The length of the integral scale of turbulence from Couniham, used by Solari for EC1:

$$L_u^C(z)=300(z/300)^{0.46+0.074\ln z_0}$$

ii) The length of the integral scale of turbulence after ESDU:

$$L_u^{ESDU}(z)=25z^{0.35}z_0^{-0.063}$$

Fig. 3. ESDU and Couniham integral scale of turbulence $(z_0=0.05)$.

3.4   Graphical analysis of the spectra

The following table forms the basis of this section:

z [m]	V(z)		L_u^C [m]		L_u^{ESDU} [m]		x_C		x_{ESDU}	
	Open	Urban	Open	Urban	Open	Urban	Open	Urban	Open	Urban
10	30.0	23.1	133	85	68	60	4.4n	3.7n	2.2n	2.6n
30	36.5	30.4	173	128	99	89	4.8n	4.2n	2.7n	2.9n
90	42.7	37.6	225	192	146	130	5.3n	5.1n	3.4n	3.5n
150	45.6	41.0	254	232	174	156	5.6n	5.7n	3.8n	3.8n

Tabel 7. Spectrum parameter $x=nL_u/V$ for different heights above the ground and integral scale of turbulence (Couniham and ESDU)

Note the difference in the values of spectral parameter x for different integral scales of turbulence. Using this table, we can easy examine the differences in the spectra due to the height above the ground and/or the choice of the turbulence length. Solari spectra in Fig.4 are represented with Couniham length of integral scale of turbulence. Von Karman spectrum in Fig.4 (left) is represented with ESDU length of integral scale of turbulence. For the frequency range of interest its values are higher than that of Davenport and Solari spectra. Von Karman spectrum in Fig. 4 (right) is represented with Couniham length of integral scale of turbulence. For the frequency range of interest for buildings and structures its values are lower than that of

Urban and suburban $z_0=0.3m$

		z=10m				z=150m		
		Dav.	Solari	v.Kar.		Dav.	Solari	v.Kar.
$V_{ref}=20m/s$	v_0	0.079	0.087	0.07	$V_{ref}=20m/s$	0.15	0.12	0.10
$V=15.4m/s$	μ_g	2.98	3.02	2.96	$V=27.4m/s$	3.19	3.12	3.06
$n_{cut-off}=5Hz$	σ_g	0.46	0.46	0.47	$n_{cut-off}=9Hz$	0.43	0.44	0.45
$V_{ref}=20m/s$	v_0	0.13	0.15	0.13	$V_{ref}=20m/s$	0.22	0.17	0.16
$V=15.4m/s$	μ_g	3.15	3.19	3.15	$V=27.4m/s$	3.31	3.24	3.21
$n_{cut-off}=10Hz$	σ_g	0.43	0.43	0.43	$n_{cut-off}=18Hz$	0.41	0.42	0.43
$V_{ref}=40m/s$	v_0	0.18	0.20	0.17	$V_{ref}=40m/s$	0.30	0.24	0.20
$V=30.8m/s$	μ_g	3.25	3.28	3.23	$V=54.8m/s$	3.40	3.33	3.28
$n_{cut-off}=10Hz$	σ_g	0.42	0.41	0.42	$n_{cut-off}=18Hz$	0.40	0.41	0.42

Table 6b. Comparison of the 3 spectra in urban area.

The main conclusions from these tables are:

i) The v_0 is extremely sensitive for a change in the cut-off frequency. The reason for this is that except for the 0th spectral moment, all other spectral moments are divergent. In the definition of v_0, we have the 2nd moment to divide by the 0th moment (a constant). If we increase the cut-off frequency, the v_0 will increase consequently. Spectral bandwidth measures, like ϵ, don't show this behaviour because the divergence of the spectral moments compensate eachother.

ii) The mean peak factor is an increasing function especially of the cut-off frequency and the reference velocity; and consequently also of the height above the ground.

iii) The σ_g parameter is almost insensitive for changes in the reference velocities, cut-off frequencies, height and terrain roughness. The σ_g stays between 0.42 and 0.47.

iv) There is not so much sensitivity to the roughness of the terrain on the μ_g and σ_g.

v) Eurocode 1 proposes a mean peak factor of 3.5. It roughly corresponds to the mean peak factor added with one standard deviation. The mean peak factor can be obtained artificially high by increasing the cut-off frequency.

3.3   Length of integral scale of turbulence

In this paper we have distinguished 2 different lengths of the integral scales of turbulence, Fig.3:

V_{ref} [m/s]	z [m]	z_0 [m]	V(z) [m/s]	NBC of Canada (Davenport'70)	EC1 (Solari'93)
20	10	0.05	20	3.6	20.0
40	10	0.05	40	7.2	40.0
20	150	0.05	30.2	5.4	15.2
40	150	0.05	60.4	10.9	30.4
20	150	0.3	35.5	4.9	13.7
40	150	0.3	70.9	9.9	27.4

Table 5. Summarization of the recommended cut-off frequencies [Hz]

Note the differences in the recommended cut-off frequencies. In comparison with the cut-off frequencies used in earthquake engineering (maximum 20-40 Hz), we must comment that the recommended cut-off frequencies by Eurocode 1 for wind engineering applications seems to be quite large. The cut-off frequencies used in full scale measuremens of wind effects on structures are usually taken around a few Herz. With the newest techniques like ultrasonic anemometers it becomes possible to resolve frequencies up to 30 Hz, but the energy content in these frequency ranges will be extremely low and uninteresting for wind loads on buildings.

The spectral peak factor of the 3 different spectra were compared. The comparisons were made at different heights (z=10 and 150m), different terrain roughnesses (z_0 = 0.05 and 0.3m), for different reference velocities (V_{ref} = 20 and 40m/s) and different cut-off frequencies; Tables 6a-b. (L_u^c in the von Karman spectrum).

Open country z_0=0.05m

		z=10m				z=150m		
		Dav.	Solari	v.Kar.		Dav.	Solari	v.Kar.
V_{ref}=20m/s	v_0	0.079	0.075	0.069	V_{ref}=20m/s	0.12	0.094	0.09
$n_{cut-off}$=5Hz	μ_g	2.98	2.97	2.93	V=30.2m/s	3.13	3.04	3.01
	σ_g	0.46	0.47	0.47	$n_{cut-off}$=7.5Hz	0.44	0.45	0.46
V_{ref}=20m/s	v_0	0.14	0.14	0.12	V_{ref}=20m/s	0.19	0.15	0.13
$n_{cut-off}$=10Hz	μ_g	3.18	3.17	3.13	V=30.2m/s	3.27	3.19	3.16
	σ_g	0.43	0.43	0.44	$n_{cut-off}$=15Hz	0.42	0.43	0.43
V_{ref}=40m/s	v_0	0.18	0.17	0.16	V_{ref}=40m/s	0.25	0.19	0.17
$n_{cut-off}$=10Hz	μ_g	3.25	3.24	3.21	V=60.4m/s	3.34	3.26	3.23
	σ_g	0.42	0.42	0.43	$n_{cut-off}$=15Hz	0.41	0.42	0.42

Table 6a. Comparison of the 3 spectra in open country.

$$\lambda_i = \int_0^\infty G_u(n) n^i dn$$

and the 0th moment is given by σ_u^2.

Analytically, for Davenport spectrum one finds $\epsilon=1.0$. Numerically, for any spectra (in the case of usual cut-off frequencies), $\epsilon=0.98\text{-}0.99$.

The mean and standard deviation of the peak factor for computing the largest extreme gust are given by Davenport as:

$$\mu_g = \sqrt{2\ln v_0 t} + \frac{0.5772}{\sqrt{2\ln v_0 t}}$$

$$\sigma_g = \frac{\pi}{\sqrt{6}} \frac{1}{\sqrt{2\ln v_0 t}}$$

where v_0 is the mean frequency of zero upcrossings:

$$v_0 = \frac{1}{2\pi} \sqrt{\frac{\lambda_2}{\lambda_0}}$$

3.2 Cut-off frequency

Calculating spectral moments and peak factors are done numerically. A question of importance is the choice of integration interval and in particular the cut-off frequency. It appears that the calculation of the spectra parameters is extremely sensitive to the cut-off frequency: Table 4. If we study for example the influence on the mean peak factor (using a Davenport wind spectrum), we see the following results:

Mean peak factor, μ_g	2.72	2.77	3.22	3.67
Cut-off frequency [Hz] (V_ref=30m/s)	1	1.5	10	100

Table 4. The mean peak factor as a function of the cut-off frequency in a Davenport spectrum

In the next table, we summarize the different recommendations for the cut-off frequencies:

3.   Power spectral density for along-wind gustiness

3.1   Spectrum types

From numerous proposals for the spectral density of along-wind gustiness: Karman (1948), Panovski (1964), Davenport (1967), Harris (1968), Flicht (1970), Kaimal (1972), Simiu (1974,1975), ESDU (1976, 1985), Naito (1978, 1983), Kareem (1985), Solari (1987,1993) were selected that of Davenport, Solari and von Karman. Attention will be paid to their spectral density functions, to the notion of cut-off frequency and integral scales of turbulence. A sensitivity study will be performed to study the influence of the terrain roughness, the reference velocity and the height above the terrain.

Davenport in NBC of Canada	Solari in Eurocode 1	von Karman in JCSS and CIB codes
$$\frac{nG_u(n)}{\sigma_u^2} = \frac{0.667x^2}{(1+x^2)^{\frac{4}{3}}}$$	$$\frac{nG_u(n)}{\sigma_u^2} = \frac{6.868x}{(1+10.32x)^{\frac{5}{3}}}$$	$$\frac{nG_u(n)}{\sigma_u^2} = \frac{4x}{(1+70.8x^2)^{\frac{5}{6}}}$$
$x = 1200\,n\,/\,V(z)$ Mean spectrum for $10 < z < 150m$	$x = L_u\,n\,/\,V(z)$, where: $L_u^{\,C} = 300(z/300)^{0.46+0.074\ln z0}$	$x = L_u\,n\,/\,V(z)$ where $L_u^{\,C} = 300(z/300)^{0.46+0.074\ln z0}$ or $L_u^{\,ESDU} = 25z^{0.35}z_0^{-0.063}$

Table 3. Power spectra of the along-wind gust velocity.

The Longuett-Higgens indicator of the frequency bandwidth of the gust velocity process is:

$$\epsilon = \sqrt{1 - \frac{\lambda_2^2}{\lambda_0\lambda_4}}$$

where the spectral moments for $i=1,2,...$ are defined by:

2.3 The gust factor

The gust factor is the ratio of the peak velocity pressure to the mean pressure of the wind:

$$C_{gust}(z) = \frac{q_{peak}(z)}{Q(z)} = \frac{Q(z) + g\sigma_q}{Q(z)} = 1 + gV_q \approx 1 + g[2I(z)]$$

Where $Q(z)$ is the mean value of the wind velocity pressure, σ_q the root mean square value of the along wind velocity pressure fluctuations from the mean, g the peak factor and V_q the coefficient of variation of the velocity pressure fluctuations. V_q is approximately equal (second moment order formats) to the double of the intensity of turbulence $I(z)$; Table 2. The recommended values of the peak factor are 2.8 (ASCE7-93), 3.0 (ISO) and 3.5 (Eurocode 1). The V_q is given as a logarithmic law in Eurocode 1 and ISO and as a power law in ASCE. In figure 2, we show the differences of the gust factor recommended by the different codes.
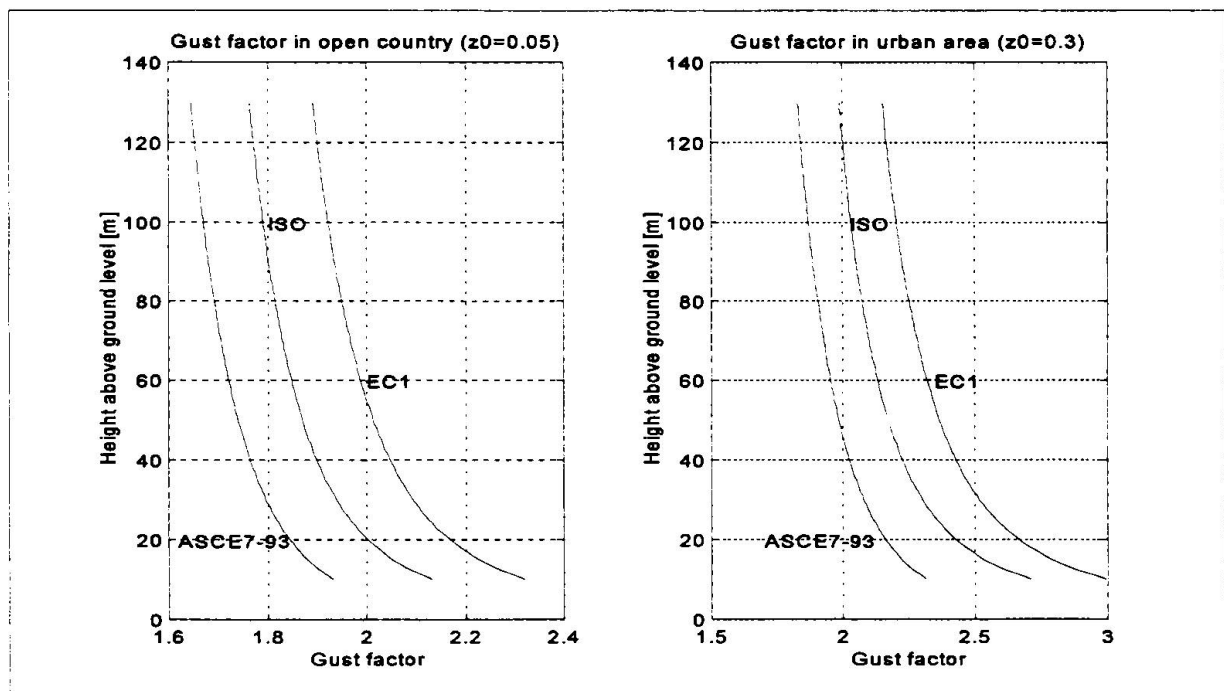

Fig. 2. Gust factor for velocity pressure averaged on 10 min, $C_{gust}(z)$.

	ASCE 7-93	ISO DIS 4354	Eurocode 1	ASCE Report	ASCE 7-95 draft
Open country	16.6	17.2	18.8	19.7	20
Suburban, urban	23.5	28.5	28.5	25.1	30

Table 2. Intensity of turbulence at 10m, I(10) - percent.

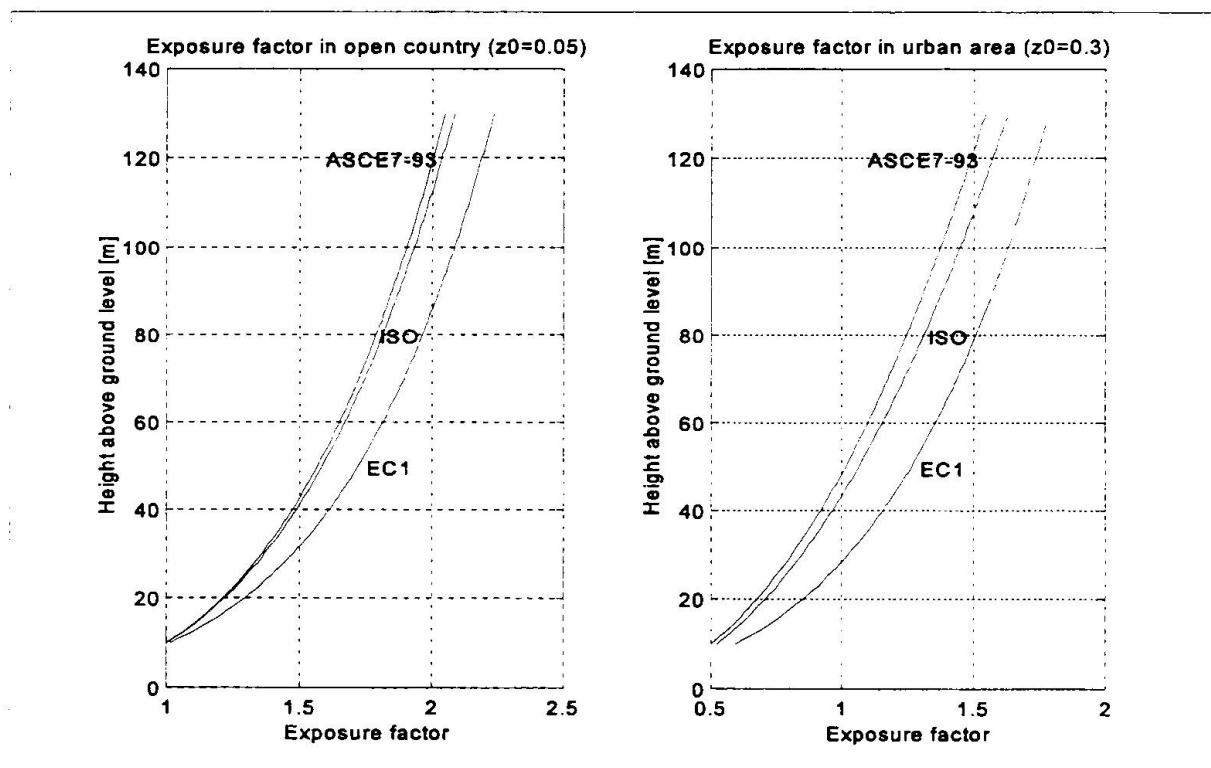| Terrain category	Logarithmic law				Power law			
	EUROCODE 1		ISO DIS 4354				ASCE 7-93	
	$k_r^2(z_0)(\ln\frac{z}{z_0})^2$		$A(z_0)(\ln\frac{z}{z_0})^2$		$B(\frac{z}{10})^{2\alpha}$		$2.58(\frac{z}{z_g})^{2\alpha}$	
	k_r	z_0 (m)	z_0 (m)	$A(z_0)$	B	α	α	z_g (m)
Open sea, flat area	0.17	0.01	0.003	0.021	1.4	0.11	1/10	213
Open country	0.19	0.05	0.03	0.030	1.0	0.14	1/7	274
Suburban, urban	0.22	0.3	0.3	0.041	0.5	0.22	1/4.5	365
Large city center	0.24	3	3	0.058	0.16	0.31	1/3	457

Table 1. Exposure factor, C_{exp} .

Fig. 1. Exposure factor (ASCE, ISO) or roughness factor (EC1), $C_{exp}(z)$.

1.   Introduction

The Eurocode 1, Part 2-4: Wind actions (ENV 1991-2-4: 1994), the ISO Draft International Standard 4354, Wind actions on structures, 1990 and the ASCE 7-93 (or the proposed revisions from ASCE 7-95), the American standard for minimum building design loads, contain accurate stochastic procedures for calculating wind effects on building and structures. However, this latest generation of standards prove the lack of international harmonization of meteorological, structural and aerodynamical data used for calculating static and dynamic design wind loads. The differences in definition of the basic parameters for the wind loading on structures create significant difficulties for unifying the formats recommended by EC1, ISO and ASCE standards for prediction of the wind loads. Additional difficulties arise in training students to apply wind standards.

2.   Basic parameters for wind loads

2.1   The reference wind velocity

According to EC1 and ISO code, the reference wind velocity is the mean velocity of the wind averaged over a period of 10 min, determined in open terrain exposure at an elevation of 10 m and having 0.02 annual probability to be exceeded (50 yr mean recurrence interval). According to ASCE7-93 code the averaging time interval of the wind velocity is about 1 min (fastest mile speed); in ASCE7-95 draft a 3 second gust speed is used. After ISO-code for different averaging time intervals, a conversion of the wind velocity is possible using the relation (in open terrain):

$$1.05V_{ref}^{1h} = V_{ref}^{10min} = 0.84V_{ref}^{1min} = 0.67V_{ref}^{3sec}$$

2.2   The exposure factor

The exposure factor describes the variation of the velocity pressure with height above ground and terrain roughness as function of reference velocity pressure:

$$C_{exp}(z) = \frac{q(z)}{q_{ref}}$$

The roughness length z_0 in metres plays an important role in this; Table 1 and Fig. 1.

National Application Document for the Wind Draft

Brian W. SMITH
Senior Partner
Flint & Neill Partnership
14 Hobart Place
London SW1W 0HH

Brian Smith graduated from Cambridge University in 1961 and obtained his Masters Degree at the University of California, Berkeley. He joined the Partnership in 1964 and became a Partner in 1977.He is a member of the BS Committees on wind loading and on towers and masts. He is Chairman of the IASS working group on masts and towers. He is convenor of the EC3 project teams on steel towers, masts and chimneys, a member of the EC1 project team on thermal actions and was co-chairman of the ad-hoc panel on ENV 1991-2-4: Wind Actions.

Summary

The background to the production of the United Kingdom National Application Document for ENV 1991-2-4: Wind Actions is described in this Paper. Following positive voting by the CEN Committee TC250/SC1 on the draft document there was considerable discussion as to the application of the Rules contained therein. An informal ad-hoc panel was set up to try to set down a consistent framework for the preparation of each Member State's NAD. This framework has been used in the drafting of the United Kingdom NAD.

1.   Introduction

The draft Eurocode on Wind Actions (ENV 1991-2-4) was drafted by the project team under the convenorship of Professor H. Ruscheweyh and published by CEN in March 1995. Such a complex subject inevitably led to much discussion in the Member States and to concerns that the National Application Documents (NAD's) may not reflect a consistent approach leading to problems of compatibility when the ENV document is converted to an EN Code.

To try to forestall this problem an informal ad-hoc panel was formed to set down a common basis for producing each country's NAD. This panel set down guidelines and advice on several aspects of ENV 1991-2-4 [1] and in doing so identified areas where the Draft needed minor technical editing before publication as an ENV.

The United Kingdom NAD is presently being drafted and is using this framework, together with calibration exercises that have been undertaken against both the existing United Kingdom Code of Practice[2] and the recently published replacement Standard[3].

2.   Outline of ENV 1991-2-4

The draft Eurocode ENV 1991-2-4 (hereinafter called 'the Draft') was developed with the intention of providing criteria for wind actions on all forms of structures. However during the course of the drafting it was recognized that certain forms of structure could not be adequately represented by the codified procedures. Specifically these were structures which respond under wind action to higher modes of vibration than the fundamental - such as cable supported structures like guyed masts, cable stayed and suspension bridges - and structures where specific guidance on pressure coefficients and wind response are required due to the nature of the structure - such as self-supported lattice towers. It was also recognized that specific Eurocodes are being developed for generic forms of structure, such as lighting columns, for which the Draft would not be used - although the procedures in such Codes should be compatible with the principles contained in the Draft.

It was also found that the basic wind data required from the Member States were in many cases obtained on different bases thus making the wind maps incompatible at borders between States.

The treatment of in-wind response to gust loading was based on work by Solari and others, leading to simplified codified procedures for the majority of 'normal' structures. Procedures are provided (in *Annex B* of the Draft) to deal with those structures which are likely to respond dynamically. The criteria for defining when the more complex rules are needed are given, although use of such procedures in any event will generally provide more economical solutions.

The pressure coefficients contained in the Draft are based on research work principally undertaken at the Building Research Establishment in the United Kingdom. The coefficients provided are upper bound values to be used for wind directions orthogonal to the building. To ensure that the most onerous conditions are covered, these pressure coefficients are the highest within a wind direction of ±45° to the normal direction (see Figure 1). Inevitably this leads to a conservative approach. To overcome this an Annex was written during the drafting programme which contained directional pressure coefficients, appropriate to wind directions in 15° sectors around each building type considered. Indeed these directional coefficients provided the data for the orthogonal values provided in the main body of the Draft. At the voting stage, however, this annex was not included in the document, primarily it is suspected because the organization of the document at that time was somewhat unwieldy.
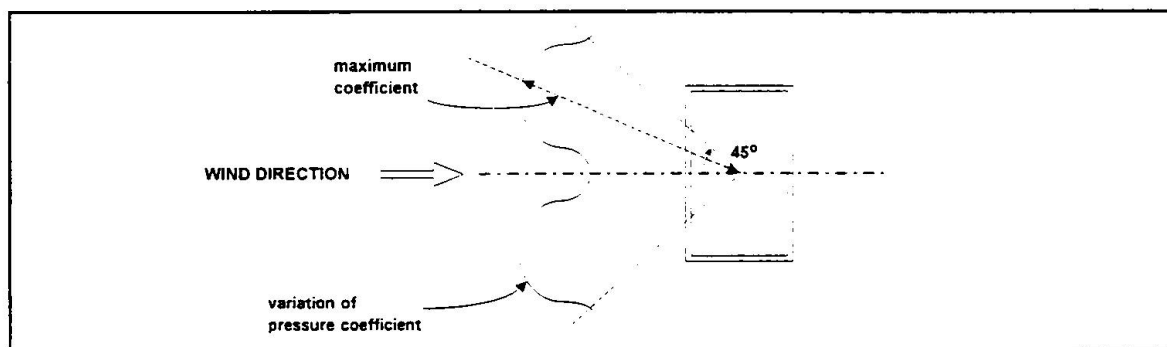
Fig. 1. Basis for orthogonal pressure coefficients.

3.   Work Undertaken by Ad-hoc Panel

3.1   General

Following the positive voting of the document to proceed to ENV status, a small informal ad-hoc panel was convened to try to develop a common strategy in the writing of Member States' NADs. It was recognized that common procedures should be made available for the derivation of the basic wind speeds, for the adoption of the informative annexes and for the incorporation of additional information, such as the inclusion of the directional pressure coefficients. The membership of the panel and details of their meetings are shown in Annex A.

3.2   Meteorological Information

At the time of positive voting of the ENV the basic wind data had not been supplied by all Member States. In certain cases the data that had been provided were not consistent, thereby making production of a European wind map impossible.

The ad-hoc panel accordingly set down in a report [4] the parameters required to produce consistent information, compatible with the principles incorporated in the Draft. These could be considered by the relevant Meteorological Offices and thus amend the data already provided or indicate the equivalent parameters adopted in developing those data.

The wind maps for each Member State are intended to represent the 10 minute mean wind velocity at 10m above sea level in uniform terrain category II, that is open countryside such as farmland, having an annual probability of being exceeded of 0.02 (i.e. 50 year return period). Guidance is given in the Draft - and in the ad-hoc panel's report - on how to derive wind speeds for other probabilities of exceedance.

The basic wind speed data are then adjusted to determine the equivalent 10 minute mean wind velocity at the site by use of altitude and direction factors. Account also needs to be taken of the terrain roughness, if not category II, and also any change in roughness from one category to another. Procedures to account for these effects are given in the ad-hoc panel's report, together with photographs and diagrams of typical

terrains to assist in the selection of the appropriate category.

Detailed procedures were developed to account for the common case of sites being in areas where there is likely to be a transition from one category type to another, as these changes do not occur instantaneously. These procedures were considered to be of value to the engineer and were recommended by the panel to be adopted in each Member State's NAD.

The engineer, in using the Draft, needs to derive the peak wind load on the structure or structural component. This is achieved in the Draft by the use of an exposure coefficient which effectively converts the mean wind speed to a peak gust load, and depends on parameters defined in the Draft. It was considered possible that the site parameters as derived by the Meteorological Office differ from those assumed in the Draft - for example the turbulent intensity could be higher or lower. In that case the Meteorological Office should either:

a)   determine the appropriate gust speed from mean wind data using their best estimate of the parameters for the site and then *by using Code parameters* work back to derive the appropriate value of mean speed for producing the map isotachs;

b)   determine the appropriate gust speed from gust speed data and *by using the Code parameters* work back to derive the appropriate value of mean speed for producing the map isotachs.

3.3   In-line Gust Response

Concern had been expressed that some Member States might develop their own analytical procedures, rather than adopt the informative annexes contained in the Draft. These aspects were discussed at length in the ad-hoc panel, and comparative calculations were undertaken to assess the sensitivity of the results to the assumptions incorporated in the draft.

The general conclusion was that by minor editing of the draft to provide clarity to the reader the recommended procedures for in-line gust response provided answers within about ± 5 per cent of other methods favoured by some panel members. However the scatter in predicting the appropriate wind speeds for the site - or in the value of the pressure coefficient for a structure or element not complying precisely with the tabulated configurations - would cause a much higher uncertainty in the wind loading.

3.4   Obstruction Heights

The effect of general roof top level, or obstruction height level, is represented simply in the Draft by the use of a parameter z_{min} which varies with terrain category and for which the wind speed is assumed to be constant at all levels from ground up to z_{min}. Thus for category IV, representing urban area, the wind speed is assumed constant up to a height of 16m above ground.

In fact in rough terrain such as towns and cities the wind tends to behave as if the ground level was raised to a height just below the average roof height, h_o leaving an indeterminate region below which is often sheltered known as the displacement height, h_d. However this is not applicable where the building to be designed is a similar height or lower than its surroundings where the displacement height is a fraction of the building height, h.

To allow for this effect the height z defined in *Clause 4.2* of the Draft as the height above ground should be replaced by an effective height z_e which is defined in the ad-hoc panel's report.

The displacement height reduces with separation distance between buildings, X, particularly across open spaces within, or at the edge of, a built up area. Rules to account for this effect are given in the panel's report and are illustrated in Figure 2.

It should be emphasized that these Rules are direction dependent, and the most onerous loading direction needs to be considered. The criteria set out in these proposals clearly depend on the continued existence of the buildings around the site. Care must be exercised to ensure that the loading is not sensitive to the dependency on the continuing existence of one or two adjacent buildings.

Accelerated wind speeds occur close to the base of buildings which are significantly taller than the displacement height. When considering low-rise buildings which are close to other tall buildings the rules for effective height will not necessarily lead to conservative values and specialist advice should be sought.
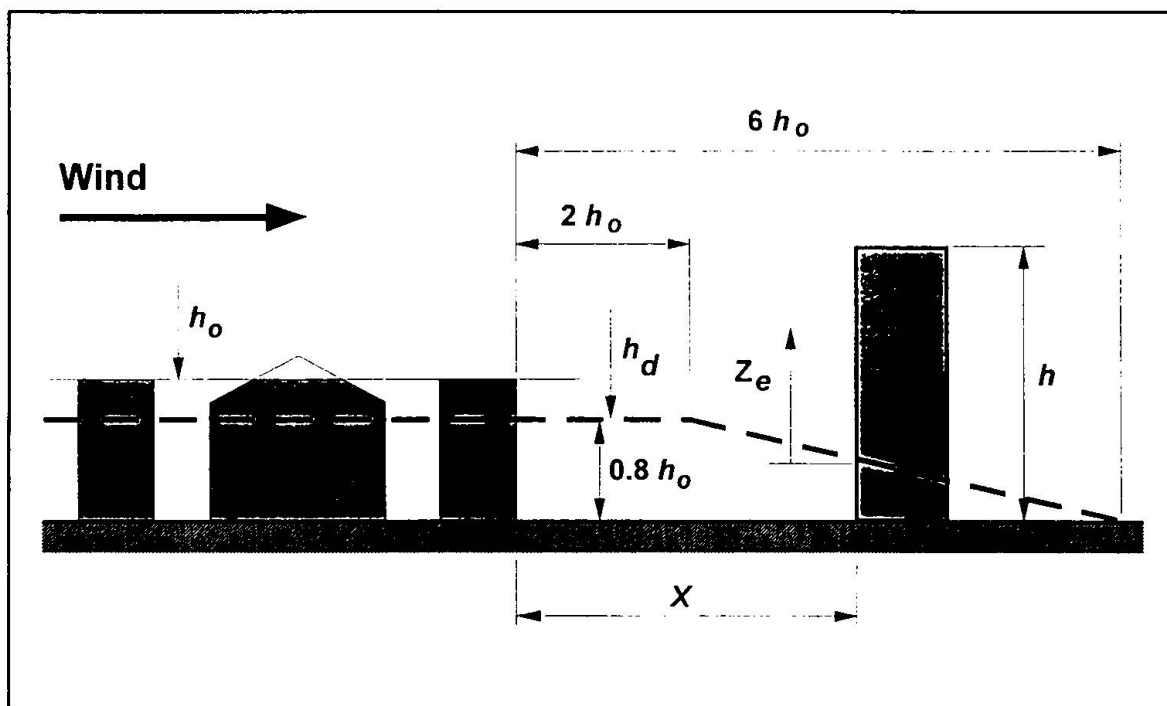

Fig. 2. Effective heights.

3.5 Direction Pressure Coefficients

The external pressure coefficients for buildings in the Draft depend on the size of the loaded area. They are given for loaded areas of $1m^2$ and $10m^2$. For areas less than $1m^2$ or greater than $10m^2$ the coefficients were assumed to be constant and with a logarithmic variation for intermediate areas.

As noted above they are also given for orthogonal wind directions but represent the highest values obtained in a range of wind directions $45°$ either side of the relevant orthogonal direction.

The panel considered that the directional coefficients, redrafted as an Annex to the Draft but excluded from the voted document, should be included in the NADs. The information contained in the Annex not only provides less conservative values but also gives values for generalised configurations which cannot be dealt with by the coefficients given in the Draft.

The Annex was thus re-examined and updated in the light of the most current information. However the coefficients provided are peak values, independent of loaded area, in the sense that they apply to different zones of the building or component. A separate adjustment for loaded area will needed to provided, for compatibility with the Draft.

4. Production of the United Kingdom's NAD for ENV 1991-2-4

The United Kingdom's NAD for ENV 1991-2-4 is presently being drafted and is following the framework of the ad-hoc panel, incorporating the proposals outlined in 3 above.

In advance of this a textual examination of the Draft was undertaken[5] to examine differences between the Draft and both the recently published British Standard BS 6399 Part 2 and its predecessor CP3 Chapter V Part 2. This identified typographical and technical errors in the Draft available at that time which were corrected prior to the publication of the ENV.

One major difference between the latest United Kingdom Wind Code, BS 6399 Part 2, and the Draft is that the United Kingdom use hourly mean wind speeds rather than 10 minute wind speeds. However the basic terrain in the United Kingdom has a z_o = 0.03 compared with a z_o = 0.05 in the Draft. It so happens that these two effects are self-cancelling, thus the map wind speeds in the Draft for the United Kingdom are identical to those in the British Standard.

Following this textual examination of the Draft a calibration exercise was undertaken to compare the results of using the draft with those obtained from BS 6399 Part 2 and CP3 Chapter V Part 2 on a series of buildings at selected locations in the United Kingdom[6]. This exercise, whilst not a comprehensive review, concentrated on the differences identified in the textual examination report. Comparative exercises were thus undertaken on:

a)   terrain effects, including obstruction heights and changes in terrain category close to the site;
b)   cladding pressures;
c)   internal pressures;
d)   overall building loads.

This exercise highlighted certain aspects of both the British Standard and the Draft which need to be addressed. Where interpretation of the Draft was found to be ambiguous, it was considered that clarification will need to be provided in the NAD. The initial conclusions from the calibration exercise were that the Draft gave higher total forces on buildings over 100m high which may be up to 30% greater than those calculated by BS 6399 Part 2 for a 200m building.

The team involved in writing the NAD are considering the conclusions of the calibration report whilst it is being finalized.

One problem faced in the production of the NAD is that no clear guidance is available on how to co-ordinate the ENVs on Actions with the already published ENVs, with their associated NADs, on design (e.g. ENV 1993-1). The latter NADs, of necessity, refer to the National Standards for loading, as ENV 1991 was not published at the time these were written. Unless amendments to these NADs are made there is, at present, no formal procedure whereby the Action and Design ENVs, with their associated NADs, can be used together.

Annex A

Membership of Ad-hoc Panel:

N. Cook	R. Sandvik
S. Desai	B. W. Smith
K. Handa	G. Solari
S. O. Hansen	P. Spehl
J. A. Hertig	G. Steinthorsson
E. Hjorth Hansen	

Meetings of Panel:

12th/13th April 1994	-	Brussels
13th June 1994	-	London
12th August 1994	-	Copenhagen

5.   References

1.   Recommendations of an Ad-hoc Panel for the production of National Application Documents, Report 386/1/95, Flint & Neill Partnership, January 1995.

2.   Code of Practice: CP3 Chapter V Part 2: Wind Loads, British Standards Institution, London, 1970.

3.   British Standard: BS 6399 Part 2: Code of Practice for Wind Loads, British Standards Institution, London, 1995.

4.   Guidance for National Meteorological Offices to provide wind data for incorporation into the Eurocode for Wind Actions, Report 386/1/94, Flint & Neill Partnership, May 1994.

5.   Textual Examination of Eurocode 1 Part 2.4: Wind Loads and Formulation of a Suitable Calibration Method, Report 434/11/95, Flint & Neill Partnership, July 1995.

6.   Calibration of ENV 1991-2-4 Eurocode 1 Part 2.4: Wind Actions. Report AM 2949/RO1 (Preliminary), W. S. Atkins Safety and Reliability, January 1996.
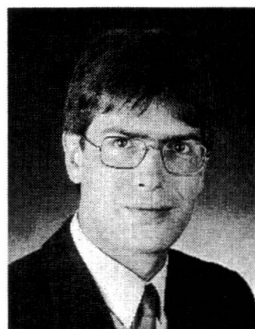
EC 1: Actions induced by cranes

EC 1:
EC 1: Einwirkungen aus Kranen

Gerhard Sedlacek
Prof. Dr.-Ing.
RWTH Aachen
Civil Engineering
Aachen, Germany

Gerhard Sedlacek, born in 1939, is Professor for Steel Construction at the RWTH Aachen. He has been convener of the Project Team for the preparation of the chapter ·Actions induced by cranes".

Dietmar Grotmann
Dipl.-Ing.
RWTH Aachen
Civil Engineering
Aachen, Germany

Dietmar Grotmann, born in 1961 is research engineer for steel construction at the RWTH Aachen.

SUMMARY

According to an agreement achieved in CEN, CEN/TC 250 prepares structural Eurocodes with design rules for buildings and civil engineering works whereas other CEN/TC´s, that prepare rules for other products e.g. CEN/TC 147 develops a code for cranes, mainly develop rules for specific actions and methods of analysis for their fields and refer to the Eurocodes for resistances where possible.

Actions for the design of crane supporting structures which are caused by crane operations at the interface between crane structures and "buildings", i.e. the contact area between wheels and rails had to be given. In cooperation between CEN/TC 250/SC 1 and the relevant working group 2 of CEN/TC 147 specific crane actions for crane supporting structures were defined which comply both with the design philosophy in CEN/TC 147 and the safety assumptions and design procedures of the Eurocodes. This paper gives some basic principles and application rules on actions on crane supporting structures.

RÉSUMÉ

ZUSAMMENFASSUNG

Gemäß der in CEN erzielten Übereinstimmung ist das technische Kommittee CEN/TC 250 beauftragt worden, Eurocodes für den Entwurf, die Berechnung und die Bemessung von Tragwerken des konstruktiven Ingenieurbaus zu entwickeln. Weitere technische Kommittees von CEN erstellen für ihre Produkte spezielle Regeln (z.B. entwickelt CEN/TC 147 eine Norm für Krane). Sie entwickeln die Regeln für die speziellen Einwirkungen und Berechnungsmethoden und verweisen was die Beanspruchbarkeit angeht auf die Eurocodes, soweit dies möglich ist.

Für die Bemessung von Kranunterkonstruktionen wären die Einwirkungen festzulegen, die durch den Kranbetrieb an der Schnittstelle "Kran - Kranunterkonstruktion" die an der Kontaktfläche zwischen Rad und Schiene entstehen. In Zusammenarbeit mit der Arbeitsgruppe 2 von CEN/TC 147 wurde die Kranlast für die Kranunterkonstruktion festgelegt, die mit der Bemessungsphilosophie in CEN/TC 147 und den Sicherheitsanforderungen und Bemessungsabläufen der Eurocodes übereinstimmen. Dieser Aufsatz beschreibt einige wesentliche Regeln für die Einwirkungen auf Kranunterkonstruktionen

1.   GENERAL AND SCOPE

Part 5 of Eurocode 1 deals with actions from cranes and machinery. It is therefore subdivided into 4 parts where Part 1 gives General rules, Part 2 deals with actions induced by cranes, Part 3 presents the Principles for determining actions from machinery and Part 4 gives practical wheel loads from transport vehicles such as lifters, helicopters, etc.

This paper presents the rules for actions from cranes, as these rules are rather detailed and operative. The rules have been developed by a Project team of CEN/TC250/SC1 in close cooperation with experts from CEN/TC147 and with the Project team of CEN/TC250/SC3 which in parallel developed rules for the resistance of steel crane supporting structures.

Actions induced by cranes comprise actions from hoists, crabs and cranes on runway beams. Accordingly the crane supporting structures are divided into 3 categories, see figure 1:

-     runway beams for hoist blocks
-     runway beams for underslung overhead travelling cranes
-     runway beams for bridge cranes

The standard gives principles and application rules for determining numerical values of crane actions defined by the forces exerted from the crane wheels to the rails.

The list of contents of part 5.2 can be taken from figure 2.
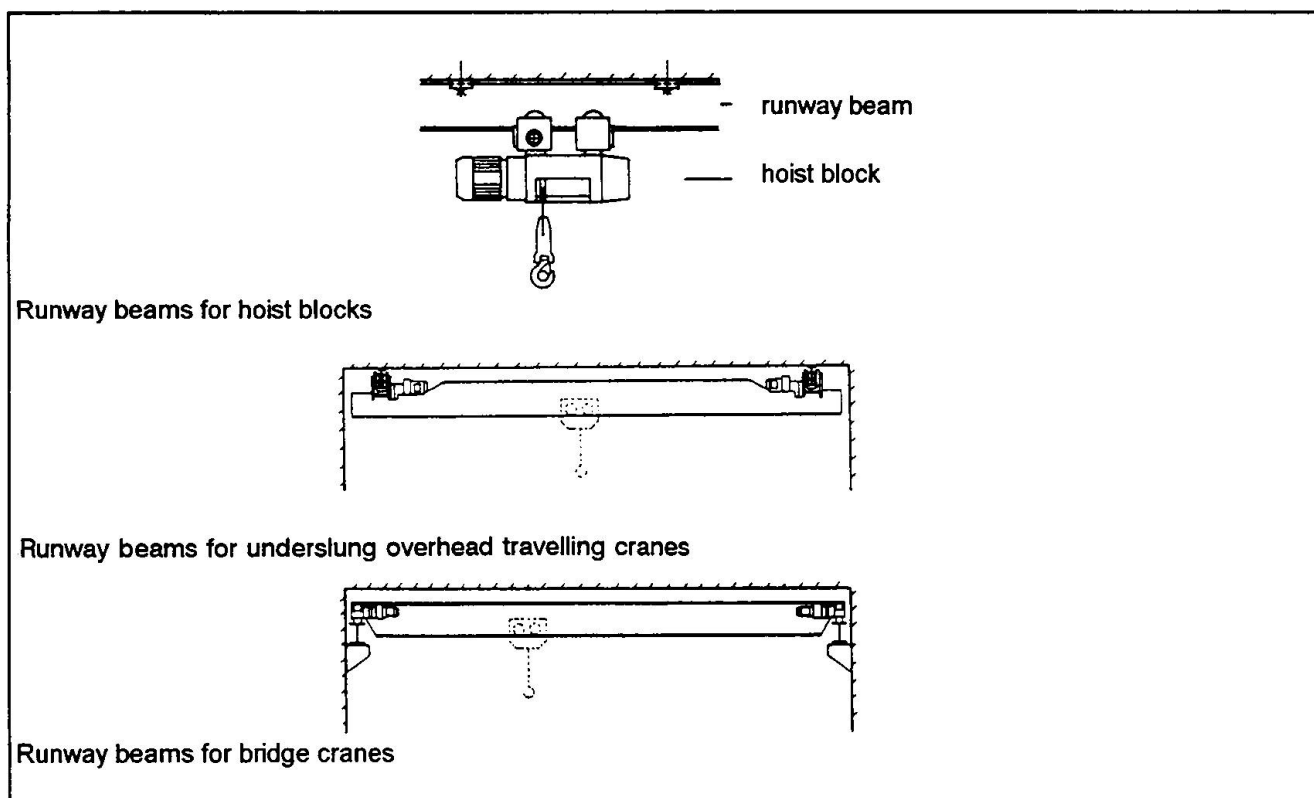
Figure 1:   3 categories of crane supporting structures

Part 5.2

Main text:
2. 1 Scope
2. 2 Definitions
2. 3 Symbols
2. 4 Classifications of actions
2. 5 Design situations
2. 6 Representation of actions
2. 7 Load arrangements
2. 8 Vertical crane loads - characteristic values
2. 9 Horizontal crane loads - characteristic values
2.10 Temperature effects
2.11 Access walkways, stairs, platforms and guard rails
2.12 Test loading
2.13 Accidental loads
2.14 Fatigue loads

Annex A: Basis of design - Supplementary clauses to ENV1991-1 for runway beams loaded by cranes

Figure 2: List of contents of part 5-2 "Actions induced by hoists, crabs and cranes on runway beams

2. BACKGROUND OF THE MODELS AND CHARACTERISTIC VALUES

2.1 General

The actions induced by cranes are classified in variable and accidental actions. Variable actions result from variation in time and location, see figure 3. They include:

- gravity loads including variable hoist loads
- inertial forces caused by acceleration/deceleration and by skewing
- dynamic effects

In addition actions are also specified for test loading, in case tests are performed with cranes on the supporting structures

Accidental situations lead to buffer forces, tilting forces etc.

Actions may be vertical and/or horizontal and are composed of a static and a dynamic component. The dynamic component in general is expressed in terms of a dynamic magnification factor to the static load:

$$Q_{k,i} = \varphi_i F_{k,i}$$

where $F_{k,i}$ is the static wheel load
         φ_i is the dynamic magnification factor
         $Q_{k,i}$ is the characteristic wheel load

Figure 4 gives a survey on the type of the magnification factors to be considered for the static loads.
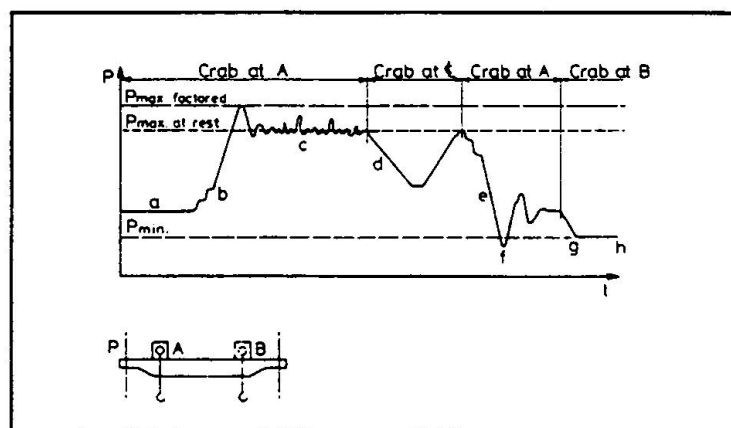
Figure 3: Example for the fluctuation of crane wheel reaction during a work cycle

Dynamic magnifica-tion factors	effects to be considered	to be applied to
φ_1	- vibrational excitation of the crane structure due to lifting the hoist load off the ground	selfweight of the crane structure
φ_2 or φ_3	- dynamic effects of transferring the hoistload from the ground to the crane - dynamic effect of sudden release of the payload if for example grabs or magnets are used	hoistload
φ_4	- dynamic effects induced when travelling on rail tracks or roadways	selfweight of the crane and hoistload
φ_5	- effects caused by drive forces	horizontal forces
φ_6	- when a test load is moved by the drives in the way the crane is used	test load
φ_7	- considers the elastic effects of impact on buffers	buffer loads
φ_8	- gust response factor	wind loads

Figure 4: Various dynamic magnification factors φ_i

The simultaneity of the crane load components is taken into account by considering groups of loads defined in figure 5. Each of these groups of loads shall be considered as defining one characteristic crane action for the combination with non-crane loads.

2.2   Characteristic values

2.2.1   Basis

To determine the design values of the crane loads for ultimate limit state a reference period of 50 years and a reliability index ß = 3,80 has been adopted. Based on these definitions the characteristic values Q_k were determined from the design values Q_d by

$$Q_k = \frac{Q_d}{\gamma_Q}$$ where a single safety factor γ_Q = 1,35 was used for all characteristic crane actions

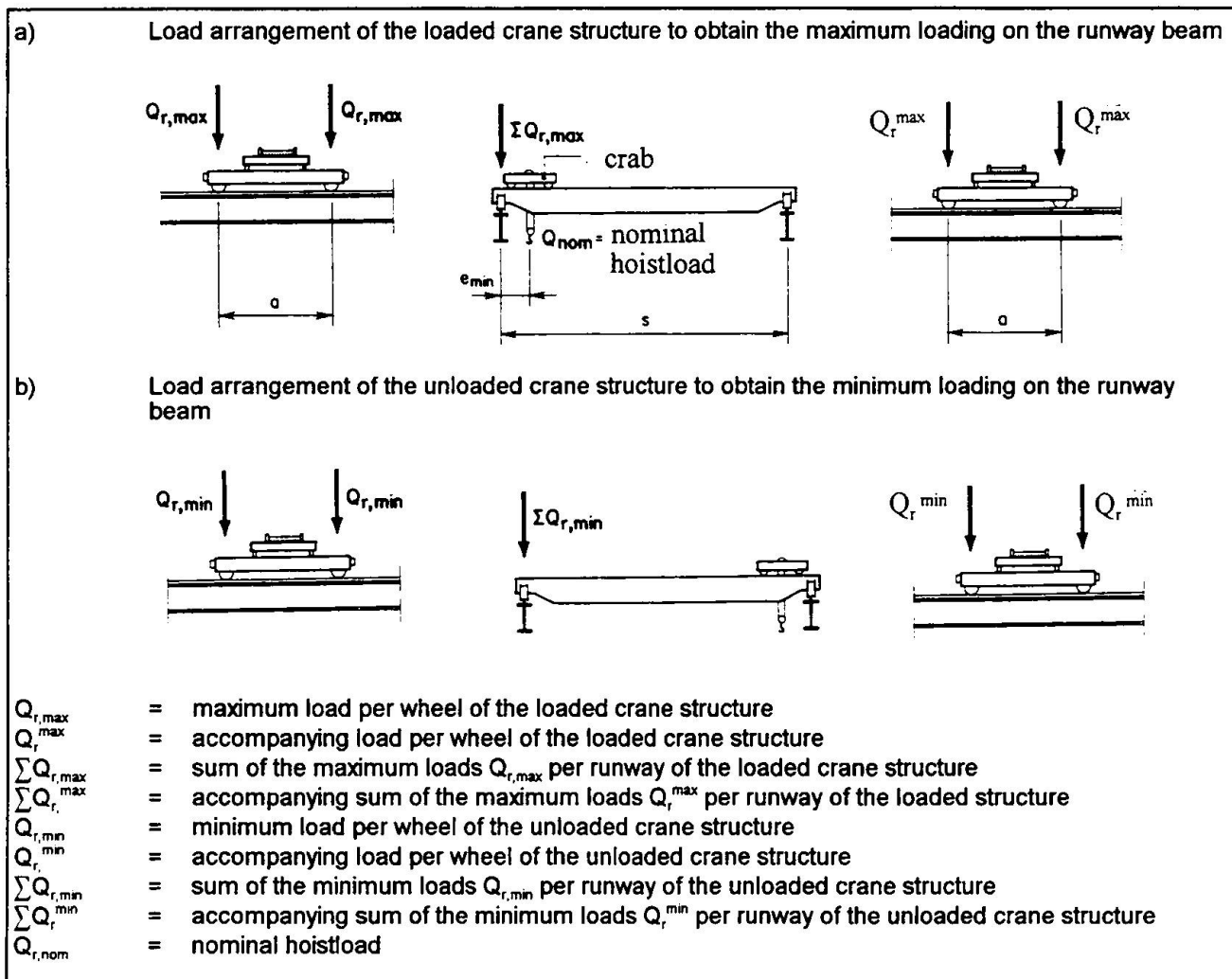a) Load arrangement of the loaded crane structure to obtain the maximum loading on the runway beam

b) Load arrangement of the unloaded crane structure to obtain the minimum loading on the runway beam

$Q_{r,max}$	=	maximum load per wheel of the loaded crane structure
Q_r^{max}	=	accompanying load per wheel of the loaded crane structure
$\sum Q_{r,max}$	=	sum of the maximum loads $Q_{r,max}$ per runway of the loaded crane structure
$\sum Q_r^{max}$	=	accompanying sum of the maximum loads Q_r^{max} per runway of the loaded structure
$Q_{r,min}$	=	minimum load per wheel of the unloaded crane structure
Q_r^{min}	=	accompanying load per wheel of the unloaded crane structure
$\sum Q_{r,min}$	=	sum of the minimum loads $Q_{r,min}$ per runway of the unloaded crane structure
$\sum Q_r^{min}$	=	accompanying sum of the minimum loads Q_r^{min} per runway of the unloaded crane structure
$Q_{r,nom}$	=	nominal hoistload

Figure 6   Load arrangements to obtain the relevant vertical actions to the runway girders

$$e = \frac{1}{4} b_r$$

where

e = eccentricity
b_r = width of the rail head
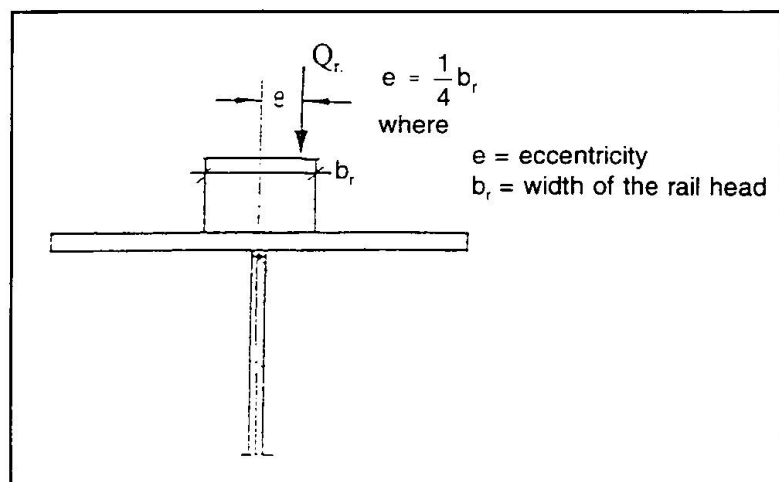
Figure 7   Eccentricity of the load introduction

(a)   Definition of the drive force

$K = \mu \, \Sigma Q_{r,min}$
μ = friction factor (e.g. μ = 0,2 for steel to steel)
$\Sigma \, Q_{r,min}$ is the sum of the minimum vertical wheel loads
$M = K \, \ell_s$

$H_{L,i} = \varphi_5 \, K \, \dfrac{1}{n_r}$

n_r number of runway beams

$H_{T,i} = \varphi_5 \, \xi_i \, \dfrac{M}{a}$

$\xi_1 = \dfrac{\Sigma \, Q_{r,max}}{\Sigma \, Q_r}$

$\xi_2 = 1 - \xi_1$

Σq_r is the sum of the vertical wheel load per runway

(b)   Longitudinal and transversal horizontal wheel loads caused by acceleration
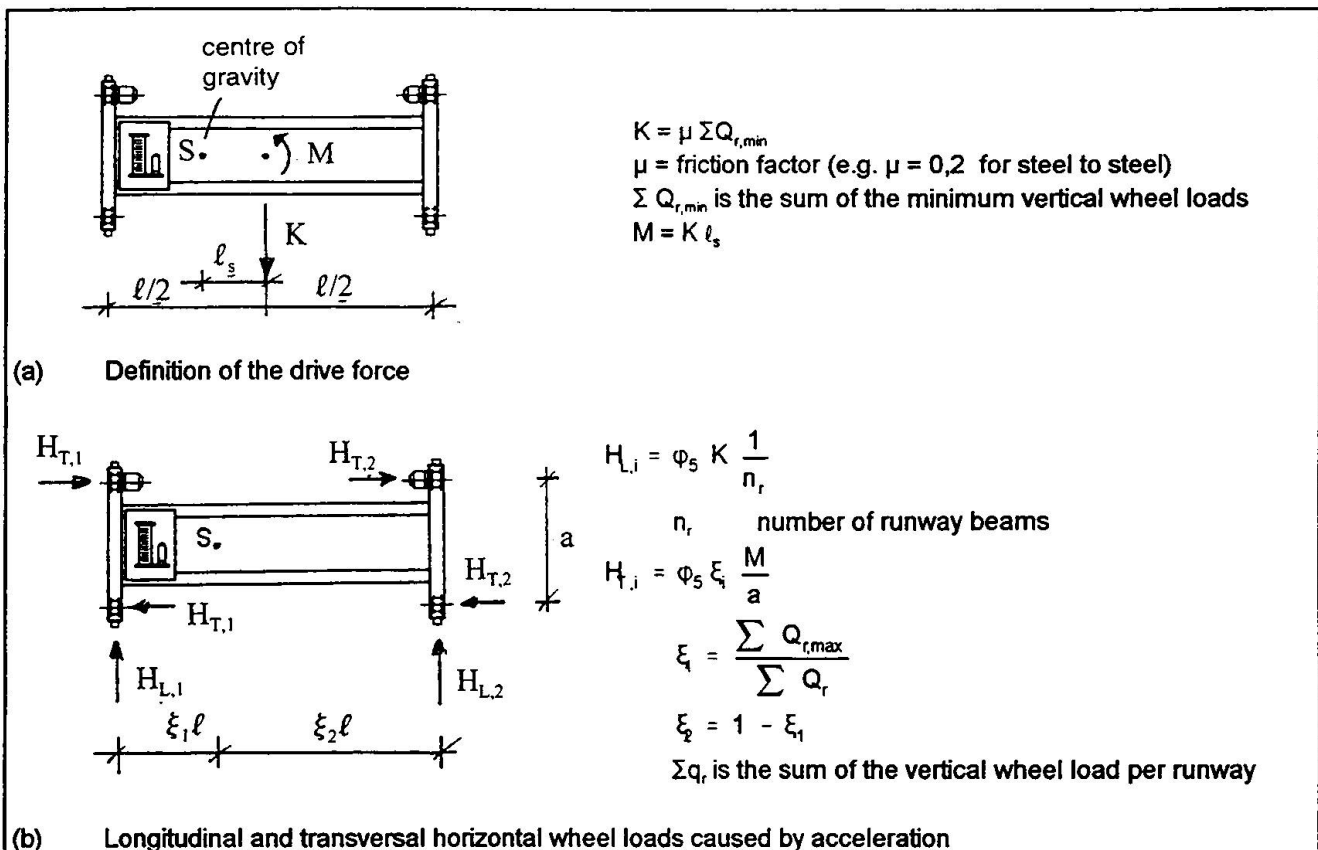
Figure 8   Horizontal wheel loads caused by acceleration

The horizontal crane loads caused by skewing are induced by guidance reactions which force the wheel to deviate from their free rolling natural travelling or traverse direction. These loads should be applied as longitudinal or transversal horizontal wheel loads H_{sL} and H_{sT} to the runway beams as shown in figure 9.

The horizontal wheel loads caused by skewing may be obtained from:
$H_{s,i} = f \, \lambda_{s,ij} \, \Sigma \, Q_{r,max}$

where f   is a non-positive factor defined as
         f   = 0,3 (1 - exp (-250 α)) $\leq$ 0,3
         α = skewing angle, see figure 9
$\lambda_{s,ij}$ is a force factor for i = L (longitudinal) or i = T (transversal) and the wheel j

The force factor $\lambda_{s,ij}$ is depending on the combination of the wheel pairs and the distance h, determined according to figure 10(a) between the instantaneous slide pole and the guide means, see figure 9. The value of the force factor $\lambda_{s,ij}$ may be determined by the expressions given in figure 10(b).

The simultaneity of the horizontal loads caused by acceleration and skewing is defined in figure 5 where the relevant groups of loads are given.

2.2.4   Test loading

After fabrication cranes are checked by test loads. If relevant the crane supporting structure shall be designed for these test loads to secure that no irreversible serviceability conditions occur.

When considering these test loads in the design of crane supporting structures the following two cases shall be distinguished:

case a: Dynamic test load:
        The test load is moved by the drives in the way the crane will be used. The test load has to be at least

110% of the nominal hoist load.

$$q_6 = 0,5 (1 + \varphi_2)$$

case b: Static test load:
   The load is increased for testing by loading the crane without the use of the drives. The test load has to be at least 125% of the nominal hoist load.
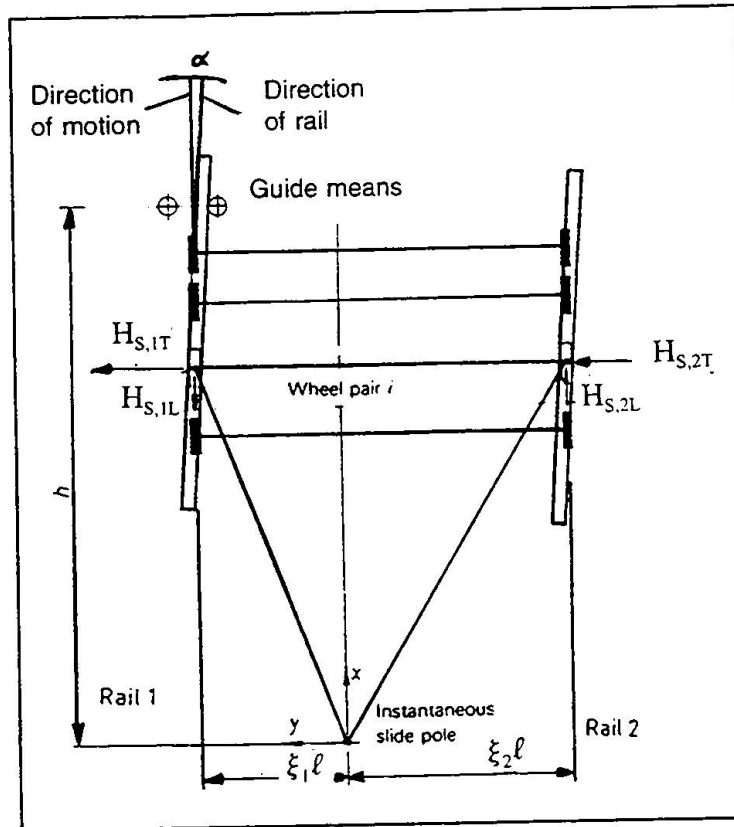
$$q_6 = 1,0$$

Figure 9   Definition of the horizontal forces caused by skewing

2.2.5   Accidental loads

Cranes may generate accidental actions due to collision with buffers or collision of lifting attachments with obstacles (tilting forces). These actions should be considered for the structural design where appropriate protection is not provided.

2.2.6   Fatigue loads

The fatigue loads shall be determined such, that the operational conditions of the distribution of hoist loads and the effects of the variation of crane positions to the fatigue details are duely considered for normal service condition .

In case detailed studies are not possible the fatigue loads may be expressed for practical reasons in terms of fatigue damage equivalent loads Q_e that may be taken as constant for all crane positions to determine fatigue load effects:

$$Q_e = \varphi_{fat} \, \lambda \, Q_{max}$$

where Q_{max} is the maximum value of the characteristic vertical wheel load

	Combination of wheel pairs		h
	coupled (c)	independent (i)	
Fixed/Fixed FF	CFF	IFF	$\dfrac{m\xi_1\xi_2\,\ell + \Sigma e_i^2}{\Sigma e_i}$
Fixed/Movable FM	CFM	IFM	$\dfrac{m\xi_1\,\ell + \Sigma e_i^2}{\Sigma e_i}$

h = distance between the instantaneous slide pole and the guide means
m = number of pairs of coupled wheels (m = 0 for independent wheel pairs)
ξ_1 = distance of the instantaneous slide pole from rail 1
ξ_2 = distance of the instantaneous slide pole from rail 2
ℓ = span of the appliance
e_i = distance of the wheel pair i from the guide means

(a)

System	λ_s	λ_{S1L}	λ_{S1T}	λ_{S2L}	λ_{S2T}
cFF	$1 - \dfrac{\Sigma e_i}{nh}$	$\dfrac{\xi_1\xi_2}{n}\dfrac{\ell}{h}$	$\dfrac{\xi_1}{n}\left(\dfrac{1-e_i}{h}\right)$	$\dfrac{\xi_1\xi_2}{n}\dfrac{\ell}{h}$	$\dfrac{\xi_1}{n}\left(\dfrac{1-e_i}{h}\right)$
iFF		0	$\dfrac{\xi_1}{n}\left(\dfrac{1-e_i}{h}\right)$	0	$\dfrac{\xi_1}{n}\left(\dfrac{1-e_i}{h}\right)$
cFM	$\xi_1\left(1 - \dfrac{\Sigma e_i}{nh}\right)$	$\dfrac{\xi_1\xi_2}{n}\dfrac{\ell}{h}$	$\dfrac{\xi_1}{n}\left(\dfrac{1-e_i}{h}\right)$	$\dfrac{\xi_1\xi_2}{n}\dfrac{\ell}{h}$	0
iFM		0	$\dfrac{\xi_1}{n}\left(\dfrac{1-e_i}{h}\right)$	0	0

n = number of wheel pairs
ξ_1 = distance of the instantaneous slide pole from rail 1
ξ_2 = distance of the instantaneous slide pole from rail 2
ℓ = span of the appliance
e_i = distance of the wheel pair i from the guide means
h = instance between the instantaneous slide pole and guide means

(b)

Figure 10   Definition of $\lambda_{s,ij}$ - values

λ is the damage equivalent factor
φ_{fat} is the damage equivalent dynamic impact factor

For determining the λ-value the use of cranes may be classified according to the load spectrum and the total number of load cycles as indicated in figure 11. The classification has been taken from the draft of the CEN standard prepared by CEN/TC147. Recommendations for the classifications of cranes are given in figure 12.

The values of the damage equivalent factor λ may be taken from figure 13 according to the crane classification chosen.

class of load spectrum / class of total number of cycles [1]	Q0	Q1	Q2	Q3	Q4	Q5
U0	S0	S0	S0	S0	S0	S0
U1	S0	S0	S0	S0	S0	S1
U2	S0	S0	S0	S0	S1	S2
U3	S0	S0	S0	S1	S2	S3
U4	S0	S0	S1	S2	S3	S4
U5	S0	S1	S2	S3	S4	S5
U6	S1	S2	S3	S4	S5	S6
U7	S2	S3	S4	S5	S6	S7
U8	S3	S4	S5	S6	S7	S8
U9	S4	S5	S6	S7	S8	S9

[1]   The classification is based on a total service life of 25 years

Figure 11   Classification of cranes according to TC 147

The damage equivalent dynamic impact factor φ_{fat} for normal conditions may be taken as:

$$\varphi_{fat,1} = \frac{1 + \varphi_1}{2}$$

$$\varphi_{fat,2} = \frac{1 + \varphi_2}{2}$$

2.2.7   Load combinations with other variable loads

For any combination of groups of loads induced by cranes together with actions specified in other parts of ENV 1991 any such combination shall be considered as one action.

When considering the groups of loads induced by cranes with other actions the following cases should be distinguished:

case a: runways outside buildings; the runways are then fully exposed to climatic actions.

case b: runways inside buildings where climatic actions are resisted by the buildings and structural elements of the buildings may also be loaded directly or indirectly by crane loads.

The combination factors ψ-factors for crane loads are as given in figure 14.

item	Type of crane		classes
1	Hand-operated cranes		S0, S1
2	Erection cranes		S0, S1
3	Powerhouse cranes		S1, S2
4	Storage cranes	intermittend operation	S3, S4
5	Storage cranes, spreader bar cranes, scrap yard cranes	continuous operation	S5 to S9
6	Workshop cranes		S2 to S4
7	Bridge cranes, ram cranes	grab or magnet operation	S5 to S9
8	Casting cranes		S5 to S9
9	Soaking pit cranes		S7 to S9
10	Stripper cranes, charging cranes		S7 to S9
11	Forging cranes		S5 to S9
12	Transporter bridges, semi-portal cranes, portal cranes with trolley or slewing crane	Hook operation	S3 to S6
13	Transporter bridges, semi-portal cranes, portal cranes with trolley or slewing crane	grab or magnet operation	S5 to S9
14	Travelling belt bridge with fixed or sliding belt(s)		S2 to S4
15	Dockyard cranes, slipway cranes, fitting-out cranes	hook operation	S2 to S4
16	Wharf cranes, slewing, floating cranes, level luffing slewing	hook operation	S3 to S6
17	Wharf cranes, slewing, floating cranes, level luffing slewing	grab or magnet operation	S5 to S9
18	Heavy duty floating cranes, gantry cranes		S1, S2
19	Shipboard cargo cranes	hook operation	S2 to S4
20	Shipboard cargo cranes	grab or magnet operation	S3 to S6
21	Tower slewing cranes for the construction industry		S2
22	Erection cranes, derrick cranes	hook operation	S1, S2
23	Rail mounted slewing cranes	hook operation	S2 to S4
24	Rail mounted slewing cranes	grab or magnet operation	S3 to S6
25	Railway cranes authorized on trains		S3, S4
26	Truck cranes, mobile cranes	hook operation	S2 to S4
27	Truck cranes, mobile cranes	grab or magnet operation	S3 to S6
28	Heavy duty truck cranes, heavy duty mobile cranes		S0, S1

Figure 12   Recommended classification of cranes

λ factors	S0	S1	S2	S3	S4	S5	S6	S7	S8	S9
normal stresses	0,198	0,250	0,315	0,397	0,500	0,630	0,794	1,00	1,260	1,587
shear stresses	0,379	0,436	0,500	0,575	0,660	0,758	0,871	1,00	1,149	1,320

Figure 13   λ-values according to classification of cranes (service life 25 years)

Action	Symbol	ψ_0	ψ_1	ψ_2
group of load induced by cranes	Q_r	1,00	0,90	- [1]
Wind Force	F_{wk} F_w^* [2]	0,6 1,0	0,5 0	0 0
Snow and ice	S	0,6	0,5	0
Temperature Effects	T_K	0,6	0,6	0,5

[1] ratio between the permanent crane action and the total crane action
[2] Corresponding to maximum in service wind speed

Figure 14   ψ-factors for crane loads

REFERENCES

[1]   A.J. Beuker, H. Gulvanessian, G. Sedlacek, C. Urbano, G. Wagner, D. Grotmann: Members of CEN/TC250/SC 1/PT 13

[2]   ENV 1991-1: Eurocode 1: Basis of Design and Actions on Structures; Part 1: Basis of design, 1994

[3]   Crane Safety - Design General Proof calculation to prevent mechanical hazards by design; Part 1 to Part 3; Draft CEN/TC 147/ WG 2/ N 23 October 1995

[4]   Draft ENV 1993-6: Eurocode 3 - Part 6: Crane supporting structures

[5]   J. Oxfort: Zum Betreibsfestigkeitsnachweis für die Radlastwirkungen in Kranbahnträgern noch DIN 4132, Stahlbau 1/1983, pp 50-54

[6]   SIA 160: Einwirkungen auf Tragwerke, Ausgabe 1989

Leere Seite
Blank page
Page vide

Design Philosophy for Accidental Actions

Ivar HOLAND
Professor, dr. techn.
SINTEF
Trondheim, Norway
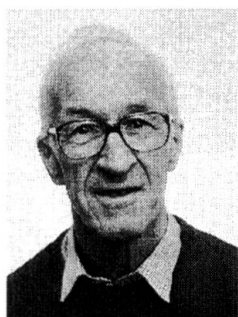
Ivar Holand, born 1924, was awarded his civil engineering degree at the Norwegian Institute of Technology in 1948. He received his doctoral degree from the same institution in 1958, and became a Professor of Structural Mechanics in 1963, and Director of the Cement and Concrete Research Institute in 1981. He retired in 1992 and is now a senior research consultant to SINTEF.

Summary

The objective of a design for accidental actions is to give the structure an adequate robustness, reducing the risk of a structural catastrophe to an acceptable level. As a consequence, such a design is not needed for categories of structures with a limited risk potential. For traditional structures with a medium risk potential, the robustness may be obtained by prescriptive detailing rules or a simplified analysis, whereas an analysis-based design for defined accidental actions is needed for structures with a high risk potential.

1. ENV 1991 Eurocode 1: Part 2.7 Accidental Actions

A draft for Eurocode 1: Part 2.7 Accidental Actions was completed in January 1996. The author has been a member of the Project Team, and the present paper has been influenced by the work there, and in broad terms reflects the attitude of the Project Team. However, the author is solely responsible for the formulations, which have not been discussed in the Project Team, except to the extent they are identical with formulations in the draft for Part 2.7.

Parts 2.1 to 2.7 should ideally only prescribe load values. Since the design philosophy for accidental actions differs from the design philosophy for permanent and variable actions, it has been unavoidable to also consider design to a limited extent in the draft. Thus, in the development of ENV 1991-1 [1] to EN, it should be considered if certain parts ought to be transferred from Part 2.7 to Part 1.

2.   Definition of accidental design situations and accidental actions

2.1   Formulations in ENV 1991 Part 1 and Part 2.7

The term "Design situation" is defined in ENV 1991-1 to mean the circumstances in which the structure may be required to fulfil its function. The selected design situations are to be sufficiently severe and varied enough to encompass all conditions which can reasonably be foreseen to occur during the execution and use of the structure.

The phrase "which can reasonably be foreseen" is somewhat ambiguous in the case of accidental situations, the characteristics of which are that they cannot easily be foreseen. The PT has therefore qualified this phrase by saying that in the present case this shall be interpreted as "which have a reasonable probability of occurrence and can be counteracted in an economical way".

2.2   Probability of Accidental Actions. Residual Risk

With regard to accidental actions, the structure is designed to resist, with appropriate degrees of reliability, actions with low probability of occurrence, with severe consequences of failure and usually of short duration.

Only in some cases can the probability of occurrence of an accidental action and the probability distribution of its magnitude be determined from statistics and risk analysis procedures. Thus, design values in practice are often nominal values.

The PT has not defined any annual probability for an accidental action, but refers in a note to ISO DP 10252 "Accidental Actions due to Human Activities" [2], which specifies that the representative value of an accidental action should be chosen in such a way that there is an assessed probability less than $p = 10^{-4}$ per year for one structure that this or a higher impact energy will occur.

Hence, there will always be a residual risk which will have to be accepted. The residual risk will refer to accidental actions on a low probability level, which are not considered at all in the design, as well as actions that are identified and considered, but for which the design nevertheless will necessitate the acceptance of a residual risk. The residual risk will be determined by the cost of safety measures weighed against the consequences of a serious failure, including the conceivable public reaction after an accident.

2.3   Causes of Accidental Actions. Risk Analysis

Causes of accidental situations include:

-    failure of equipment (cranes, gas piping, vehicle brakes etc.) due to poor design, fabrication or maintenance
-    improper use or operation (due to insufficient teaching or training, indisposition, negligence or unfavourable external circumstances)
-    natural hazards like tornadoes, earthquakes, avalanches, landslides etc.

A risk analysis may be a valuable tool to study risk scenarios, in particular when accidental situations developing through a complex chain of events have to be considered. However, the complexity needed will be dictated by the problem at hand, and risk analysis in a rigorous form including extensive statistical analyses will be used only in special cases. Risk analysis ideas may, however, also be applied to provide a systematic procedure for identification of risks, and, furthermore, for assessment of accidental actions to be included. The actual assessments may often be made by comparison with known structures, and with risks implied in accepted designs for which experience exists.

A severe consequence requires the consideration of extensive hazard scenarios, while less severe consequences allow less extensive hazard scenarios. Consequences are to be assessed in terms of injury to humans, or unacceptable change to the environment, or large economic losses for the society.

2.4 Man-Made Accidents and Natural Accidents

Accidental design situations are defined in ENV 1991-1 to include (Article 1.5.2.5) "design situation involving exceptional conditions of the structure or its exposure, e.g. fire, explosion, impact or local failure". Thus, accidental actions arising from the natural environment like waves and tides, flooding, tornadoes, extreme erosion or dropping rocks are not included. In accordance with this, the draft for Part 2.7 states that "This part refers to exceptional conditions applicable to the structure or its exposure caused by human activities, e.g. fire, explosion or impact. " However, in ENV 1991-1 Article 4.1(4) states that "Some actions, for example from seismic actions and snow loads, can be considered as either accidental and/or variable actions ...". The restriction to man-made accidents is thus a choice, presumably motivated by a need to restrict the number of sources of accidental actions to be considered in Part 2.7.

Regarding design principles, there is no reason to distinguish between man-made accidents and acts of God, neither in the striving for reducing risks of structural failures, nor in the design philosophy to reach this objective. The logical consequence is that design to mitigate accidental actions should follow the same principles, irrespective of the source of the accidental action. Accordingly, the Project Team has formulated the principles of their draft as generally valid for all categories of accidental actions. Future versions of the Prestandards "Earthquake resistant design of structures" (ENV 1998) and "Actions on structures exposed to fire" (ENV 1991-2-2) should thus comply with ENV 1991-2-7, also where this may not fully be the case in the present documents.

2.5 Acceptance of Local Damage

It is an essential premise for the definition of an accidental action that localised damage (cross section failure/component failure) will be acceptable, provided that it will not endanger the whole structure (i. e. cause system failure), or that the loadbearing capacity is maintained long enough for necessary emergency reactions to be taken, for instance evacuation of the building and its environs. This philosophy will govern the choice of accidental situations to be considered. As a result, some types of events which are generally denoted as accidents, like persons falling through windows or ceilings, are not classified as accidental actions in the present context, since they have no potential to

damage the structural system.

Distinguishing between component failure and system failure allows a systematic discrimination between design for variable actions, essentially focusing on cross section/component failure, and for accidental actions, essentially focusing on system failure.

2.6 Accidental and variable actions from the same source

As indicated in ENV 1991-1 Article 4.1(4), accidental actions as well as variable actions may originate from the same sources of action in some cases. This may for instance be the case for impact from ships, where a ship out of control may be the source of an accidental action, whereas actions from fendering and mooring of ships are variable actions.

If abnormal values may occur for actions in the category variable, with the result that the catastrophe safety is not sufficiently taken care of by the load factors and the normal check of component failure under variable loads, a check for such abnormal loads may be needed. Examples are:

-     wave and wind loads on offshore structures
-     wind and ice loads on masts and towers
-     wave and tide loads on dikes

The corresponding safety checks may follow the principles described for accidental situations, even if the loads are not classified as accidental actions according to ENV 1991 Part 2.7.

3.   Application of accidental actions in design. Safety Categories

3.1   Objective of design

Risk may be defined as the danger that undesired events represent. Risk is expressed in terms of the probability and consequences of undesired events. Thus, risk reducing measures consist of probability reducing and consequence reducing measures, including contingency plans in the event of an accident. Risk reducing measures should be given high priority in design for accidental actions, and also be taken into account in design. No structure can be expected to resist all actions that could arise due to an extreme cause, but there is to be a reasonable probability that it will not be damaged to an extent disproportionate to the original cause.

A result of the acceptance of local failure (which in most cases may be identified as a component failure) provided that it does not lead to a system failure, is that redundancy and non-linear effects both regarding material behaviour and geometry play a much larger role in design to mitigate accidental actions than variable actions. The same is true for a design which allows large energy absorption.

3.2   Safety Categories

Design for accidental situations is implemented to avoid structural catastrophes. As a consequence, only structures where a collapse may cause large consequences in terms of injury to humans, damage to the environment or economic losses for society need to be designed for accidental situations. Exempted are thus in particular low-rise buildings, where the consequences of an accidental action are small. Nevertheless, consequence reducing measures like fire protection of steel members and design measures like favouring ductile design in earthquake areas are relevant also for low-rise buildings.

A convenient measure to decide what structures are to be designed for accidental situations is to arrange structures or structural components in categories according to the *consequences* of an accident.

The draft for Part 2.7 arranges structures in the following safety categories based on consequences of a failure:

-    Safety category 1   Limited consequences
-    Safety category 2   Medium consequences
-    Safety category 3   Large consequences

Less important individual structural members or sub-systems may be placed in a lower safety category than the overall structural system.

Examples of placing structures in safety categories are shown in an informative annex to the draft, which also is included in Table 1 to illustrate the concept of categorization.

Table 1. Safety categories suggested in draft for EC 1 Part 2.7

Safety categories	Structure
1	Residential buildings of maximum three storeys and comparable structures Agricultural buildings
2	Buildings generally Small road and railway bridges
3	Industrial plants with high risk potentials Large road and railway bridges Dams and dikes implying heavy damage in case of flood Structures for large numbers of persons (e. g. large grandstands or very high-rise buildings) Nuclear reactors

Reliability differentiation is also discussed in ENV 1991-1, Section 2.2. As argued there, there may be various reasons for reliability differentiation, and the choice of categories or classes may to some extent depend on particular needs. A possible unification of safety categories suited for several applications may be a task in the development of ENV 1991 into an EN.

3.3 Design Strategies

Design with respect to accidental actions may pursue one or more as appropriate of the following strategies, which may be mixed in the same building design:

- preventing the action occurring or reducing the probability and/or magnitude of the action to a reasonable level. (The limited effect of this strategy must be recognised; it depends on factors which, over the life span of the structure, are commonly outside the control of the structural design process)
- protecting the structure against the action (e.g. by traffic bollards)
- designing in such a way that neither the whole structure nor an important part thereof will collapse if a local failure (single element failure) should occur
- designing key elements, on which the structure would be particularly reliant, with special care, and in relevant cases for appropriate accidental actions
- applying prescriptive design/detailing rules which provide in normal circumstances an acceptably robust structure (e. g. tri-orthogonal tying for resistance to explosions, or minimum level of ductility of structural elements subject to impact)

Partial load factors to be applied in analysis according to strategy no. 3 are defined for buildings in [1], Table 9.2, to be 1.0 for all loads (permanent, variable and accidental) with the following qualification in 9.4.2(4): "Combinations for accidental design situations either involve an explicit accidental action A (e.g. fire or impact) or refer to a situation after an accidental event (A = 0)". After an accidental event the structure will normally not have the required strength in persistent and transient design situations and will have to be strengthened for a possible continued application. In temporary phases there may be reasons for a relaxation of the requirements e.g. by allowing wind or wave loads for shorter return periods to be applied in the analysis after an accidental event. As an example Norwegian rules for offshore structures [3] are referred to.

For prescriptive rules Part 2.7 refers to the relevant ENV 1992 to ENV 1999.

3.4 Methods of Analysis

Analysis for accidental actions may be achieved with different levels of refinement, e. g. by:

- an appropriate (dynamic, non-linear etc.) analysis of the structure for an adequate model of the accidental action
- analysis for a static equivalent load model
- without analysis, if prescriptive detailing rules are applied

The different safety categories may be considered in the following manner:

- Safety category 1: no specific consideration of accidental actions
- Safety category 2: depending on the specific circumstances of the structure in question: a simplified analysis by static equivalent load models, or by applying prescriptive design/detailing rules, or, alternatively, as for safety category 3
- Safety category 3: extensive study of accident scenarios and using dynamic analyses and non-linear analyses if appropriate

The analysis and design for accidental actions is according to ENV 1991-1 [1] based on characteristic actions and material strengths as for check of cross section strength. The adequacy of this approach for check of system failure may, however, be questioned [4,5]. Since a system failure assumes a simultaneous failure in several sections, it may be more appropriate to base the analysis on mean values of material characteristics and use a global safety factor to establish a sufficient distance between the mean global strength and the loads. Such an approach is, however, not in accordance with the present ENV 1991-1.

References

1   ENV 1991-1 EUROCODE 1: Basis of Design and Actions on Structures. Part 1: Basis of Design. CEN 1994
2   ISO DP 10252 "Accidental Actions due to Human Activities" ISO 1995.
3   Norwegian Petroleum Directorate: Regulations concerning loadbearing structures in the petroleum activities 1992.
4   Eibl, J.: Fragen zum Nachweis der Tragsicherheit bei Berücksichtigung nichtlinearer Stoffgesetze. Tagung "Sicherheit von Bauwerken - Günter Breitschaft Symposium". Eigenverlag des IfBt, Berlin, Märtz 1989.
5   Eibl, J., Schmidt-Hurtienne, B.: Grundlagen für ein neues Sicherheitskonzept. Bautechnik 72 (1995) Heft 8 pp 501-506.

Leere Seite

Blank page

Page vide

Accidental Actions: Fire
Influence of the Active Fire Protection Measures
(Annex D of ENV1991-2-2)

CAJOT L.-G.	FONTANA M.	SCHWEPPE H.	KIRCHNER U.
SCHLEICH J.B.	Civil Engineer	KINDMANN R.	Civil Engineer
Civil Engineers	ETH Zürich	Civil Engineers	Engineering Office
ProfilARBED		Univ. of Bochum	Halfkann/Heister/Kirchner
Research			
Esch/Alzette	Zürich	Bochum	Erkelenz
LUXEMBOURG	SWITZERLAND	GERMANY	GERMANY

Summary

The rule (3) of D.1 of Annex D of ENV1991-2-2 [1] defines a Fire Load reduction factor γ_n accounting for active fire protection measures. This factor γ_n is equal to 0,6 for approved fire extinguishing systems. This short definition of γ_n leading to this very rough procedure is the only reference on the Active Measures influence in the ENV1991-2-2 [1]. This points out one of the main improvements to be undertaken for ENV1991-2-2 [1].

This paper describes some existing methods considering the Active Measures (DIN18230, New-Zealand Method, Austrian Standards TRVB A126 and TRVB A100, SIA81, FRAME) and provides a summary table which should enable to improve the details given in ENV 1991-2-2 concerning the fire load reduction factor γ_n.

1. Introduction

Many methods of Fire Safety Engineering have pointed out the influence of the Active fire fighting measures:

- DIN 18230 "Baulicher Brandschutz im Industriebau" for Germany [2, 3, 4, 5]
- The Austrian Standards TRVB A126 et TRVB A100 "Brandschutztechnische Kennzahlen verschiedener Nutzungen, Lagerungen, Lagergüter" and "Brandschutzeinrichtungen rechnerischer Nachweis" [6]
- Fire Engineering Design for Structural Stability in New-Zealand [7]
- SIA 81 "Evaluation du risque d'incendie" for Switzerland [8]
- FRAME for Belgium [9]

Moreover it is obvious that people sleep safer in a hotel with smoke detectors and sprinklers with a structural fire resistance of R30 than in a R90 building without any active protection measures. Nevertheless only one sentence can be found in Annex D of ENV 1991-2-2 about this major factor.

2.   Annex D of ENV 1991-2-2 [1]

EC 1 part 2-2 [1] considers the influence of active fire protection measures by the differentiation factor γ_n in Annex D. It is used in the scope of equation (D.1) determining the design fire load q_d.

$$q_d = \gamma_q \cdot \gamma_n \cdot q_k \qquad (D.1)$$

The characteristic value of the fire load q_k has to be multiplied by the global safety factor γ_q for the accepted failure risk in connection with the expected fire occurrence probability. The multiplication with γ_n finally leads to the design fire load.

Annex D of EC 1 does not contain much information about numerical values of γ_n. Beside the advice to fix γ_n to 0,6 for approved fire extinguishing systems the Eurocode only refers to national regulations.

3.   DIN 18230 "Baulicher Brandschutz im Industriebau" [2, 4, 5]

3.1   General description of DIN 18230

In connection with the German Industriebaurichtlinie, DIN 18230 offers a calculation method to determine the requested fire resistance time of a compartment. The application of this standard which generally takes active and passive fire safety measures into account is restricted to industrial buildings with a limited floor area of 30000 m^2 [3]. Buildings which are not involved in industrial production or storage, e.g. skyscrapers, silos and power plants are excluded.

The first step in DIN 18230 is to calculate the fire load q_R by the following equation (1). It mainly depends on the combustibility of the component parts and the stored material in the compartment. Beiblatt 1 to DIN 18230 contains a summary of the combustion factor m and the calorific value H_u for commonly used materials. q_R is generally referred to the floor area A_f of the compartment.

$$q_R = \frac{\sum (M_i \cdot H_{ui} \cdot m_i \cdot \psi_i)}{A_f} \qquad (1)$$

The equivalent time t_a is calculated by the following equation:

$$t_a = q_R \cdot c \cdot w$$

The transformation factor c considers the heat transfer through the fire compartment enclosure. It is equal to the conversion factor k_b in table E.1 of EC 1 part 2-2 Annex E [1]. The numerical values differ between 0,04 $\frac{min.\,m^2}{MJ}$ and 0,07 $\frac{min.\,m^2}{MJ}$ resp. between 0.15 to

0.25 $\frac{min.\,m^2}{kWh}$ in the German code, in relation to the thermal properties of the enclosure walls, ceilings and floor.

The ventilation factor w in equation (2) considers the ventilation conditions in the compartment. For its determination DIN V 18230 (sept. 1987) [2] defines the estimated

opening area A_{v+h} which has to be calculated by adding the vertical opening area A_v to the horizontal opening area A_h multiplied by a dimensionless factor k_1 ($\Rightarrow$ DIN V 18230 (sept. 1987) [2] diagram 1).

$$A_{v+h} = A_v + k_f \cdot A_h$$

The ratio of the estimated opening area A_{v+h} to the floor area A_f of the compartment is required for table 3 of the standard leading to the ventilation factor w. This table differentiates between the position of the openings.

Openings Position	Ground Plan	Section	A_{v+h} / A_f					
			to 0.05	>0.05 to 0.10	>0.10 to 0.15	>0.15 to 0.20	>0.20 to 0.25	>0.25
Compartment with openings on only one side			3.2	2.0	1.5	1.2	1.0	0.9
Compartment with openings on at least two sides			2.2	1.5	1.0	0.9	0.7	0.6
Compartment with horizontal opening			1.8	1.2	0.9	0.7	0.6	0.5

Tab. 1: Table 3 of DIN 18230 (sept. 1987) [6] for the ventilation factor w

Finally the required fire resistance time erf t_F can be calculated:

erf $t_F = t_a \cdot \gamma \cdot \gamma_{nb}$

γ is a global safety factor which depends on the compartment size and the relevant fire safety class SK_b 1 - 3. The fire safety class corresponds to the required safety level of each component part, e.g. dividing walls and load bearing elements are generally classified into class SK_b 3 (high requirements). For instance, for a column in a multi-storey building of 2500 m^2, γ is equal to 1.25.

γ_{nb} considers the influence of active fire safety measures like sprinkler systems or work fire brigades, e.g. if an automatic sprinkler system is provided, γ_{nb} gets to 0.6.

Other values for γ_{nb} can be taken from the following table which is the translation of the table 6 of DIN V 18230 (sept. 1987) [2].

work fire brigade number of firemen	sprinkler system	no sprinkler system
0	0.6	1.0
1 team	0.55	0.9
2 teams	0.5	0.8
3 teams	0.4	0.7
4 teams	0.35	0.6

Tab. 1 : Additional factor γ_{nb} according to DIN V 18230 (sept. 1987)

After its calculation the required fire resistance time has to be related to the corresponding fire resistance class R.

$$0 < \text{erf } t_F \leq 15 \text{ min} \rightarrow \text{no fire protection}$$
$$15 < \text{erf } t_F \leq 30 \text{ min} \rightarrow \text{R 30}$$
$$30 < \text{erf } t_F \leq 60 \text{ min} \rightarrow \text{R 60}$$
$$60 < \text{erf } t_F \leq 90 \text{ min} \rightarrow \text{R 90}$$
$$90 < \text{erf } t_F \leq 120 \text{ min} \rightarrow \text{R 120}$$

DIN 18230 only determines the required fire resistance time for a compartment. The verification and the design of each component part has to be done according to DIN 4102 part 4 [10].

3.2 Draft on DIN 18230 (july 1994 and september 1995) [4, 5]

In comparison to the prestandard of 1987 the draft editions of DIN 18230 from 1994 [4] and 1995 [5] do not contain substantial differences concerning the general calculation method of the equivalent fire resistance time. The determination of the ventilation factor w has been revised. The estimated opening area A_{v+h} has been replaced by the partial factors a_w and w_0. The factor a_w takes the height of the compartment into account, while w_0 depends on the ratios of the vertical and horizontal openings to the floor area. Both factors are determined by diagrams. Finally the ventilation factor can be calculated by a simple multiplication:

$$w = w_0 . a_w$$

The values of the global safety factors have been modified slightly.

The following table contains the values of the additional factor for the influence of active fire safety measures. The symbol for this factor has been changed from γ_{nb} to a_L. The application has been enlarged to non-professional work fire brigades, detectors and manual sprinkler systems.

(1)			(2)	(3)	
work fire brigade					
number of firemen	professional	non-professional	detectors	manual fire extinguishing systems	automatic sprinkler systems
0	1.0	1.0			
1 team	0.9	0.95			
2 teams	0.8	0.85	0.9	0.85	0.6
3 teams	0.7	0.8			
4 teams	0.6	0.75			

Tab. 3: Additional factor a_L - DIN 18230 (draft july 1994) [5]

The final value of a_L is made up of a multiplication of column (1), (2) and (3).

4. Austrian standards TRVB A126 and TRVB A100 [6]

The basic concept of the Austrian standard TRVB is similar to the Swiss one used in SIA [8]. The specific fire risk B is determined according to the main equation in accordance with the

individual factors as fire load Q, fire danger C, smoke danger R etc., which are given as table values.

$$B = Q. C. R. K. P. E. H$$

The characteristic risk number SF is depending upon the fire risk B and the measures of smoke exhausting.

$$SF = (G + K_1) \cdot B/K_2$$

The presence or absence of a sprinkler system is not taken into account in the formula above. The necessary active fire protection measures according to the fire resistance duration of the structural components are determined in accordance with the characteristic risk number SF.

Hereby, the possibility of changing fire protection measures exists.

For example, for the calculated characteristic risk number SF 3.0, both following solutions are allowed, the fire resistance class R60 with a fire alarm system or unprotected steel structures with a sprinkler system (in both cases a work fire brigade has to exist).

5. New-Zealand Method [7]

The chapter "Fire Engineering Design for Structural Stability" of [7] provides the following formula:

$$S_c = c_1 \cdot c_2 \cdot c_3 \cdot c_4 \cdot \omega \cdot q_f$$

where:

S_c = calculated security rating (minutes)

c_1 = enclosure (firecell) surface thermal coefficient
= 0.067 for typical applications

c_2 = structural element ductility or compression gravity loading factor

c_3 = 1.0 for unsprinklered firecells
= 0.6 for sprinklered firecells

c_4 = ventilation configuration coefficient
= 1.0 for satisfactory ventilation configuration when $A_v > 0.03\ A_{df}$
= 1.25 for unsatisfactory ventilation configuration when $A_v > 0.03\ A_{df}$
= 1.0 for any ventilation configuration when $A_v \leq 0.03\ A_{df}$

ω = ventilation factor

q_f = design fire load energy density/m^2 floor area (FLED)

The ventilation factor, ω, is given by:

$$\omega = \frac{A_{df}}{A_{dt}(A_v\sqrt{h_v} / A_{dt.})^{0.5}}$$

where:

A_{df} = design fire area = lesser of A_f or 150 m^2

A_f = firecell floor area

A_v = ventilation area considered accessed by the fire

h_v = weighted mean height of openings A_v

A_{dt} = total surface area occupied by the area of design fire

As in ENV 1991-2-2 [1], the sprinklers are considered by multiplying the fire load by a factor 0,6. The reduction is based on a paper of Malhotra [11].

6. Fire risk evaluation according to SIA documentation 81 [8]

6.1 Description of the method

In 1960 Dipl. Ing. ETH Max Gretener, head of the Brand-Verhütungs-Dienst BVD (Swiss Fire Protection Association) in Zurich, started to study possibilities to calculate the fire risk in industrial premises and other large buildings. He developed an easy to use risk assessment method which was first published in 1965 and focused on the needs of the fire insurance companies. In 1968 it was proposed to use the method also to set the fire protection measures by the fire police.

In 1984 the Fire Risk Evaluation Method SIA Documentation 81 was published. It was derived from the work of Max Gretener. The method was completely revised by a project team consisting of members from the VKF (association of monopolistic state insurance companies) the BVD (representing also the private fire insurance companies) and the Swiss Association of Engineers and Architects SIA. This project team adapted the method to new national and international knowledge and experience. Emphasis was given to make the method easy to use by fire police, insurance people, engineers and architects.

The method is well accepted in Switzerland and even recommended in the fire regulation as a tool to evaluate and compare the fire risk of alternative concepts (trade-off between sprinkler and detection and passive fire protection).

Below a short description of the method is given:
It is a method based on a large statistical survey on fire loads and on building losses. It consists in the verification of a global fire safety factor γ_{Fire}:

$$\gamma_{Fire} = R_{accepted} / R_{calculated} \geq 1$$

It is a check to verify that the calculated risk of given compartment is smaller than the accepted risk.

$R_{accepted}$ is a function of the number and the mobility of the persons involved and of the location of the relevant fire compartment within the building.

$R_{calculated} = A \times B$ A representing the probability of occurrence of a fire
           B representing the probable amount of losses $B = P_{danger} / M_{applied}$

P_{danger} is a function of the following parameters:
* fire load density and distribution
* combustibility of the fire loads
* smoke production
* production of corrosive agents

* combustibility of the building components
* area of the compartment or building
* storey of the compartment to be checked/height of the building

$M_{applied}$ is a function of:
* basic normal measures which includes the:
  * quality and number of internal fire fighting devices such as portable fire extinguisher and internal hydrants
  * reliability and quality of water supply
  * distance to nearest hydrants
  * quality of staff instruction in case of fire
* active measures which includes the:
  * type of fire detection devices and measures
  * reliability and rapidity of alarm transmission
  * reliability, rapidity and quality of fire brigades
  * type of fire suppression devices
  * presence of smoke and heat extraction devices
* passive, structural measures which includes the:
  * level of structural fire resistance
  * the type of the facade used as a barrier against the spread of fire
  * the fire resistance level of compartmentation
  * the ventilation characteristics of the fire compartment

With regard to questions of validity, the Swiss Fire Risk Assessment method has the advantage of not just claiming to have a purely scientifical background, but to be an empiricalistic procedure tested by a wide practical application. However it is based on a large background statistical data, and a scientific validation for this method could certainly be developed if needed.

6.2   Influence of active measures

The SIA-method grades the influence of active measures on the global fire risk. With regard to sprinklers the following parameters are taken into account:

- detection   (sprinklers activate an alarm bell if water is flowing through the main valve)

- alarm transmission   (the sprinkler alarm is often - in Switzerland mandatory - connected directly to the fire brigade)

- suppression function   (water discharge on fire)

The method proposes the following risk reduction factors:

- detection (parameter S_{13})   : $S_{13} = 1.20$
- alarm transmission by specially protected telephone lines (parameter S_{24}) : $S_{24} = 1.20$
- suppression function   : $S_{51} = 1.7$

or for annually checked sprinkler system designed according to
regulations (*) $: S_{51} = 2.0$ (*)

The global risk reduction factor $\gamma_n = 1/(\Sigma s_i)$ is found to be:

- Sprinkler without automatic alarm to fire brigade:

$$\gamma_{n1} = \frac{1}{S_{13} \cdot S_{51}} = 0.49 \text{ (or 0,42 see*)}$$

- Sprinkler with automatic alarm to fire brigade:

$$\gamma_{n2} = \frac{1}{S_{13} \cdot S_{24} \cdot S_{51}} = 0.41 \text{ (or 0,35 see*)}$$

These values are lower than the value for the reduction of the design fire load in Annex D of ENV1991-2-2 [1]. $\gamma_n = [0.6]$.

While Annex D mainly considers the suppression function (reduction of fire load), the SIA method also considers alarm and alarm transmission (e.g. earlier evacuation and fire brigade action). This may explain the better rating of sprinkler systems within the SIA method. This better rating is supported by the insurance companies who apply premium reductions up to 60 % and more for sprinkler systems. This could lead to the assumption that their risk assessment systems also come to the conclusion of a risk reduction of roughly 60 % e.g. $\gamma_n = (1-0.6) = 0.4$.

7.   Method FRAME [9]

The method FRAME for Fire Risk Assessment Method for Engineering is based on the Swiss SIA 81 made by Mr. E. De Smet and published by ANPI (Association Nationale pour la Protection Incendie) in Belgium. This method enables one to calculate two risks in case of fire, the risk for the contents and the risk for the people.

In the case of the risk of the contents, the sprinklers have an influence on the detection and on the fire extinction.
The risk reduction factor is 1,22 for the detection which can be considered only if there is a connection to the fire brigade. Concerning the fire suppression function, the risk is again reduced by a factor equal to 1,71 for sprinklers without independent water source, to 1,98 for sprinklers with one independent water source and to 2,65 for sprinklers with two independent water sources. This last case leads to a value of γ_n equal to $1/(2,65 \cdot 1.22) = 0,31$.

In the case of the risk for the people, the fire risk reduction factor is the same for the detection. But the sprinklers also play a part in the protection of the evacuation. The reduction factor is 1,27 if there are sprinklers only in high risk areas and is equal to 1,63 if there are sprinklers in the whole building.

8. Fire Safety Engineering taking into account the active fire fighting measures - Practical Example

A practical example came with the realization of the ARBED OFFICE BUILDING in Esch-sur-Alzette, Luxembourg. This new construction was erected between 1991 and 1993, is composed of two wings with nine levels and a total volume of 61 m³ [12,13,14,15].

The Fire Engineering Design has used the new structural fire design standards of CEN by performing a global structural analysis on the entire steel structure, considering the combination rules for actions during fire and applying the estimated natural fire evolution according to the specific features of this building.

When it came to the natural fire evolution a first evaluation of the natural temperature-time curve was based on real fire loads existing in offices (900 MJ/m²) and common areas (650 MJ/m²) (i.e. 53 kg and 38 kg of wood respectively per m² of floor area), on ventilation conditions and on the size of the fire compartment. This produced a natural fire curve with a maximum temperature of 800°c at 20 minutes.

Due to the large size of the compartment because of the atrium connecting levels, the decision was taken to install a sprinkler system. Which meant, refering to Annex D of ENV 1991-2-2 [1], it was reasonable and on the safe side compared to the other standards to adopt a fire load density reduced for design by 40% . This lead to a natural fire with a maximum air temperature of only 400°C (figure 1).

Due to a possible problem in the water supply and delay in the intervention of the fire brigade, it was supposed that this natural fire would spread onto two consecutive levels over a total floor area of 300 m² (figure 2).

This fire scenario was applied to the entire structure and the numerical calculation by CEFICOSS proved that widely unprotected steel structure will not fail (Figure 3 shows the global deformations after 30 minutes).

The reason for this remarkable conclusion is the global frame behaviour, which could be activated by strong beam connections able to transmit bending moments and the natural fire which, if it occurs, is assumed to be softened by a complete set of active fire safety and fire fighting measures (figure 4)

The influence of this complete set of active fire measures should be defined more in details in ENV 1991-2-2 and can surely not by summarized by the single value 0,6 for the γ_n as it is now the case. An ECSC research [16] is now working on this topic and should offer the possibility to improve the ENV 1991-2-2 in the future.

9. Conclusion

The following table enables one to compare the Annex D of ENV 1991-2-2 [1] to the other methods.

Method	Sprinkler effect (Detection and extinction): γ_n
ENV 1991-2-2 [1]	0,6
DIN 18230 [2, 3, 4, 5]	0,54 (= 0,6 x 0,9)
New Zealand [7]	0,6
SIA 81 [8]	0,35 to 0,49
FRAME [9]	0,31 to 0,48
Insurance Companies	Premium reduction: Initial premium multiplied by up to 0,4

The value 0,6 of γ_n in Annex D of ENV 1991-2-2 appears very high and should be divided into sub-coefficients taking into account the sprinkler types, the water supply, the detection and the communication of the alarm to the fire brigade.

10. Bibliography

[1] ENV 1991-2-2 "Eurocode 1: Basis of design and actions on structures - Part 2-2: Actions on structures exposed to fire", 9.2.1995

[2] DIN V 18230 - Baulicher Brandschutz im Industriebau - Teil 1 - Rechnerisch erforderliche Feuerwiderstandsdauer - September 1987

[3] Richtlinie über den baulichen Brandschutz im Industriebau (Industriebaurichtlinie-IndBauR), Ministerialblatt für das Land Nordrhein-Westfalen, Nr.74, 5.12.1989.

[4] Entwurf DIN 18230 - Baulicher Brandschutz im Industriebau - Teil 1 - Rechnerisch erforderliche Feuerwiderstandsdauer - Juli 1994

[5] Entwurf DIN 18230 - Baulicher Brandschutz im Industriebau - Teil 1 - Rechnerisch erforderliche Feuerwiderstandsdauer - September 1995

[6] TECHNISCHE RICHTLINIEN VORBEUGENDER BRANDSCHUTZ, TRVB A 100 87 and TRVB A 126, Österreichischer Bundesfeuerwehrverband, Ausgabe 1987

[7] "New Zealand Structural Steelwork Limit State Design Guides" Volume 1, HERA report R4-74(I), R4-80, Clifton, Manukau City, May 1993 and July 1994.

[8] "Evaluation du Risque d'Incendie"; Méthode de Calcul, Société Suisse des Ingénieurs et des Architectes, documentation N° 81, 1984

[9] E. DE SMET, "Evaluation des Risques", ISSN 0772-7267, ANPI, octobre 1988.

[10] DIN 4102 -Brandverhalten von Baustoffen und Bauteilen Teil 4 - Zusammenstellung und Anwendung klassifizierter Baustoffe, Bauteile und Sonderbauteile, März 1994.

[11] Malhotra H.L.; Trade-Offs and Fire Safety; Fire Prevention Journal, No. 240, 1991.

[12] Bruognolo, B. and Matthes, G.: Die neue Hauptverwaltung der ProfilARBED in Esch-sur-Alzette (Luxembourg). OFFICE DESIGN 1/94, Baden-Baden, 1994

[13] Schleich, J.B.: Stahlbauarchitektur und Brandschutz; Oesterreichischer Stahlbautag, Linz, November 1993. Stahlbau Rundschau, Wien, April 1994

[14] Schleich, J.B.: Brandschutz im Stahlbau. BAUMEISTER, Sonderheft, Oktober 1995

[15] Schleich, J.B.: Bauen mit Stahl- Neue Brandschutzkonzepte. Deutsches Architektenblatt 6/94, Stuttgart, Juni 1994

[16] J.B. Schleich, L.G. Cajot, M. Pierre, CEC Agreement 7210-SA/125, 126, 213, 214, 323, 423, 522, 623, 839, 937 "Competitive Steel Buildings Through Natural Fire Safety Concept" Technical Reports n°1 and n°2, 1994 - 98.
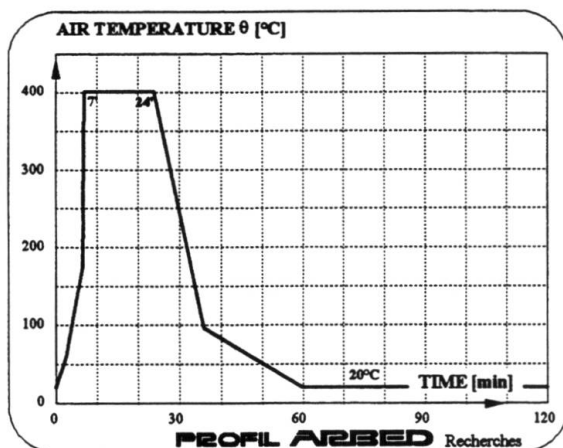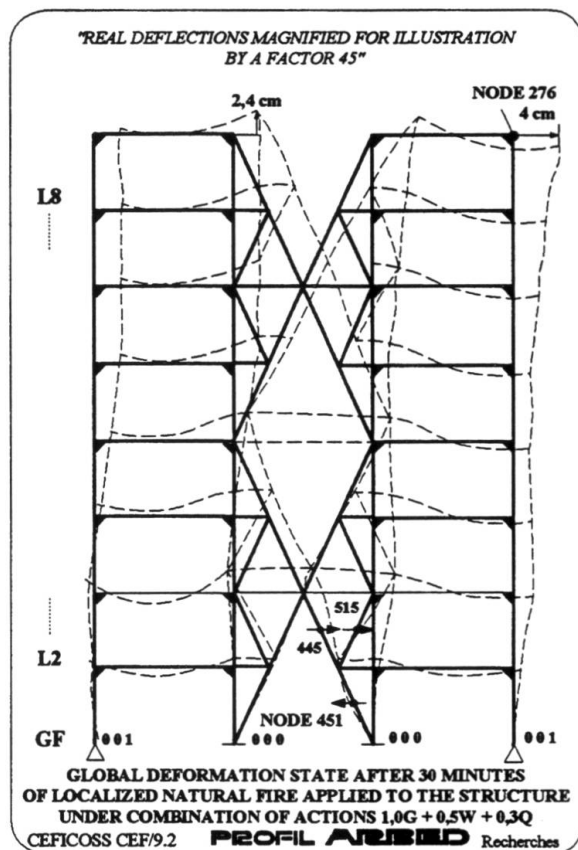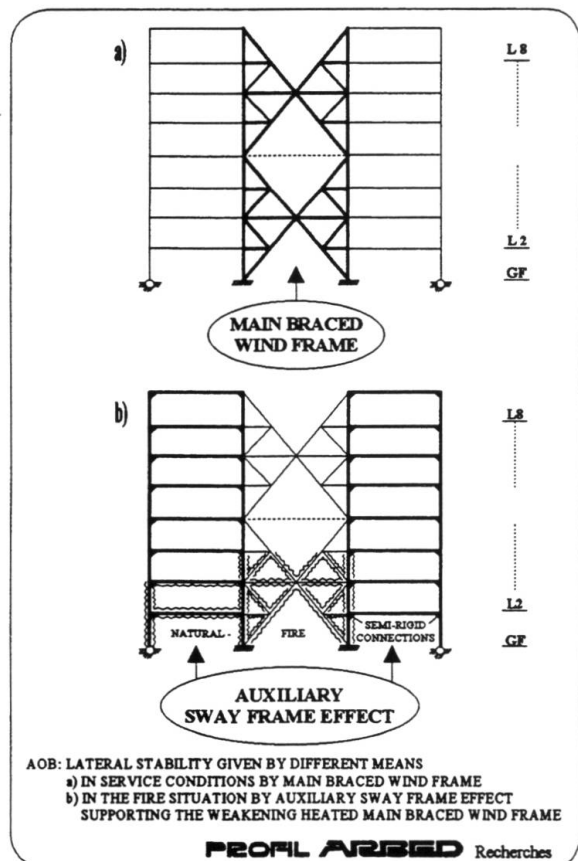
Figure 1

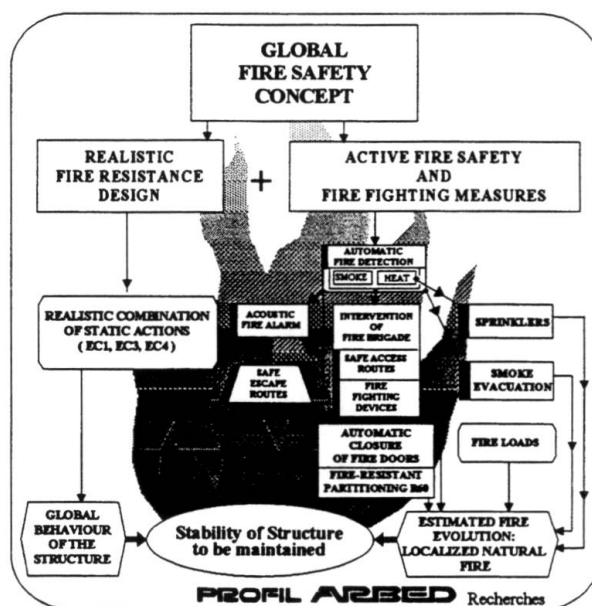GLOBAL DEFORMATION STATE AFTER 30 MINUTES
OF LOCALIZED NATURAL FIRE APPLIED TO THE STRUCTURE
UNDER COMBINATION OF ACTIONS 1,0G + 0,5W + 0,3Q
CEFICOSS CEF/9.2

Figure 3

AOB: LATERAL STABILITY GIVEN BY DIFFERENT MEANS
a) IN SERVICE CONDITIONS BY MAIN BRACED WIND FRAME
b) IN THE FIRE SITUATION BY AUXILIARY SWAY FRAME EFFECT
SUPPORTING THE WEAKENING HEATED MAIN BRACED WIND FRAME

Figure 2

Figure 4

Leere Seite

Blank page

Page vide

Input data for the natural fire design of building structures

TWILT, Leen
VAN DE LEUR, Peter
TNO Bouw
Delft
The Netherlands

CAJOT, Luis-Guy
SCHLEICH, Jean-Batist
Profil ARBED Research
Esch/Alzette
Luxembourg

JOYEUX, Daniel
KRUPPA, Joël
CTICM
Paris
France

1. INTRODUCTION

Traditionally, structural fire safety design is based on conventionally rather than on physically based thermal actions. This certainly holds for the international standards in the field, see e.g. [1]. Therefore, the release of Eurocode 1, part 2-2: "Actions on structures exposed to fire" [2], should be seen as a turning point: for the first time in international standardization, the natural fire concept is presented as an - for the time being -informative option. This option opens the possibility for a more nuanced and functionally based design, enabling to achieve rational and uniform fire safety levels.

It should be noted however that the Eurocode approach is a first and still incomplete attempt to arrive at more physically based thermal actions. Hence, the aim of this paper is:
- to identify the input data, necessary for a natural fire design;
- to critically discuss the input data, required by EC1, part 2-2;
- to demonstrate the potential of the natural fire design.

2. THE VARIOUS FIRE MODELS AND NECESSARY INPUT DATA

In order of increasing level of complexity, the following models are distinguished:

- Nominal Fire Curves
These are fire models in which the gas temperature time relationships are set by convention, i.e. no physical parameters are taken into account. In some models of this kind, the fire duration is related to the fire load density. Differentiation with respect to the type of combustible materials (e.g. cellulosic vs. hydrocarbon based curves).

- One Zone Models
In One Zone Models, the temperature in the fire compartment is assumed to be uniformly distributed. Gas temperature development is calculated by solving the heat and mass balance for the system consisting of the fire compartment (= fire zone) with its boundary structure including ventilation openings. Input data are the amount of combustible materials (representative for the total available heat of combustion), the ventilation conditions (representative

for the rate of heat release) and the thermal inertia of structural elements bounding the fire compartment (representative for the convective heat losses to the environment).

- Multi Zone Models

These models are used when the fire is localized, e.g. in the growth phase of a fire. The fire compartment is divided into a hot zone, with a uniform temperature, above a fresh air zone and a fire plume which feeds the hot zone just above the fire. For each of the zones, the heat and mass balance is solved. (Semi-) empirical relations govern plume entrainment, radiative heat exchange between zones and mass flow through openings to adjoining compartments. Besides the input data necessary for one zone models, the (growth of the) fire size should be known. Only some of the available models can handle oxygen-starved conditions.

- C(omputational) F(luid) D(ynamics) Models

CFD models are based on two- or three-dimensional heat and mass transport, solving the equations of conservation of mass, momentum and energy for discrete points in the enclosed compartment and are, therefore, commonly referred to as "field models". Input data as for the multi zone models, however a more nuanced approach is viable. E.g., material properties and boundary conditions may be defined as function of the temperature, if necessary.

3.   INPUT DATA REQUIRED BY EUROCODE 1, PART 2-2

Of the various fire models reviewed in the above section, only the Nominal Temperature-Time Curves and the One Zone Models are recognized in Eurocode 1, part 2-2.

Three types of Nominal Fire Curves are specified: the ISO standard curve, the hydrocarbon curve and a curve representative for external fire exposure. See Fig. 1. None of these curves require physical input data.
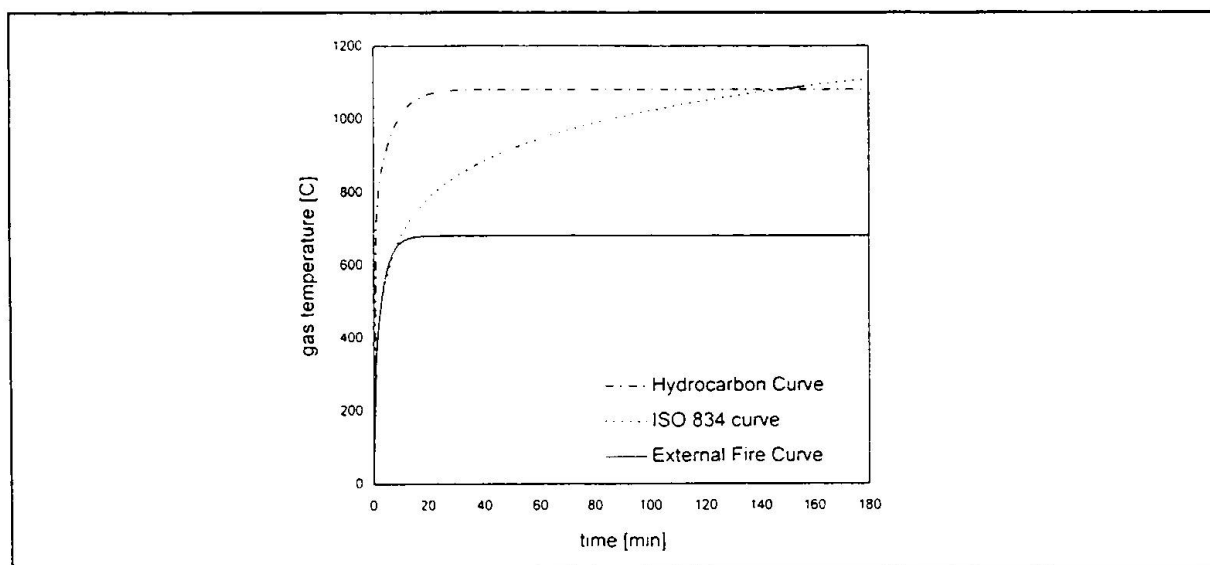
Fig. 1: Nominal fire curves.

As an alternative to nominal fire curves, thermal actions for internal members may be based on a One Zone Model ("Parametric Fire Exposure"). See Fig. 2. This requires the following input data:

- the total amount of combustion energy per unit of floor area, represented by the fire load density (see section 4);
- the so-called opening factor, representative for the rate of heat release (see section 5) and the heat loss through the ventilation flow (see section 6);
- the thermal inertia of the boundary enclosure, representative for the convective heat losses through the solid boundaries (see section 6).
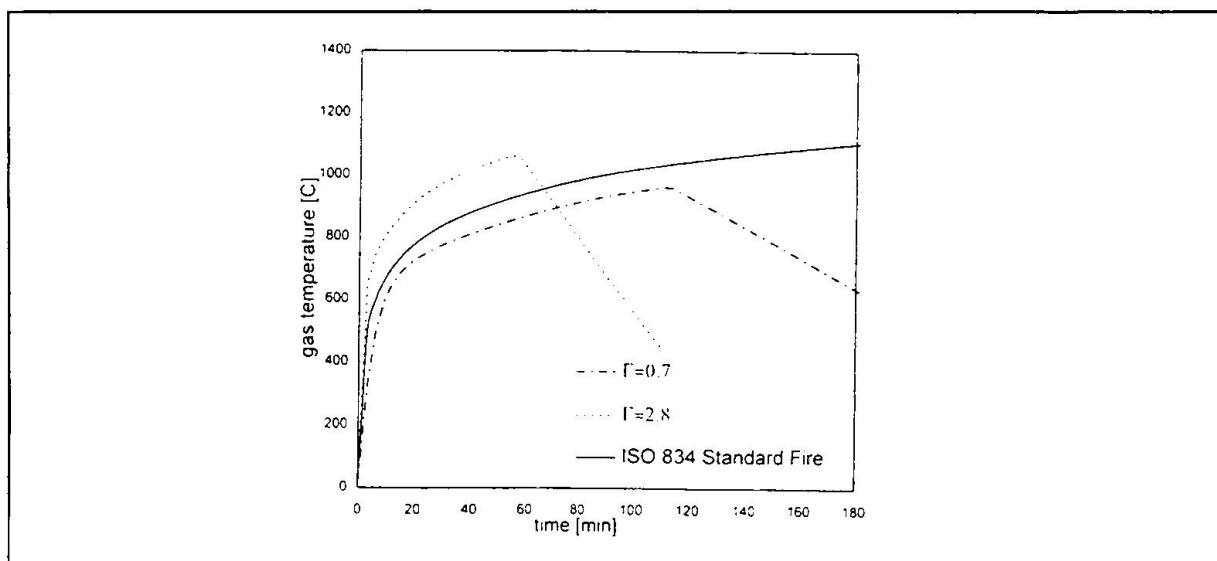
Fig. 2: Parametric fire curves

The thermal actions for external members may, alternatively, be based on an external fire exposure model in which size and temperature distribution of the flames from the openings of the fire compartment are determined. In essence the underlying fire model is a One Zone Model. In principle similar input data as for the Parametric Fire Exposure play a role, complemented with some geometrical parameters . However, especially the rate of heat release is treated in a somewhat different manner. See section 5.

4.   FIRE LOAD DENSITY

The fire load Q in a fire compartment is defined by the total energy liable to be released. Building components such as wall and ceiling linings, and building contents, such as furniture constitute the fire load. Divided by a reference area (generally the floor area), the fire load Q gives the fire load density q_f. The fire load density is the source of the fire development and is also the production-source term in the heat balance equation solved by calculation models.

In the EC 1, the characteristic fire load density is defined by the following equation:

$$q_f = \frac{1}{A_f} \sum_i \psi_i \, m_i \, H_{ui} \, M_i \qquad\qquad (1)$$

where: M_i =   the mass of the material i (kg)
   H_{ui} =   the net calorific value of the material i (MJ/kg)
   m_i =   the factor describing the combustion behaviour of the material i
   ψ_i =   the factor of assessing protected fire load of the material
   A_f =   the floor area of the fire compartment

$M_i H_{ui}$ represents the total amount of energy contained in material and released assuming a complete combustion.

The 'm' factor is a non-dimensional factor between 0 and 1, representing the combustion efficiency: m = 1 corresponds to complete combustion and m = 0 to the extreme situation in which a combustible material contributes no heat at all to the fire process. The m-factor is a function of the type of fuel (solids, liquids) and its geometrical properties (porosity, massivity), its position in the fire compartment (exposed area to radiation) and the fire characteristics (temperature, oxygen content, etc.). So far, no international agreement exists on the way to determine the m-factor. Apparently, the m-factor may be assumed conservatively as m = 1.

The ψ-factor in equation (1) is introduced to take into account protection of the fire load, for example by putting it inside a cabinet. It has a value between 0 (complete protection for the full fire duration) and 1 (the protection has no influence on the energy release). The protection may reduce the energy release, but often does so for a limited period of time, which depends on the fire conditions (radiation, temperature). This is not reflected in the present concept of the ψ-factor which is time independent. For many practical applications, $\psi = 1.0$ is a realistic value.

According to EC 1, the fire load density may be determined from a national fire load classification system, or - for an individual project - by performing a fire load survey. The classification on the basis of the occupancy of the fire compartment calls for a statistical approach. A summary of statistics available in Europe is well represented in a CIB/W14 workshop report [3]. Operational guidance on application for non specialists is however lacking. This should be provided for the next version of EC 1.

The EC option for a specific study of the fire load may be extended to give a general procedure as follows:
- The net calorific value of numerous materials is known. A limited overwiew is presented in EC 1, part 2-2. If necessary, H_{ui} can be determined on basis of a generally accepted test method (calorific bomb, ISO 1716).
- In addition, the m-factor should be known. As mentioned earlier however, an internationally accepted test method is not available. A concept of such a method is under development within the scope of ECCS project "Natural Fire Safety Concept" (NFSC). Basic ideas behind that work are, that the conditions under which the m-factor is determined should follow real fire conditions closely, and that modern measuring techniques should be applied. Until such a method is available, a conventional value for the m-factor of 0.7 is proposed.

- The fire model of Annex C determines whether the fire is fuel or ventilation controlled, and then uses the appropriate relationship to calculate the RHR.

$$R = \min \left(\frac{L}{\tau_F} \; ; \; 0.18 \; (1-e^{-0.036 \cdot \eta}) \; A_w\sqrt{h.W/D}\right) \qquad (2)$$

where:
R	=	rate of burning (kg of wood/s)
L	=	fire load ($=A_F.Q$) (kg of wood)
τ_F	=	free burning fire duration (assumed to be 1200 s)
A_w	=	sum of window area on all walls ($A_w = \sum_i A_{wi}$) (m^2)
h	=	weighted average of window height on all walls ($h = \sum_i A_i h_i / A_w$) (m)
W	=	width of wall containing window(s) (m)
D	=	depth of fire compartment (m)
η	=	$A_T/A_w\sqrt{h}$ (m$^{-1/2}$)
A_T	=	all surfaces minus windows (m^2)

The first term in equation (2) relates to fuel controlled fires and the second to ventilation controlled fires. The expression for fuel control is only approximate as it assumes that all fuel controlled fires have a duration of twenty minutes.

For the ventilation controlled regime, various sets of equations exist for the RHR but the differences are small. This can be seen in graphical form in Fig. 4, which compares expressions for RHR from different sources with experimental data [4,5].
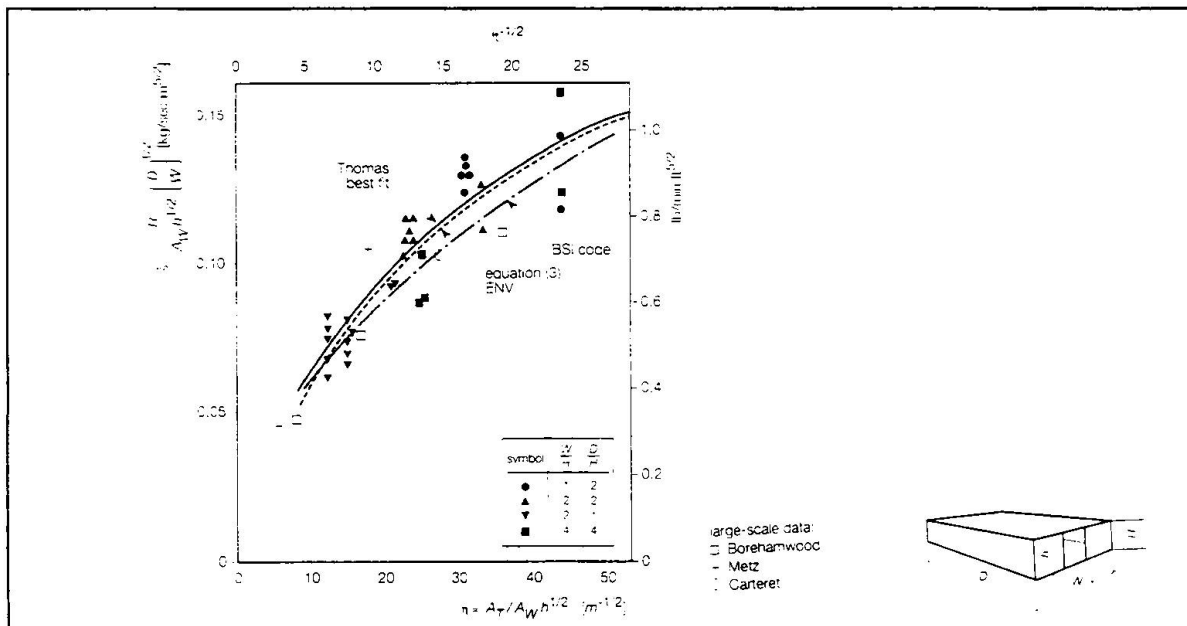
Fig. 4: Rate of heat release, ventilation controlled fires.

Pre-flashover fires are not dealt with in the Eurocode, but they are important in egress analysis and in the design of heat and smoke extraction systems. They will also gain relevance for structural fire safety when the concept of localised fire is accepted. For pre-

- The Eurocode parametric fire models use $\sum_i \psi_i \, m_i \, H_{ui} \, M_i$ but more advanced models use the rate of heat release directly (see next section).

5.   RATE OF HEAT RELEASE AND VENTILATION CONDITIONS

An essential parameter in a fire is the rate of heat release (RHR). It is the source of the gas temperature rise, and the driving force behind the spreading of gas and smoke.

A typical fire starts small and goes through a growth phase. Two things can then happen: either during the growth process there is always enough oxygen to sustain combustion. In that case, when the fire size reaches a maximum, the RHR is limited by the available fire load (fuel controlled fire). Or, the size of openings in the compartment enclosure is too small to allow enough air to enter the compartment. Then, the RHR is limited by the available oxygen and the fire is said to be ventilation controlled. Both ventilation and fuel controlled fires can go through flashover. This important phenomenon marks the transition from a localised fire to a fire involving all the exposed combustible surfaces in the compartment.

The two regimes are illustrated in Fig. 3, which presents graphs of the rate of burning (kg/s) vs. the ventilation parameter $A\sqrt{h}$, with A being the opening area and h being the opening height. Graphs are shown for different fire load densities. Starting on the left side of the figure in the ventilation controlled regime, with increasing ventilation parameter the rate of burning grows up to the limiting value determined by the fire load density and then remains approximately constant (fuel controlled region).
The models described in the annexes to EC 1 treat the RHR in different ways.

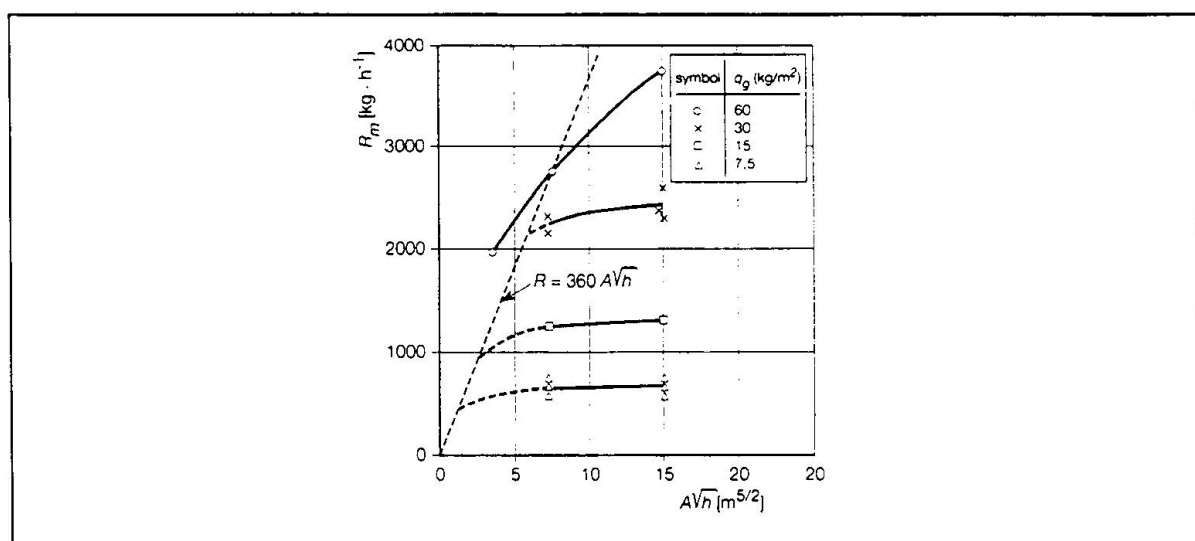| symbol	q_g (kg/m²)
○	60
×	30
□	15
△	7.5

$R = 360\, A\sqrt{h}$

Fig. 3: Rate of heat release for different ventilation regimes.

- The parametric fires of Annex B do not deal with the RHR explicitly. Implicit in the model however, a ventilation controlled post-flashover fire is assumed and the RHR is calculated proportional to $A\sqrt{h}$.

flashover fires one method of calculating the RHR uses conventional or calculated values of the RHR per unit area, and estimates the rate of fire spread (i.e. the rate of growth of the area involved in fire) to calculate RHR as a function of time. In other cases it may be acceptable to simply assume a fixed area involved in fire and find a corresponding value for the rate of heat release. In all cases the RHR per unit floor surface must be available. A British draft standard [6] only states two values as a guideline, depending on the building occupancy:

Building use is "retail"   : 0.5 MW/m^2
Building use is "offices"   : 0.25 MW/m^2

The Belgian standard for the design of heat and smoke venting systems [7] contains tables with values of the RHR density for specified combustibles in storage halls. As default values to be used when the exact nature of the combustible is unknown, 0.5 and 0.25 MW/m^2 are mentioned for mechanical and natural ventilation respectively.

6. HEAT LOSSES

The heat losses suffered by the combustion gases are important factors to the temperature development of a compartment fire. Heat losses occur to the compartment boundaries by convection and radiation. A substantial amount of heat can also be removed from the compartment by the ventilation flow. This last contribution to the heat loss is quite easy to model. In this paper, attention will be focused on the heat losses to the compartment boundaries.

It has long been known that the heat losses to the compartment boundaries can play a decisive part in determining whether a given fire will develop to flash over or not. This is why even the simpler approaches to fire modelling take this aspect into account.
The most popular way to do that is through the concept of the "thermal inertia" b of the wall material. This factor is defined for a homogeneous wall construction by:

$$b = \sqrt{\lambda \cdot \rho \cdot c} \tag{3}$$

where: λ =   heat conductivity (W/mK)
        ρ =   mass density (kg/m^3)
        c   =   heat capacity (J/kgK)

It can be shown that under certain conditions (among others, "thermally thick" wall, constant surface temperature) the heat flux into the wall depends on b only.

The parametric fire models in the Eurocode have b as the single parameter to account for the convective heat losses. For the important case of walls consisting of multiple layers of different materials, an effective value of b is calculated from the contributions of the different layers, according to:

$$b = \sqrt{\sum s_i \cdot c_i \cdot \lambda_i \Big/ \sum \frac{s_i \cdot c_i \cdot \lambda_i}{b_i^2}} \tag{4}$$

where: λ_i =   heat conductivity of material i (W/mK)

                  s_i =   thickness of material i (m)

                  c_i =   heat capacity of material i (J/kgK)

                  b_i =   b-factor of material i $(J/m^2 s^{1/2} K)$

The expression has some obvious shortcomings:

- The sequence of the different materials is not accounted for; a brick wall insulated with wood panels gives the same result as a wood panel 'insulated' with a brick wall.
- In extreme but practical cases, the expression leads to an unrealistic value for b. Consider a wall consisting of two layers of different materials. If the first layer (heated side) is thermally thick, the other layer will have no influence on the heat flux through the surface (example: well insulated brick). The effective b should be equal to b_1. On the other side, if the first layer is thermally very thin, the effective b should be equal to b_2 (e.g. thin steel sheet covering an insulating layer). The weighing procedure in the expression does not follow these relationships.

To illustrate the consequences of the use of the b-factor, in Fig. 5 the temperature development in a fire compartment (Γ-fires), calculated by means of EC1 for different b-factors, is compared with the results of calculations based on a rigorous treatment of the 1-dimensional heat conduction equation. For the boundary construction of the fire compartment - floor area 5 x 5 m^2 - various practical sandwich constructions have been chosen. Conclusion is that use of the EC1 rule for calculating effective b-factors is not recommended. Work is currently under progress to establish an alternative 'rule of thumb' to calculate the effective b-factor. For the time being, as a first (safe) approach it is proposed to take the smallest b-factor of the materials in the sandwich construction as the effective b-factor.
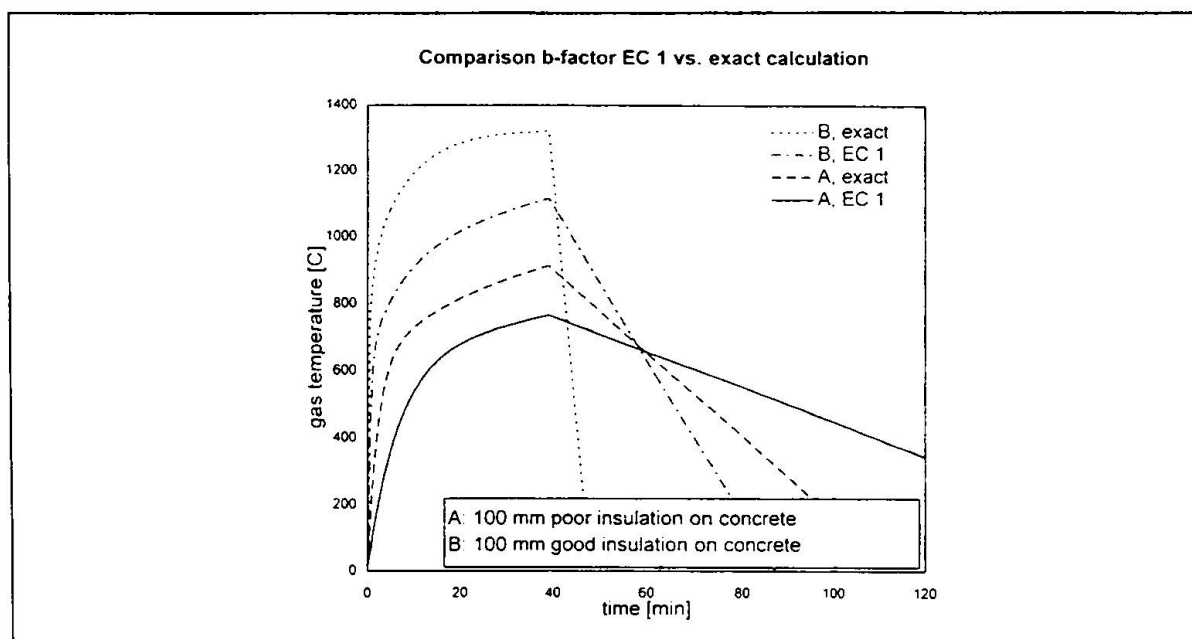

Fig. 5:   Parametric fire curves: comparison of calculation methods of the thermal inertia of the boundary construction.

7.   PRACTICAL EXAMPLES

7.1   Fires in open car parks

As a basis for the theoretical simulation of the effect of fires in open car parks, tests have been carried out in the scope of the ECSC-project "Fire Safety in Open Car Parks" [8,9]. During these tests, the rate of heat release was measured and the following "Car Fire Model" was deduced. See also Fig. 6.

During the tests flames emerged from the car mainly through the windscreen and the rear window. The hot gases in the flames move upwards due to the buoyancy. This buoyant flow is referred to as " fire plume". Two plumes are distinguished, referred to as the "front fire plume" and the "rear fire plume". The axis of these fire plumes are assumed to be 2 m apart corresponding to the dimensions of ordinary passenger cars. The rate of heat release as function of time of both the front and the rear fire plume was deduced for the measured RHR. Time integration over the RHR curves gives the total energy release (= 4.0 GJ).
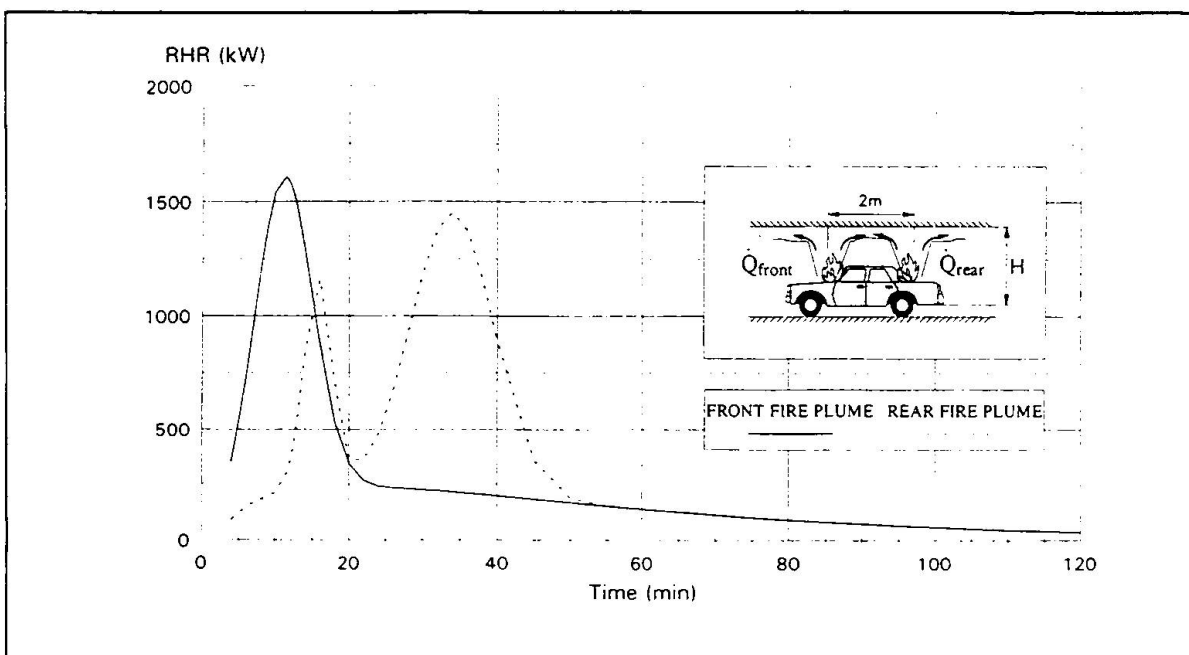
Fig. 6: Car fire model used for Open Car Parks.

The above "car fire model" was fed into a CFD model which allowed to obtain the gas temperature field. The temperatures inside the sections and the structural behaviour during the fire were analysed using advanced thermal and mechanical response models (CEFICOSS, TASEF and SISMEF). The numerical simulations have shown that composite steel concrete beams can safely be used, without any fire protection on the structural steelwork.

7.2   Fires in large compartments

In 1994 a series of two full scale fire tests have been performed in a large exhibition hall (dimensions 144 x 65 x 28 m) at the "Parc des Expositions de la Porte de Versailles", Paris

[10]. The fire load, consisting of appr. 3,500 kg wood in the form of pallets, was concentrated on a surface of 5 x 6 m^2. During one of the tests the rate of heat release was assessed by monitoring the mass loss during the fire. Also, radiative flux in the vicinity of the fire and both gas temperatures and steel temperatures at various spots in the load bearing structure have been measured. The fires were extinguished after approximately 20 minutes.

The tests allowed to evaluate the application of multi-zone models for localized fires in extremely large halls. Refer to Fig. 7 for a comparison between test results and calculation results. The agreement is satisfactory.
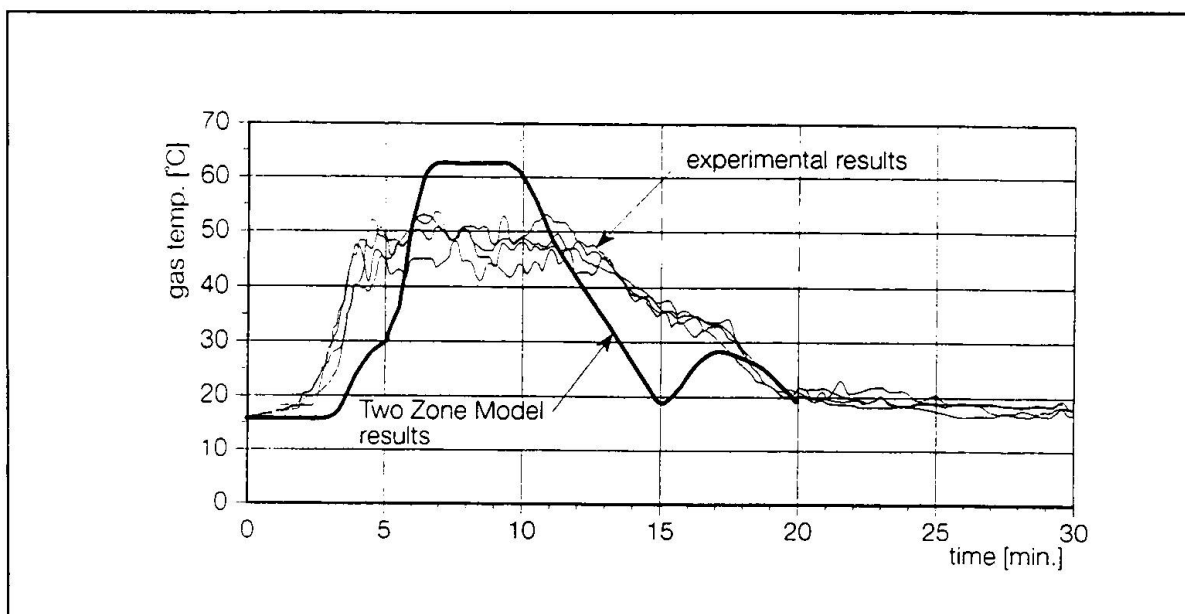
Fig. 7: Localised fire in a large compartment: comparison between test and multi zone calculation results.

8.   CONCLUSIONS

The increase of knowledge within the last decade allows performance-based codes for structural fire design. This will lead to design assumptions beyond the conventional ISO-fire approach, explicitly taking into account more realistic fire conditions.

A first step ahead is the Eurocode 1, part 2.2 which has been agreed as ENV in 1994. However, in view of the lack of operational data and the references made to national guidelines, the rules given in this first version of the document are not fully adequate.

As explained in this paper, substantial efforts are still necessary to introduce more complete and operational rules in the next version of Eurocode 1, part 2-2. This next version is expected by the middle of the year 2000.

Within the ECCS project "Natural Fire Safety Concept", efforts are under way to contribute to this goal.

9. BIBLIOGRAPHY

[1]   ISO TC 92: "Fire Resistance Tests - Elements of Building Construction".
        International Standard ISO 834, 1st edition, 1975.

[2]   Eurocode1, part 2-2: "Basis of design and actions on structures: Actions on
        structures exposed to fire". ENV 1991-2-2, November, 1994.

[3]   CIB W14: "Design Guide for Structural Fire Safety". Fire Safety Journal, vol. 10
        (2), 1986.

[4]   Thomas, P.H.: "Fires in Model Rooms"; CIB research programmes, Building
        Research Establishment current paper CP 32/74, BRE, Borehamwood, 1974.

[5]   Law, M.: "Fire Safety of External Building Elements - The Design Approach";
        AISC Engineering Journal, 2nd Quarter/1978, p. 59-74.

[6]   BSI: "Draft code of practice for the application of fire safety engineering principles
        to fire safety in buildings". Bsi 94/340340 DC, (draft for public comment), June
        1994.

[7]   Belgian Normalization Institute: "Protection incendie dans les batiments-Conception
        et calcul des installations d'évacuation de fumées et de chaleur-Partie 1: Grands
        espaces intérieurs non cloisonnés s'étendant sur un niveau". Belgian Standard NBN
        S21-208, 1st edition, August 1993.

[8]   ECCS - Technical Committee 3 - Fire Safety of Steel Structures: "Fire Safety in
        Open Car Parks-Modern Fire Engineering". Technical Note N°75, first edition,
        1993.

[9]   Mangs, J. and Keski-Rahkonen, O.: "Characterization of the fire behaviour of a
        burning passenger car. Part I : Car fire experiments". Fire Safety Journal, vol. 23,
        (1994), p. 17-35.

[10]   Joyeux , D:"Simulation of Tests in 'Parc des Expositions'". CTICM- report no.
        INC 95/34-DJ/IM, February 1995.

Leere Seite

Blank page

Page vide

Accidental Actions : Fire.
Connection between
Parametric temperature-time curves and Equivalent time of fire exposure
(Annexes B and E of ENV 1991-2-2).

Dr. FRANSSEN J-M.   CAJOT L-G.   SCHWEPPE H.
CADORIN J-F.   SCHLEICH J-B.   Prof. Dr. KINDMANN R.
Civil Engineer   Civil Engineer   Civil Engineer
Univ. of Liege   ARBED   Univ. of Bochum
Liege, Belgium   Esch, Luxemburg   Bochum, Germany

SUMMARY

The concept of parametric temperature-time curves presented in Annex B of Eurocode 1 : part 2-2. [1] and the concept of equivalent time of fire exposure presented in Annex E of the same document are briefly described. A nomogram is presented as a graphic help for the application of each method. Starting from a reference compartment, some parameters are modified and the two methods are applied. Via the calculation of maximum temperatures in 3 structures, it is possible to compare the two methods with regard to their severity.

1.   Introduction

Beyond the application of the nominal ISO temperature-time curve, Eurocode 1 proposes 2 different methods which consider more realistically the influence of some parameters on the severity of the fire such as the fire load, the geometry of the compartment and the nature of the surrounding walls. One method, proposed in Annex B, leads to parametric temperature-time curves for the air in the compartment and the other one, proposed in Annex E, leads to an equivalent time of exposure to the ISO fire supposed to have the same severity as a real fire in the compartment.

For practical situations, the designer or the authority will face the choice between one of the two methods and no indication is given in [1] concerning the correlation between them, except some limitations for the applicability of the methods. For situation where both methods are applicable, will they lead to the same "severity" ? If not, is one of the methods systematically more severe? How are different parameters taken into account in the methods?

To give some answers to those questions, a parametrical study has been undertaken on a reference case. Both methods have been applied under the same conditions and the severity of the fire has been defined as the maximum temperature obtained in a structure submitted either to the temperature-time curve given by Annex B, or to the ISO fire during the equivalent time given by Annex E.

2.   Annex B of ENV 1991-2-2: Natural Fire Curve

2.1   Introduction

This Annex is based on a paper of U. Wickström [1]. In case of a compartment with $O = 0,04\text{m}^{1/2}$ and $b = 1160\text{J}/(\text{m}^2\text{s}^{1/2}\text{K})$, the parametric curve is almost exactly the ISO curve. The nomogram explained hereafter has been developed to make easier the use of this Annex

2.2   Nomogram of Parametric temperature time curves (Annex B of ENV 1991-2-2)

The first step in finding the time dependent progress of temperature is to calculate the opening factor, $O[\text{m}^{1/2}]$, found on the upper x axis. This is done by solving the following definition:

$$O = \left[A_v \frac{\sqrt{h}}{A_t}\right]$$

$A_v=$ area of vertical openings (m^2)

$h =$ height of vertical openings (m)

$A_t =$ total area of enclosure, walls, ceiling and floor   (1)
(including openings) (m^2)

limits being: $0,02 \le O \le 0,2 \ [\text{m}^{1/2}]$.

This value is found on the upper x axis and a vertical line is extended downwards (1) from this point until it meets the corresponding materials value line, b.

The value of b is calculated by the equation:

$$b = \sqrt{(\rho,c,\lambda)}$$

$\rho =$ density of enclosure $[\text{kg/m}^3]$

$c =$ specific heat of enclosure (J/kgK)   (2)

$\lambda =$ thermal conductivity of enclosure (W/mK)

To account for enclosures with different layers of material or for different materials in walls, ceiling and floor, see points 4 and 5 of Annex B ENV 1991-2-2. [2]

For this step in the procedures the equation $\Gamma = [O/b]^2 \Big/ \left(\dfrac{0.04}{1160}\right)^2$ is used.   (3)

From this point on the materials line a horizontal line is charted across from left to right (2) to cross the time lines which emanate from the upper zero on the y axis. This line forms a new artificial time axis, the scale based upon the points where the time lines cross that artificial axis. Thus with the temperature line, the temperature path of the fire with time can be easily charted. The original equation for the temperature against time is taken from

$$\theta_g = 1325 \left(1 - 0,324e^{-0,2t^*} - 0,204e^{-1,7t^*} - 0,472e^{-19t^*}\right)$$ (4)

The next step is to find the position of maximum temperature and the time that it occurs. This is done by recommencing with the initial value for the opening factor, but this time starting on the O values found on the lower portion of the y axis.

From this point a horizontal line is charted to the corresponding fire load line (3) then charted vertically up to the lower x axis (4). Passing through this intersection, a new line starting from the upper zero on the y axis is drawn. This line continues along this path (5) until it strikes the new artificial time axis (this point being t_d). From this point a vertical line is charted up through the lower x (time) axis (this point being t_d^*) until it crosses the temperature curve (6).

This point is defined by the time t_d and the maximum temperature θ_{max} provided by the horizontal line 7.
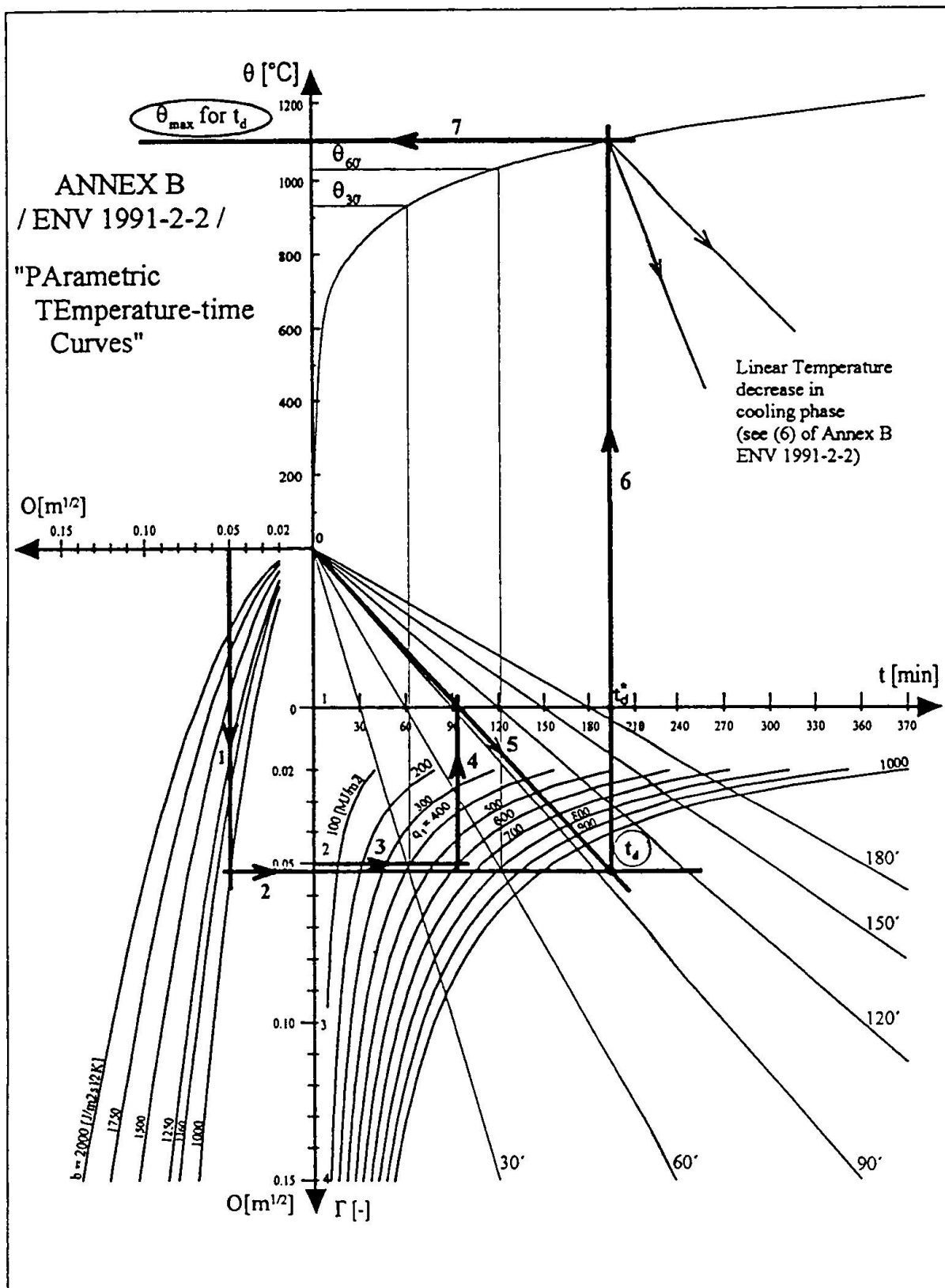
Fig. 1: Annex B Nomogram

For this step the equation base is defined by

$$t_d^* = \left(0.13 \times 10^{-3} \cdot q_{t,d} \cdot \Gamma\right)/O \quad \text{and} \quad t_d^* = \Gamma \cdot t_d \tag{5}$$

$$t_d = 0.13 \times 10^{-3} \cdot q_{t,d} / O \tag{6}$$

The value of $q_{t,d}$ is the design value of the fire load density related to the surface area A_t of the enclosure

$$q_{t,d} = q_{f,d} \cdot A_f/A_t \; [MJ/m^2] \tag{7}$$

$q_{f,d}$ = design value of the fire load density related to the surface area A_f of the floor [MJ/m^2]

At the point (t_d, θ_{max}) the linear temperature decrease will begin, this being defined by point 6 of Annex B ENV1991-2-2 as a function of t_d^*

3.   Annex E of ENV 1991-2-2: Equivalent Time

3.1   Description of the method

Annex E of Eurocode 1 offers a simple equation (8) to determine the required fire resistance time $t_{e,d}$ for a compartment, equivalent to the same duration of an ISO curve fire.

$$t_{e,d} = q_d \, k_b \, w_f \tag{8}$$

Before starting the calculation, it is necessary to determine the floor area of the compartment A_f as well as the total fire load $Q_{fi,k}$, mainly depending on the combustibility of the component parts and of the stored material. Annex D of [2] can be applied for this purpose. The design fire load density $q_{f,d}$ can be obtained from the multiplication of the characteristic fire load q_k by the safety factors γ_n and γ_q for the accepted failure risk in the case of fire and the influence of active fire measures, eq. 9.

$$q_d = \gamma_q \, \gamma_n \, q_k = \gamma_q \, \gamma_n \, \frac{Q_{fi,k}}{A_f} \tag{9}$$

The conversion factor k_b in equation (8) accounts for the heat transfer in the neighbouring component parts of the compartment. It depends on the thermal properties of the walls and ceilings of the enclosure, see table E.1 of [2].

The ventilation factor w_f can be calculated by the following equation ;

$$w_f = \left(\frac{6}{H}\right)^{0.3} \left(0.62 + 90\left(0.4 - \alpha_v\right)^4 / \left(1 + b_v \, \alpha_h\right)\right) \geq 0.5 \tag{10}$$

This equation depends on the height of the compartment H and on the ratios of the vertical (α_v) and horizontal (α_h) opening areas to the floor area A_f.

The dimensionless factor b_v can be determined by the following equation ;

$$b_v = 12.5\left(1 + 10\alpha_v - \alpha_v^2\right) \geq 10 \tag{11}$$

In case of small compartments, A_f < 100 m², Annex E allows to use the more simple equation 12. to calculate the ventilation factor ;

$$w_f = O^{-1/2} \; A_f/A_t \qquad (12)$$

with the opening factor O being calculated according to Annex B, see eq. 1.

3.2   Nomogram of Equivalent time method (Annex E of ENV 1991 2-2)

Two nomograms are presented in figure 2. The first one (upper two drawings) can be used when there is no horizontal openings in the compartment (α_h=0). The second one (lower two drawings) is made considering that the compartment has the minimum of vertical opening (α_v=2.5%). The left drawings enable to calculate w_f (equation 10) in function of the dimensionless factor α_v (upper left drawing) or α_h (lower left drawing) and in function of the height of the compartment H. The right drawings enable to calculate the equivalent time in function of the w_f factor found on the left figure and in function of the design fire load density times the conversion factor k_b (equation 8).
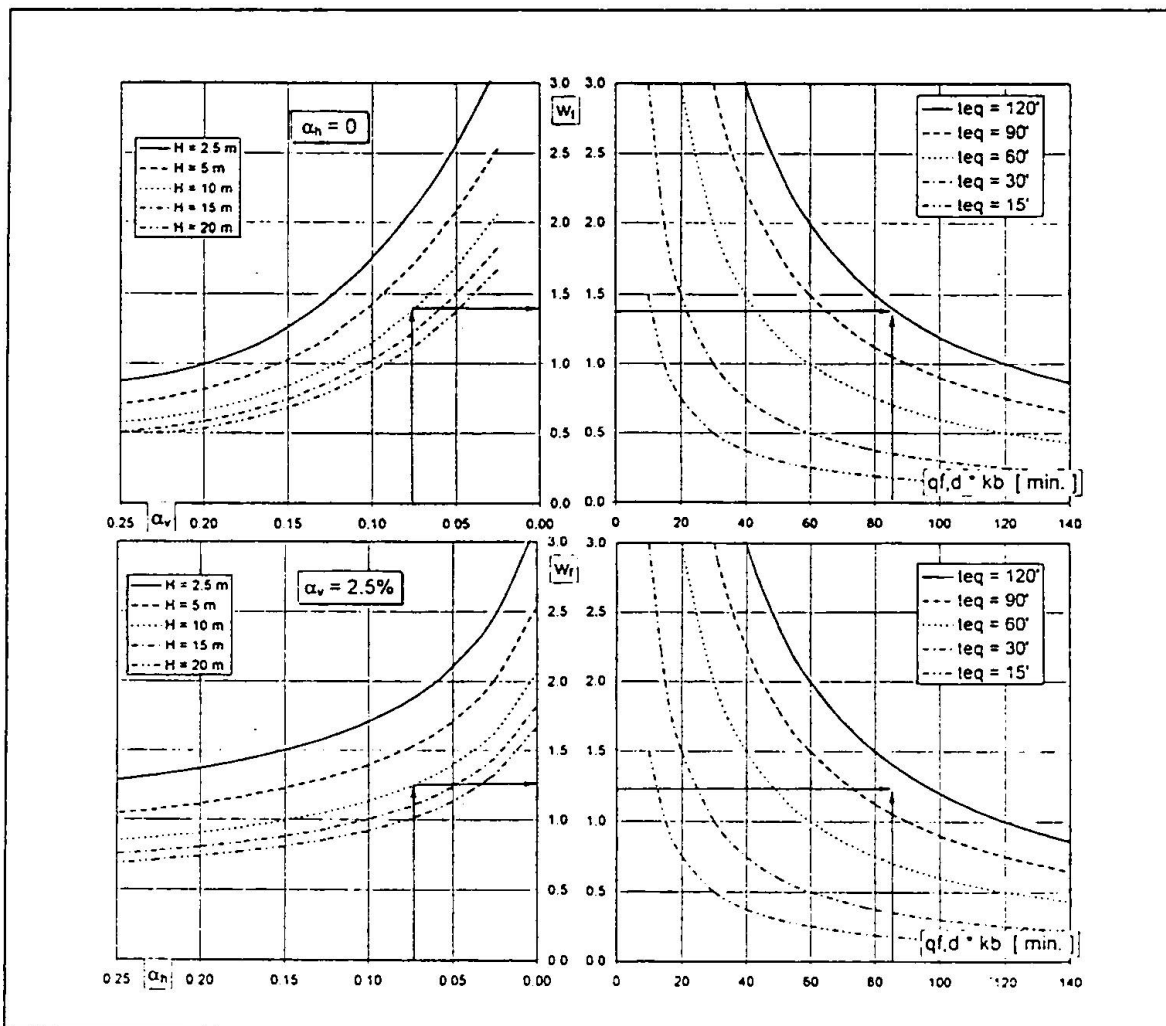
Figure 2. : Nomogram of Equivalent time

4.   Comparison between Annex B and Annex E

4.1   First look on the equations of the 2 methods

It is interesting to notice that t_d^* from Annex B can be considered as an equivalent ISO time which is related to the temperature of a very light steel element (with a very big section factor, see EC3 Part 1.2). In other words, an element whose temperature is very close to the gas temperature. In Annex B, t_d^* is proportional to the opening factor O (eq 5 & 3) while in Annex E $t_{e,d}$ is proportional to $O^{-1/2}$. It will be verified by the parametrical study whether this apparent contradiction has practical effects.

4.2   Parametrical study

A parametrical study has been made with the 2 methods. 7 parameters are taken into account:

- the floor area of the compartment, A_f in m²   16, 25, 36, 64, 100, 144, 256, 324, 400
- the height of the compartment, H in m   2.4, 2.5, 3.0, 3.5, 4.0, 4.5, 5.0
- the design fire load density, q_d in MJ/m²   250, 500, 750, 1000, 1250, 1500, 1750, 2000
- the opening height, h in m   0.2, 0.5, 1.0, 1.5, 2.0, 2.5
- the position of the sill of the opening, h_s in m   0.0, 0.5, 1.0
- the width of the opening, w in m   0.5, 1.0, 2.0, 3.0, 4.0, 5.0
- the characteristics of the walls, b in J/m²s$^{0.5}$K   500, 1000, 1300, 1600, 2000

The bold values are those of the **reference case**. The variation is made separately on the parameters. While one of them is allowed to vary from the reference case, the values of the other parameters remain fixed to the values of the reference case. This leads to 38 different cases. For the reference case we have the 7 bold values of the parameters and for the 37 other cases we have 6 bold values and one non bold value.

The results of this study are in case of annex B a set of temperature-time curves and in case of annex E a set of equivalent time. Figure 3 shows the results obtained by the 2 methods for the variation of the parameter A_f.
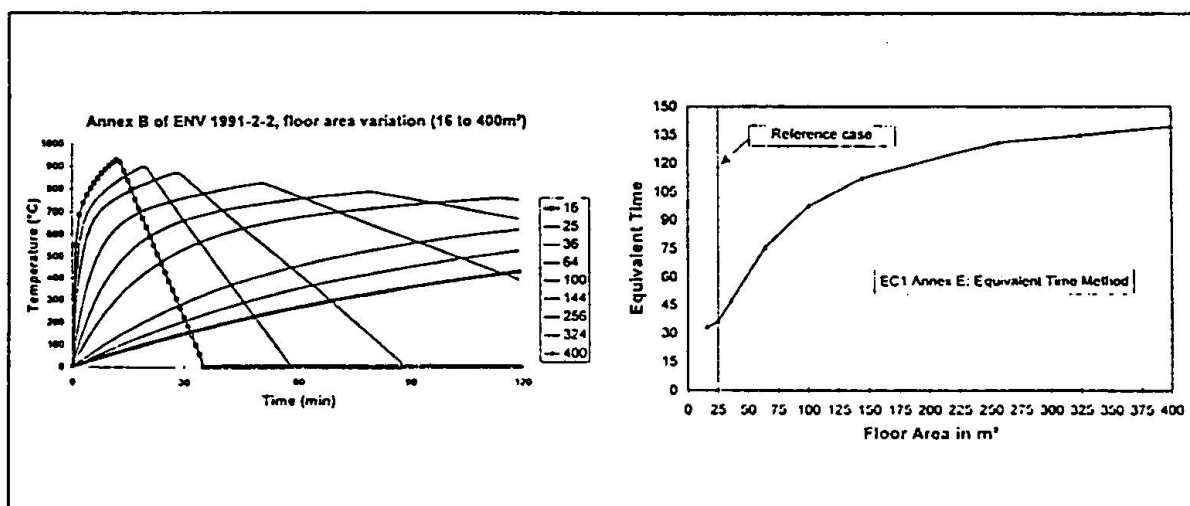

Fig. 3. Results obtained by the 2 methods.

4.3   Link between the two methods

In order to make a comparison between those methods we have to transform the results obtained with Annex B into equivalent times. This is done by calculations of temperatures in a structure and observation of the maximum temperature reached by this structure. Three structures have been chosen here;

- *Unprotected steel section.* In this case, the calculation of the uniform temperature is made by the method described in § 4.2.5.1. of Eurocode 3 : Part 1-2 [3]. A massivity of 211 m^{-1} was chosen corresponding, for example, to a HE 200 A section.

- *Protected steel section.* The same massivity is taken as for the unprotected section. The lightweight insulating material has the following properties: $c_P = 850$ J/(kgK); $\lambda_P = 0.15$ W/(m²K); $\rho_P = 300$ kg/m³ ; thickness = 20 mm. Those characteristics are similar to, say, vermiculite. Here the calculation of the uniform temperature is made by the method described in § 4.2.5.2. of Eurocode 3 : Part 1-2 [3].

- *Concrete structure.* The temperature is calculated in a semi-infinite concrete volume, at a penetration depth of 3 cm. The calculations are made with the non linear finite element code SAFIR of the University of Liège.

For the thermal calculations, steel and concrete thermal properties are taken from Eurocode 4 : part 1-2 [4].

The temperature in the structures submitted to the ISO curve is first calculated as a function of time. The same calculation is made for the same structures submitted to the natural fire curves obtained from annex B. In each case, the maximum temperature obtained in a structure submitted to a parametric temperature-time curve is reported on the corresponding curve obtained by the first calculation when the structure was submitted to the ISO curve. The moment when this temperature was obtained is defined as the equivalent time.
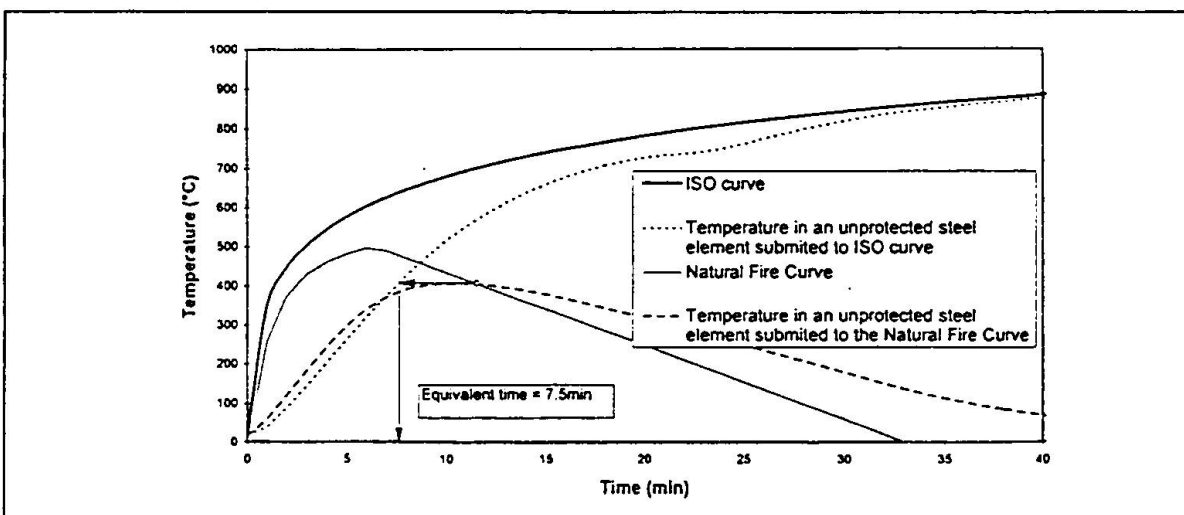

Fig. 4: Link between Natural Fire Curve and Equivalent Time

In other words, the equivalent time is the time during which a defined structure has to be submitted to the ISO fire curve in order to obtain, in the structure, the same effect (maximum temperature) as the natural fire curve would have produced.

4.4   Results

The position of the sill of the opening has no influence on the results, for the annex B method as well as for the annex E method. The 6 other results of the parametrical study are shown on the figures 5.a and 5.b. The equivalent time is given in minutes as a function of the different parameters. Dotted lines are segments linking at least one point which is out of the field of application of the method used to obtained this point. The zones which are beyond the applicability limits of the methods have been shaded in grey on the figures.

It appears that the equivalent times calculated with a concrete structure and with a protected steel structure are very close to each other. This is because those two structure have the same thermal behaviour, i.e. a delay in time between the increase of temperature in the air and the temperature increase in the structure. Whether the delay is caused by a thermal protection or by a cover of concrete does not make a difference. It is also observed that these two curves are generally very similar to the equivalent time curves given by Annex E.

In some cases, the variation of the equivalent time calculated from the results of the Annex B with a parameter is different for the unprotected steel element than for the two protected elements. This is due to the fact that the maximum temperature calculated in the unprotected steel is mainly influenced by the maximum temperature in the air, whereas the maximum temperature in the protected elements is also influenced by the duration of the fire. Going from a severe but short fire to a less severe but longer one is generally favourable for a pure steel section, but it can be more critical for a protected element.

The same effect also explains why the apparent contradiction between Annex B and Annex E mentioned in § 4.1. disappears when temperatures are calculated in protected elements, but not in unprotected elements.

5.   Conclusions

Two different methods are proposed in ENV 1991-2-2 [2] to take into account the influence of physical parameters on the severity of the fire. Those parameters are the fire load, , the geometry of the compartment and the thermal properties of the surrounding material.

This study shows that, despite apparent contradiction in the equations, the methods proposed in Annex B and in Annex E are coherent while evaluating the temperature in a protected steel element or in a concrete element.

When considering an unprotected steel element, these two methods have lead in some cases to very different results. None of two methods is systematically safer than the other.

If it is considered that Annex B provides a good approximation of the air temperature-time curve in the compartment, based on more refined models, thus allowing the calculation of the temperature in each structure type, whereas Annex E is an attempt to simplify the solution even further and to propose equivalent time irrespective of the structure, then this study tends to indicate that the approximation is valid in case of protected elements, but may not be valid in case of unprotected steel elements.

It can be noticed that the method of Annex E gives equivalent times which in each case are higher than 30 minutes. Nevertheless 30 minutes of ISO curve heating is an upper bearing limit for an unprotected steel element.
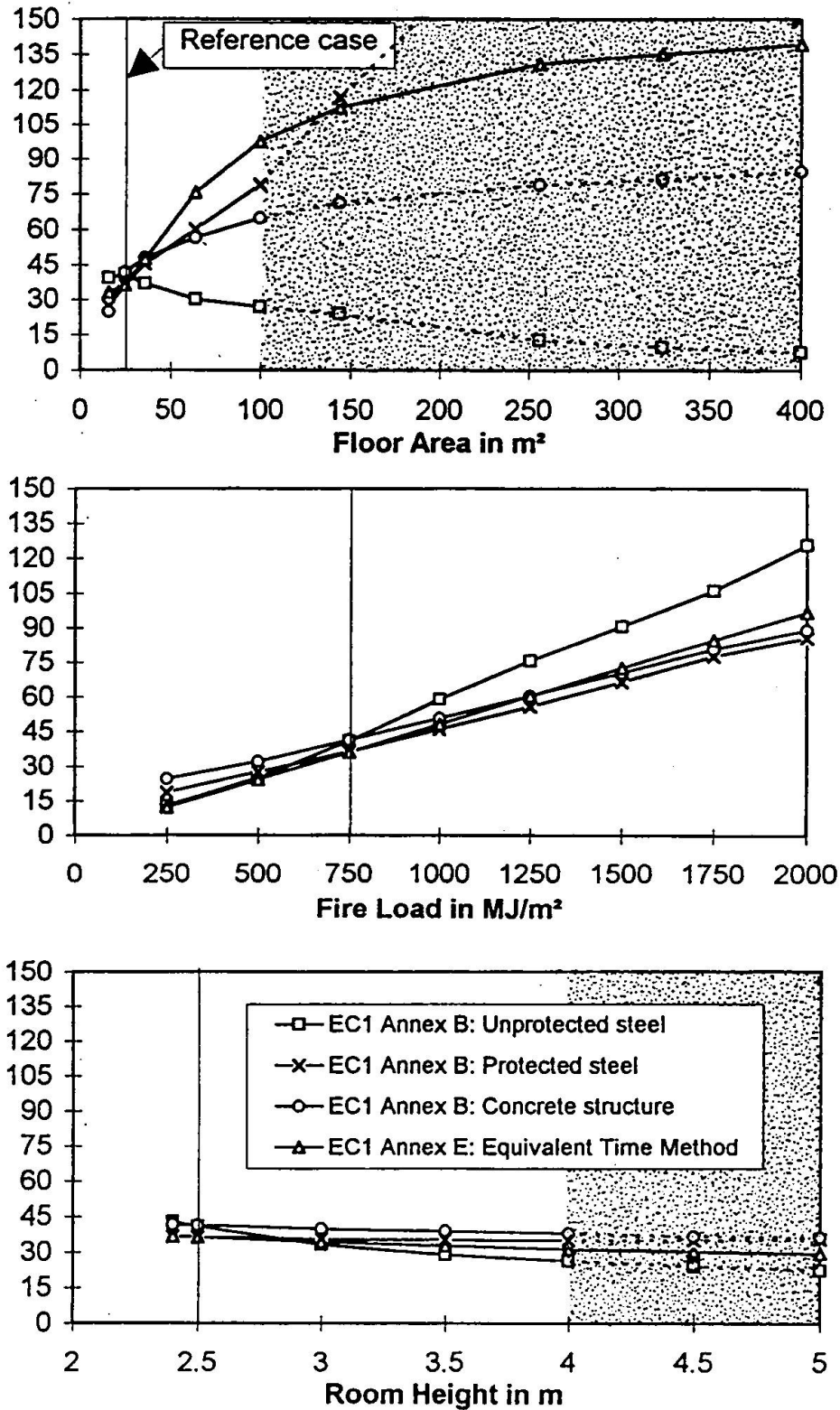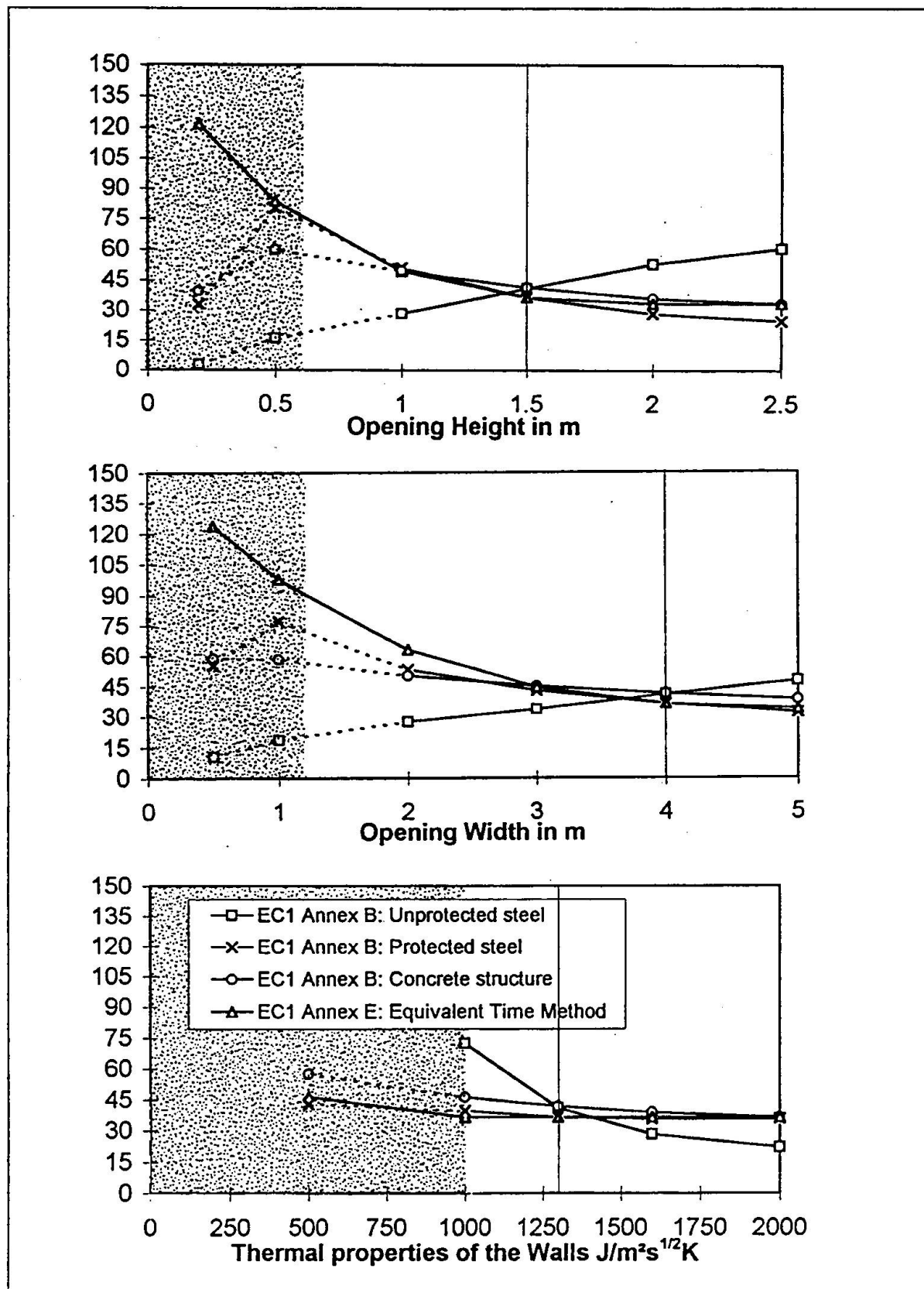
Fig.5.a: Results of the parametrical study

Fig. 5.b: Results of the parametrical study

6. Acknowledgement

7. References

[1] Wickström, "Application of the Standard Fire curve for Expressing Natural Fires for Design Purposes".

[2] Eurocode 1: Basis of design and actions on structures. Part 2-2: Actions on structures exposed to fire, ENV 1991-2-2.

[3] Eurocode 3: Design of steel structures Part 1.2: General rules Strucural fire design, DRAFT ENV 1993-1-2.

[4] Eurocode 4. Design of Composite Steel and Concrete Structures. Part 1.2 : Structural Fire Design, prENV 1994-1-2, CEN , April 1994.

[5] J.B. Schleich, L.G. Cajot, M. Pierre, CEC Agreement 7210-SA / 125, 126, 213, 214, 323, 423, 522, 623, 839, 937 "Competitive Steel Buildings Through Natural Fire Safety Concept" Technical Report n° 1 Semestrial Report (01.07.1994 to 31.12.1994)

[6] J.B. Schleich, L.G. Cajot, M. Pierre, CEC Agreement 7210-SA / 125, 126, 213, 214, 323, 423, 522, 623, 839, 937 "Competitive Steel Buildings Through Natural Fire Safety Concept" Technical Report n° 2 Semestrial Report (01.01.1995 to 30.06.1995)

Leere Seite

Blank page

Page vide

Large Compartment Fire Tests at Cardington and the Assessment of Eurocode 1

Yong WANG	Gordon COOKE	David MOORE
Consultant	Fire Safety Specialist	Head, Steel Section
Building Research	Fire Research Station	Building Research
Establishment	BRE	Establishment
Garston, Watford	Garston, Watford	Garston, Watford
UK	UK	UK

Summary

This paper describes a series of large compartment fire tests performed at BRE's Cardington laboratory. One of the objectives of these tests was to collect high quality data to assess the fire recommendations in Eurocode 1 Part 2.2. This paper presents comparisons between the fire temperature-time relationships, predicted by Eurocode 1, and those predicted by the method of Pettersson, Magnusson and Thor, and the test results. To relate realistic fires to the standard fire exposure, Eurocode 1 gives recommendations to calculate the equivalent time of exposure for a real fire. Predictions for the equivalent time of the large compartment fire tests using the Eurocode 1 method are compared with the test results and also with predictions from other methods. Finally, a parametric study is conducted to compare the sensitivities of the maximum fire temperature to the material properties of the compartment lining, predicted using the Eurocode 1 method and the method of Pettersson et al.

1. Introduction

With the advance in fire safety engineering, the design of structures subject to fires is now moving away from the traditional prescriptive approach to a performance based methodology. In the performance based method, the fire is treated as a type of accidental loading and the structure is designed to sustain this loading without loss of stability.

Essentially, there are four steps in this new approach. The design starts with the specification of a fire load, obtained from a statistical analysis of actual fires. This is followed by a fire behaviour analysis based on the fire load and ventilation condition of the fire compartment which gives the fire exposure in the form of a fire temperature - time relationship for the fire. Using this relationship and the thermal properties of the building materials, a thermal calculation is then performed to obtain the temperature rise in the structural members. Finally, a structural design incorporating the strength and stiffness of the structural elements at high temperatures is carried out to check the stability of the structure.

Various parts of the Eurocode system give recommendations on the thermal response and structural behaviour of the different materials used in construction. For example, Eurocode 3 Part 1.2 [1] describes in detail the procedures for the determining the fire resistance of steel framed buildings.

The method for calculating the time-temperature relationship of the fire is given in Eurocode 1 Part 2.2 [2]. Various appendices give other details such as the fire load, the equations for calculating the fire temperature-time relationships inside and outside a compartment and the calculations for the equivalent time of the fire. The equations for the latter relate a realistic fire scenario to the traditional standard fire exposure.

Although the information contained in Eurocode 1 has a sound scientific basis, its validation was based on comparisons against fire tests performed in small compartments [3]. Clearly, the applicability of the method to the large open plan offices found in modern buildings needs critical examination. The main differences between fires in small compartments and those in large compartments are:

(a)   The temperature distribution in a large compartment is generally more non-uniform than the temperature distribution in a small compartment;

(b)   The air movement in a large compartment is generally more turbulent than the air movement found in a small compartment.

Against this background, the Building Research Establishment in conjunction with British Steel Technical carried out 9 large compartment fire tests in BRE's Cardington laboratory (referred to as BRE/BST tests in the paper). More recently, as part of an ambitious project to investigate the behaviour of a whole building under fire conditions, a fire test in a full scale 8-storey steel framed building (referred to as the BRE corner test) was carried out to examine the provisions of Eurocode 1 Part 2.2 [2].

The objectives of this paper are twofold: first, to briefly describe the above mentioned fire tests and secondly, to assess the recommendations given in Eurocode 1 Part 2.2. This assessment includes the following comparisons:

(a)   A comparison between the temperature-time relationship of the compartment predicted using the recommendations given in Eurocode 1 Part 2.2 and the same relationship calculated using Pettersson et al's method. Both these predictions are also compared with the test results.

(b)   The equivalent time of exposure of a fire calculated using Eurocode 1 Part 2.2 is compared with the test results and other empirical methods.

(c)   An assessment is made on the sensitivity of the maximum fire temperature to the properties of the compartment lining materials $(k\rho c_p)^{1/2}$.

2. Description of fire tests

2.1 BRE/BST fire tests

A full description of these fire tests is given in a British Steel Technical report[5]. This paper gives a brief account of the more important test parameters and of the measurements taken.

The fire tests were conducted in a compartment built inside the BRE Large Building Test Facility (LBTF) at Cardington, to the north of London. Overall, the compartment measured nominally 23 m x 6 m x 3 m high. Test 7 was carried out in the 1/4 size compartment.

The compartment roof was constructed of 200 mm thick reinforced autoclaved aerated concrete slabs with two layers of 25 mm thick standard grade ceramic fibre blanket. Test 8 had an additional lining of two layers of 12.5 mm thick Fireline plasterboard. The walls of the compartment were made of 215 mm thick lightweight concrete blocks with the same lining as the ceiling. The floor of the compartment was 75 mm thick dense concrete covered with a 125 mm deep layer of fluid sand.

Fire load was uniformly distributed in the compartment. Ventilation was provided via an opening in one wall. Table 1 gives the fire load density and the opening width and height for each fire test.

During the fire, three crib lines in the compartment, one near the back, one in the middle and one near the front were adopted as measuring stations for monitoring the compartment air temperature. At each of these stations, an array of 3 mm thermocouples were used.

Short steel sections with and without fire protection were suspended below the compartment roof at the three monitoring stations and their temperatures recorded. These temperatures were used to determine the equivalent time of fire exposure and for validating thermal response analysis.

The mass loss of timber stacks (every other stack in the centre row) was monitored using 1 m square load cell platforms.

2.2 BRE fire test in the 8-storey building

The Building Research Establishment in collaboration with a number of European parties is carrying out an ambitious experimental programme to study the behaviour of whole buildings under fire conditions. These tests are being carried out in an eight storey three bay by five bay steel framed composite building erected in BRE's Cardington laboratory. Although the main objective of this programme is to provide high quality test data on the structural behaviour of the whole building under fire conditions, this data can also be used to calibrate the recommendations in Eurocode 1 Part 2.2 [2]. To date (January 1996), only two compartment fire tests using timber

cribs have been carried out, one by the Building Research Establishment and one by British Steel Technical. Since the fire conditions of both these two tests are the same, only the BRE test is described here.

The BRE fire test was conducted in one corner of the building, simulating the dimensions of a typical office room. This room measured 9 m long, 6 m wide and 4.185 m high.

The floor of the building was constructed of in-situ concrete acting compositely with corrugated steel decking. The floor of the fire compartment was covered with sand to simulate the serviceability load and to protect the instrumentation. The external end wall was made of lightweight concrete blocks, while the window side of the compartment consisted of a 1.5 metre high wall of lightweight concrete blocks supporting a 2.685 m high aluminum frame sealed with double glazing. The remaining internal walls of the fire compartment were formed using plasterboard to give a two hour fire resistance.

The fire load consisted of 40 kg/m^2 of timber distributed uniformly over the compartment floor.

Various instruments were placed inside and outside of the fire compartment to record combustion gas temperatures, the steel beam and column section temperatures and the strains and displacements in various locations in the compartment.

3. Analysis of fire tests

In this paper, three types of analysis are conducted. First, combustion gas temperature-time curves from these tests are compared against various predictions. These predictions include the parametric temperature - time curves proposed in Eurocode 1 Part 2.2 [2], predictions according to the method of Pettersson et al [4] and a simple equation based on the observation that the hot gas flowing out of the compartment constitutes a significant proportion of the total heat release of the fire. Secondly, the equivalent times of fire exposure predicted by Eurocode 1 are compared against the test results and predictions by other methods. Thirdly, the sensitivity of the predicted maximum combustion gas temperature to the properties of the compartment lining materials is compared with that of the predictions using the method of Pettersson et al [4].

3.1. Compartment fire temperature-time relationship

3.1.1: Eurocode 1 parametric temperature-time curve
For convenience, the equations in the Eurocode 1 Part 2.2 [2] are reproduced here. The temperature-time curve of a compartment fire is divided into a heating phase and a cooling phase. The expression for the heating phase is given by:

$$T_g = 1325(1 - 0.325e^{-0.2t^*} - 0.204e^{-1.7t^*} - 0.472e^{-19t^*}) \qquad (1)$$

where T = the temperature in the fire compartment (C°),

t^* = $t.\Gamma$ (h) with

t = fire exposure time in hours,

Γ = $(O/b)^2 / (0.04/1160)^2$

in which b is the average value of $(k\rho c_p)^{1/2}$ of compartment structure within the range of $1000 \le b \le 2000$ ($J/m^2s^{1/2}K$)

O = opening factor $A_v h^{1/2} / A_t$ within the range of $0.02 \le O \le 0.2$ ($m^{1/2}$) with

A_v = area of vertical openings (m^2)

h = height of vertical openings (m)

A_t = total area of enclosure of the fire compartment (m^2), i.e. walls, ceiling and floor, including opening.

The fire exposure time t_d^* at which the fire temperature in the enclosure starts to decrease is given by the following expression:

$$t_d^* = 0.00013 q_{t,d} \Gamma / O \qquad (2)$$

in which $q_{t,d}$ is the fire load density related to the total area A_t of the fire compartment. During the cooling phase, the temperature is assumed to decrease linearly at a rate depending on the time t_d^*.

The combustion gas temperature-time curves for all the large compartment fire tests have been predicted using Eurocode 1 method. Typical results are shown in figures 1-4. For BRE/BSC fire tests 5 and 6, the ventilation factor was lower than the lower bound value of 0.02 ($m^{1/2}$) permitted in Eurocode 1 Part 2.2 [2]. However, using the test value seems to give better agreement with the test temperature-time curves than using this lower bound.

It seems that Eurocode 1 Part 2.2 [2] predicts the maximum combustion gas temperature reasonably well but grossly underestimates the time of fire exposure. This prediction would be acceptable for unprotected steel structures since their maximum temperatures would be very close to that of the fire. However, Eurocode 1 Part 2.2 [2] may significantly underestimate the temperature rise in other structures such as protected steel and concrete structures.

3.1.2: Predictions according to the method of Pettersson et al [4]

The method used by Pettersson et al [4] is the most widely quoted one in the fire safety engineering literature for the calculation of combustion gas temperatures in fully developed compartment fires. The method is based on the assumptions of a uniform temperature field and no-moving air in the fire compartment. While these assumptions are reasonable for fires in small enclosures, the results from the BRE/BST large compartment fire tests clearly show that the

combustion gas temperature in the compartment is not uniform. For example, figure 5 shows the three time-temperature curves recorded at the three combustion gas measurement stations for BRE/BST Test 2.

However, including a non-uniform temperature distribution will make the study of the compartment fire behaviour very complicated. For applications to structural fire resistant design, this degree of complexity may not be necessary since the maximum temperature of a structural member may not be particularly sensitive to a non-uniform temperature field. For example, figure 6 shows the measured temperature-time curves of steel sections at the three recording stations of BRE/BST Test 2. Clearly, the differences in the maximum temperatures of steel at these locations are much smaller than the differences in fire temperatures at the same locations. It is therefore considered acceptable to use the average combustion gas temperature in the compartment for determining the temperature of the structural elements.

The method developed by Pettersson et al [4] is based on a heat balance: heat produced equals heat lost. The heat produced is the heat generated by combustion of the fire load. The heat lost is made up of: heat lost in escaping gases; heat absorbed by the structure and fabric of the compartment, heat lost by radiation through the ventilation opening and heat required to produce mass of volatile [3].

Clearly, the total rate of heat release in the fire is the most important parameter. In this study, this value was calculated from the measured burning rates of the timber cribs during steady burning and are given in table 2, which also includes the predicted burning rates using the equation known as the CIB equation [3].

The maximum heat release rate is obtained from the burning rate of timber cribs, assuming a combustion efficiency coefficient of 0.7 and a heat production of 18 MJ/kg for timber. The complete rate of heat release-time curve of the compartment fire is constructed from three parts: a linearly growth part consuming 10% of the fire load, a steady burning rate consuming 50% of the fire load and a parabolic cooling phase until complete burn-out of the fire load.

Studies in the 1950's and 1960's established an empirical burning rate of about $5.5A_vh^{1/2}$ kg wood/minute based on ventilation conditions and the maximum heat required for stoichiometric combustion. It is noticed from table 2 that in BRE/BST Tests 5 and 6, the burning rates of timber are significantly higher than this value. At present, there lacks a comprehensive theory to explain these higher burning rates. However, the equivalent heat of $5.5A_vh^{1/2}$ kg wood/minute may still be regarded as the maximum rate of heat release for the fire development.

Predicted combustion gas temperature-time curves are compared with the test results and also with the predictions from Eurocode 1 Part 2.2 [2] in figures 1-4. It seems that this method generally predicts more severe fires than Eurocode 1. However, the degree of over prediction

using the method of Pettersson et al [4] is about the same as the degree of under prediction using the Eurocode 1 [2] method.

During the fire analysis using the method of Pettersson et al [4], it was observed that the heat loss due to hot gas flowing out of the fire compartment openings accounted for about 70%-80% of the total heat release. Since the fire compartments were highly insulated, this is in agreement with the observation of Thomas and Heselden [3] who noticed that radiation heat loss through opening was less than 30%. Since the mass rate of air flowing out of the compartment openings is expressed as[7]:

$$m_{air} = 0.5 A_v \sqrt{h} \qquad (3)$$

The combustion gas temperature can be determined from the following expression:

$$T_g = T_\infty + \frac{0.75 * RHR}{0.5 A_v \sqrt{h} C_a} \qquad (4)$$

where RHR is the total rate of heat release and the coefficient of 0.75 implies that 75% of the total rate of heat release of the fire flows out of the fire compartment openings as convective heat loss. T_∞ is the ambient temperature and C_a the specific heat of ambient air, $C_a = 1150$ J/kg.°C.

Figures 1-4 compare the predicted fire temperature-time curves using equation (4) with the test results and predictions from Eurocode 1 [2] and the more complicated method of Pettersson et al[4]. The accuracy of equation (4) is comparable to that of the other two methods. However, equation (4) is much easier to use.

3.2: Equivalent time of fire exposure

Eurocode 1 [2] provides an equation to calculate the equivalent time of a realistic fire. This equivalent time is the time in the standard fire exposure (e.g. ISO 834 [7]) for a structural member to reach the maximum temperature obtained when the structural member is subjected to the realistic fire exposure.

Alternative methods to calculate the equivalent time of fire exposure are provided by Law [8] and Harmathy [9]. Results of the predicted equivalent times for the BRE/BST fire tests using these three methods are compared with the test results in table 4. The test equivalent times are obtained from measured temperatures of the protected steel sections.

Eurocode 1 [2] gives three different values of k_b (0.04-0.07) according to the value of $(k\rho c_p)^{\frac{1}{2}}$ of the compartment lining materials. However, using the value of 0.09 gives the best agreement.

Table 3 shows that while the methods of Eurocode 1 [2] and Law [8] are reasonably close to each other and to the test results, the predictions of Harmathy [9] are quite different. This is because

there is a fundamental difference in the way Harmathy's [9] equations are derived.

The derivation of Harmathy's equations [9] was based on temperature calculations at the position of the reinforcement inside a concrete slab, while the methods of Eurocode 1 [2] and Law [8] were based on temperature calculations for steel sections.

In summary, the equivalent time of exposure of a fire may not be unique. Its values may depend on the construction material and the fire protection of the structural members.

3.3. Effect of $(k\rho c_p)^{\frac{1}{2}}$ of enclosure lining materials on maximum fire temperature

In Eurocode 1 [2], the property $(k\rho c_p)^{\frac{1}{2}}$ of the enclosure lining material plays an important role in the calculation of the parametric temperature-time curves. Whilst it is possible to check the accuracy of this recommendation by performing a series of experiments in which only the lining materials are varied, the cost of such a series of tests would be prohibitive. Instead, the method of Pettersson et al [4] is used. Although this method has not proved to be very accurate as shown in figures 1-10, it is thought that this is the result of inaccurate information on the rate of heat release of the fire. For comparative studies to check the influence of other parameters on the fire temperature development, this method is acceptable.

Table 4 compares the predicted maximum temperatures of a fire in an enclosure with different lining materials. Other conditions are the same as the BRE corner fire test. In the calculations using the Pettersson et al [4] method, the rate of heat release is unchanged.

Table 4 shows that for this range of lining materials, the maximum difference in the predicted maximum temperature using the Pettersson et al method [4] is only about 7%, whilst the maximum difference in the maximum temperatures predicted using Eurocode 1 [2] is about 30%.

The results of table 4 imply that the heat release rates of the same fire in enclosures with different lining materials will be different. However, existing prediction for the burning rate of a fire do not include this influence. Nevertheless, the effect of different enclosure lining materials on the fire temperature development as predicted using the Eurocode 1 [2] method should be explored further.

4. Conclusions

In this paper, a series of fire tests in large compartments in the BRE's Large Building Test Facility at Cardington are briefly described and results are analysed. The results are compared with predictions using Eurocode 1 [2] and other methods. From the results of the analyses, the following conclusions can be drawn:

(1)   The Eurocode 1 [2] underestimates the temperature-time relationships for fires in large compartments. Generally, Eurocode 1 gives a reasonable prediction for the maximum

combustion gas temperature, but grossly underestimates the fire exposure time.

(2)   The method of Pettersson et al [4] gives similar accuracy. It is thought the inaccuracy in the prediction is not in the method itself, but the assumption concerning the amount of energy released per unit mass of timber.

(3)   Equation 4 may be used as a very simple way to estimate the combustion gas temperature. The accuracy of this equation is comparable to Eurocode 1 and Pettersson et al's method.

(4)   The fire temperature is very sensitive to the properties of the compartment lining materials, according to Eurocode 1. However, predictions using the method of Pettersson et al [4] do not show such sensitivity. It is recommended that a thorough study is made to investigate the influence of lining materials on the fire temperature development, including a study on the influence of this parameter on the heat release rate.

(4)   The equivalent time of exposure of a fire may not be a unique. Its values may depend on the construction material and fire protection of the structural members. A thorough study is required to validate the recommendations in Eurocode 1.

5. References

1.   European Committee for Standardization, "Eurocode 3: Design of Steel Structures: Part 1.2: General Rules, Structural Fire Design", Draft ENV 1993-1-2, July 1995

2.   European Committee for Standardization, "Eurocode 1: Basis of Design and Actions on Structures, Part 2.2: Actions on Structures Exposed to Fire", ENV 1991-2-2:1994

3.   Thomas, P.H. and Heselden, A.J.M., "C.I.B. International Co-operative Programme on Fully-Developed Fires in Single Compartments: Comprehensive Analysis of Results", Fire Research Station Internal Note No. 374, April 1970

4.   Pettersson, O., Magnusson, S.E. and Thor, J., *Fire Engineering Design of Steel Structures*, Publication 50, Swedish Institute of Steel Construction, Sweden, 1976

5.   Kirby, B.R., Wainman, D.E., Tomlinson, L.N., Kay, T.R. and Peacock, B.N., "Natural Fires in Large Scale Compartments - British Steel Technical, Fire Research Station Collaborative Project", June 1994

6.   Drysdale, D., An Introduction to Fire Dynamics, John Wiley and Sons, pp. 315, 1985

7.   ISO, "Fire Resistance Tests - Elements of Building Construction, International Standard 834" , 1975

8.   Law, M., "A Relationship between Fire Grading and Building Design and Contents", Fire Research Note No. 877, JFRO, London, 1971

9.   Harmathy, T.Z., "The Possibility of Characterizing the Severity of Fires by a Single Parameter", *Fire and Materials*, Vol. 4, No. 2, pp. 71-76, 1980

Parameter	Test 1	Test 2	Test 3	Test 4	Test 5	Test 6	Test 7	Test 8	Test 9
Fire load density (kg/m^2)	40	20	20	40	20	20	20	20.6	20
Window width (m)	5.595	5.595	5.195	5.195	2.139	5.195	1.37	5.065	5.195
Window height (m)	2.75	2.75	1.47	1.47	1.73	0.375	2.75	2.68	2.75

Table 1:   *Fire load density and ventilation conditions for each test*

Test	Test burning rate (kg/min)	CIB burning rate (kg/min)	test burning rate/A$_v$h (kg/min.m$^{3/2}$)
BRE/BST 1	84	59.7	3.55
BRE/BST 2	87	59.7	3.67
BRE/BST 3	36.6	36.3	3.95
BRE/BST 4	51.6	36.3	5.57
BRE/BST 5	40.2	26.5	8.25
BRE/BST 6	21.6	13.1	18.15
BRE/BST 7	30	32.9	4.8
BRE/BRE 8	60.6	55.2	2.73
BRE/BST 9	69	57.6	2.91
BRE corner	--	133.8	3.38

Table 2:   *Test and predicted burning rates*

Equivalent time method:	test 1 min	test 2 min	test 3 min	test 4 min	test 5 min	test 6 min	test 7 min	test 8 min	test 9 min
Measured	118.0	71.5	81.5	142.0	99.8	110.5	54.3	67.5	74.0
Eurocode 1	101.2	50.6	79.0	157.9	100.6	112.1	50.6	57.0	53.7
Law	79.5	43.3	55.7	111.3	79.4	109.1	34.2	43.5	41.2
Harmathy	44.4	28.9	57.1	101.9	93.2	162.2	45.3	30.6	30.3

Table 3: Equivalent times of exposure, BRE/BST fire tests

	Maximum combustion gas temperature (°C)	
$(k\rho c_p)^{\frac{1}{2}}$ of lining material/ (1160 J/m² s$^{1/2}$ °K)	Pettersson prediction	EC1 Part 2.2 prediction
0.5	927.4	1253.6
0.6	921.8	1201.3
0.7	915.7	1152.7
0.8	909.1	1110.9
0.9	902.6	1075.3
1.0	895.6	1044.3
1.1	889.3	1016.4
1.2	882.4	990.7
1.3	872.5	966.7
1.4	869.5	944.0
1.5	863.5	922.8

Table 4: Predicted maximum combustion gas temperature
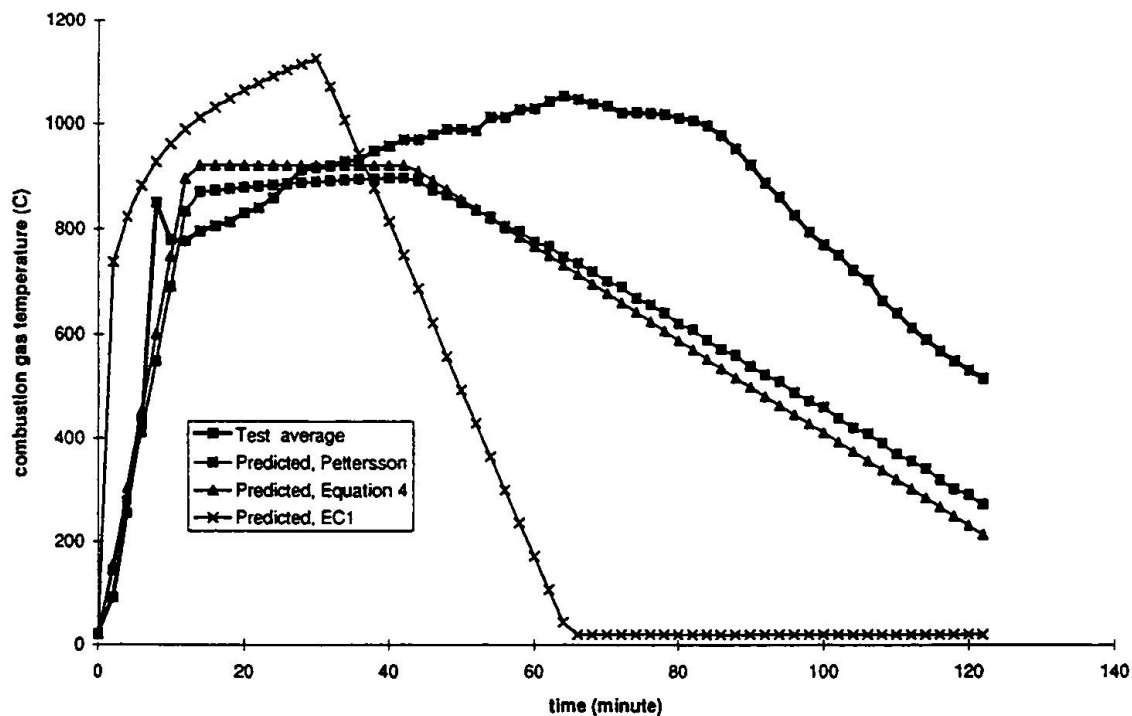
Figure 1:   Comparison of combustion gas temperatures, BRE/BST Test 1
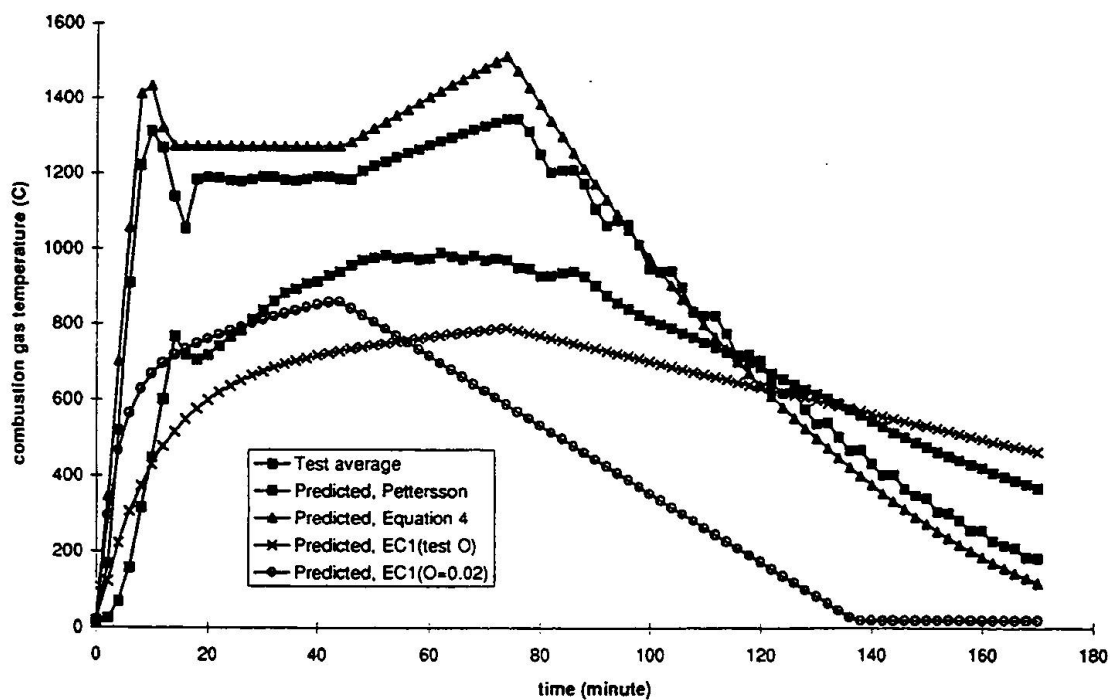
Figure 2:   Comparison of combustion gas temperatures for BRE/BST Test 5
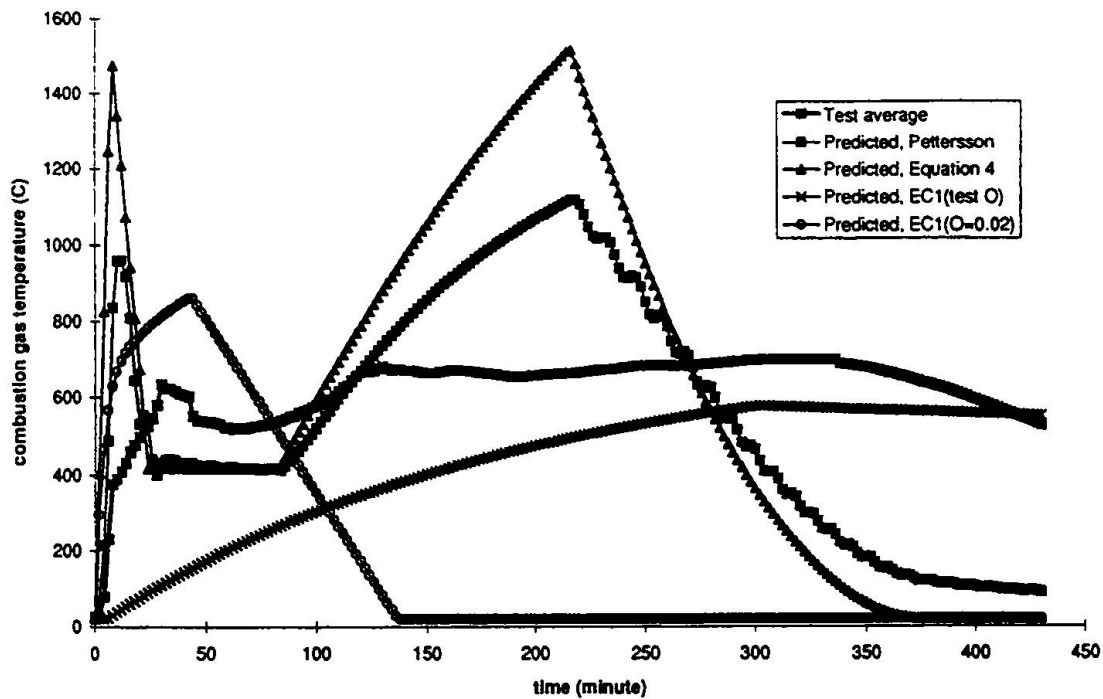
Figure 3: Comparison of combustion gas temperatures for BRE/BST Test 6
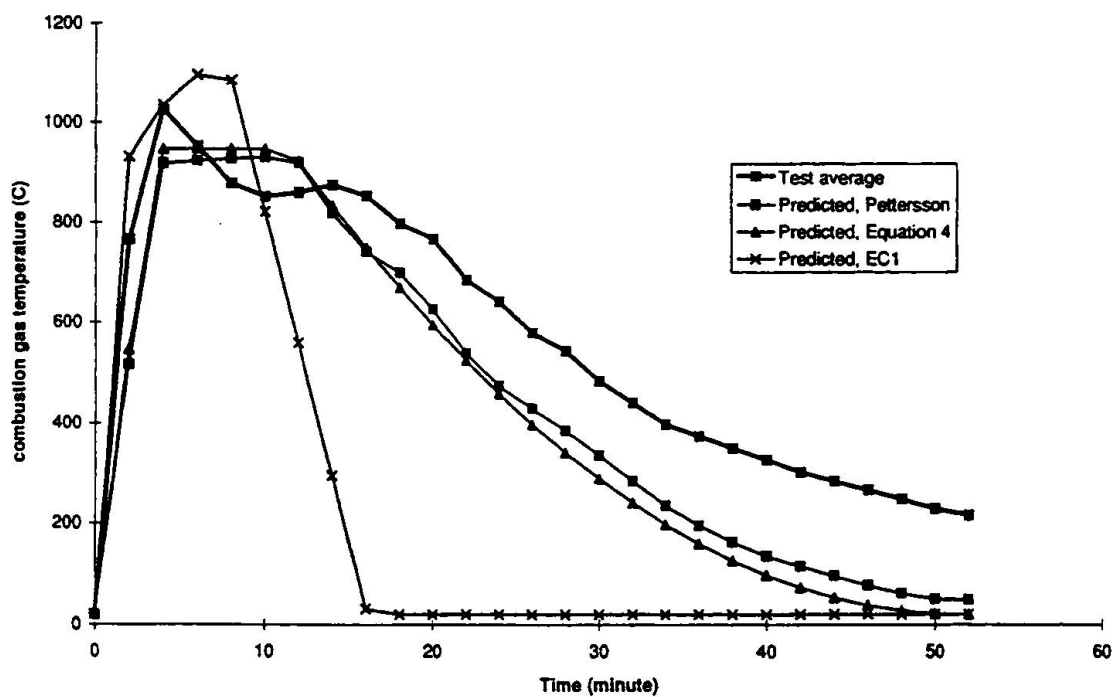
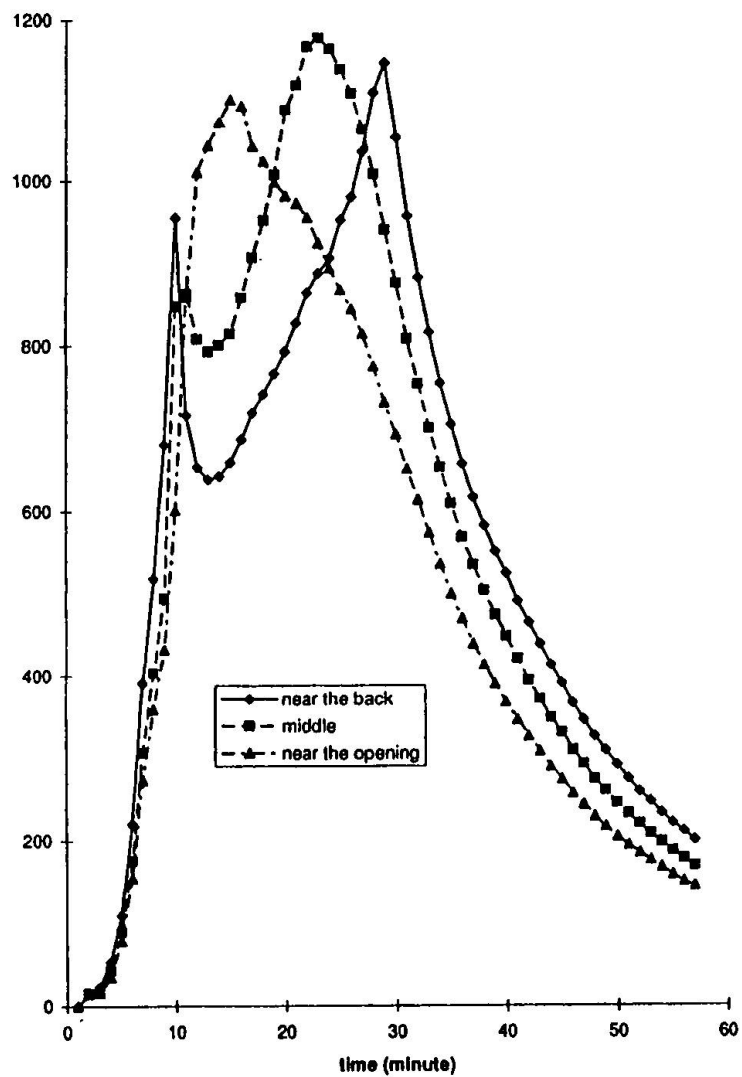Figure 4: Comparison of combustion gas temperatures for BRE corner test

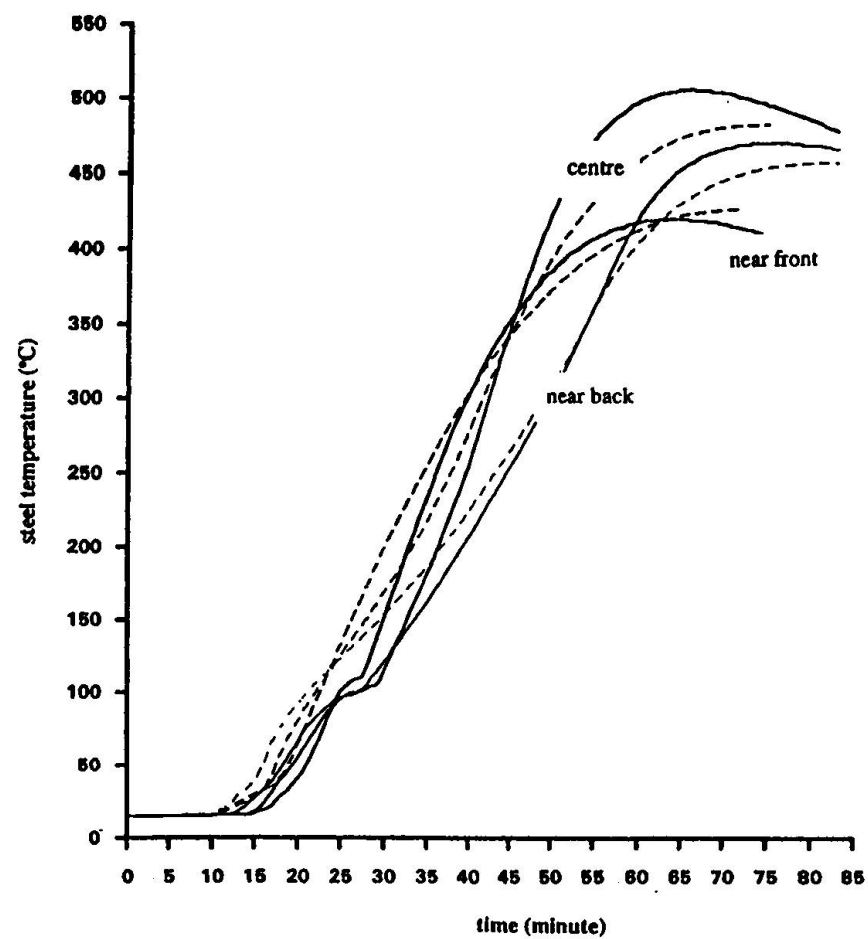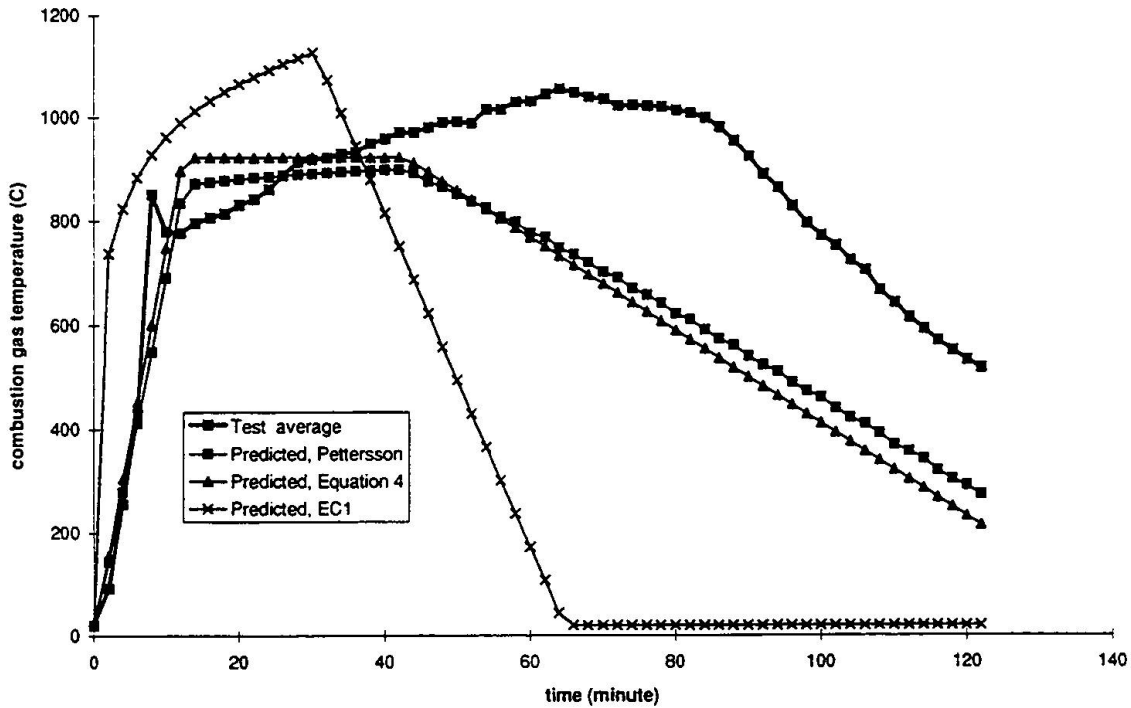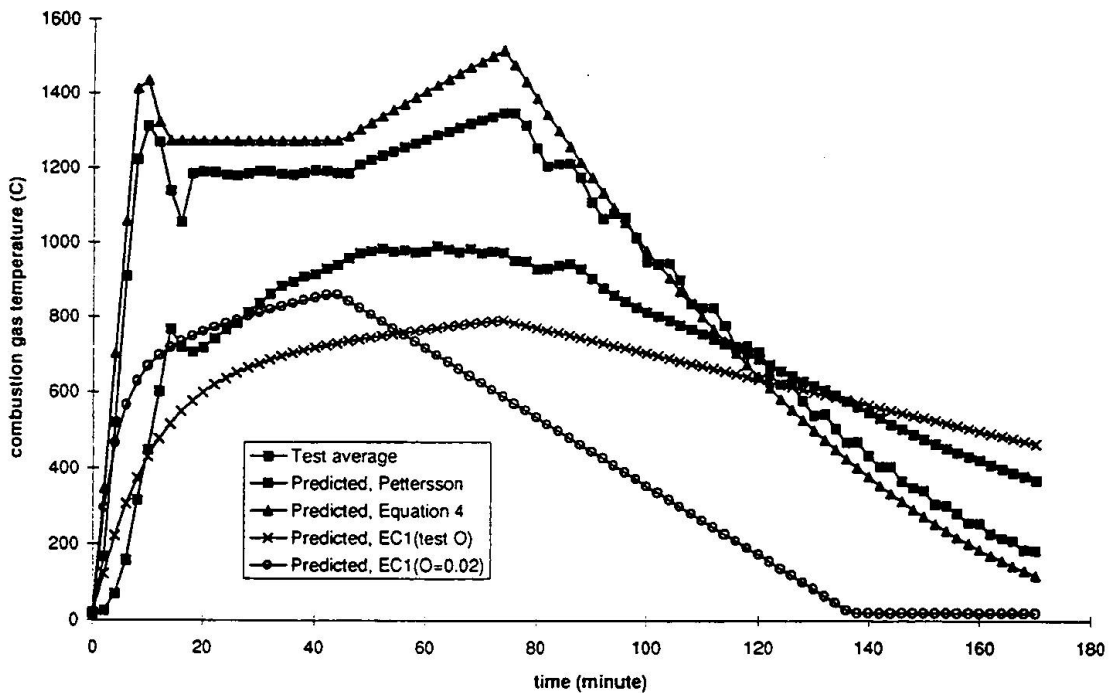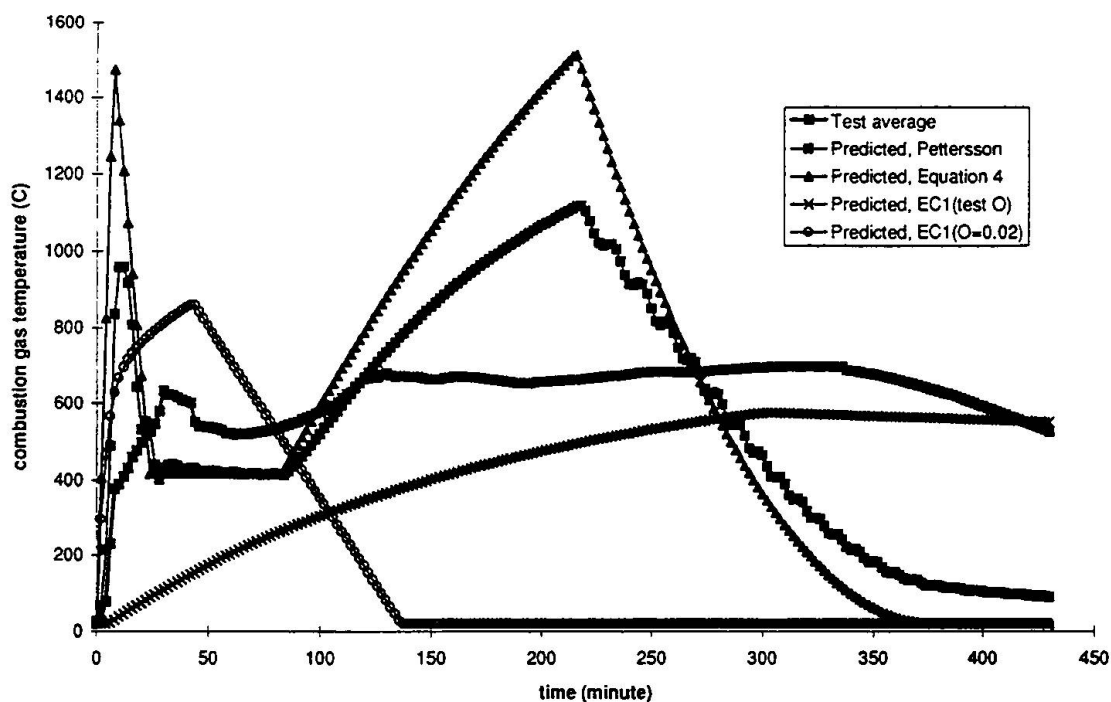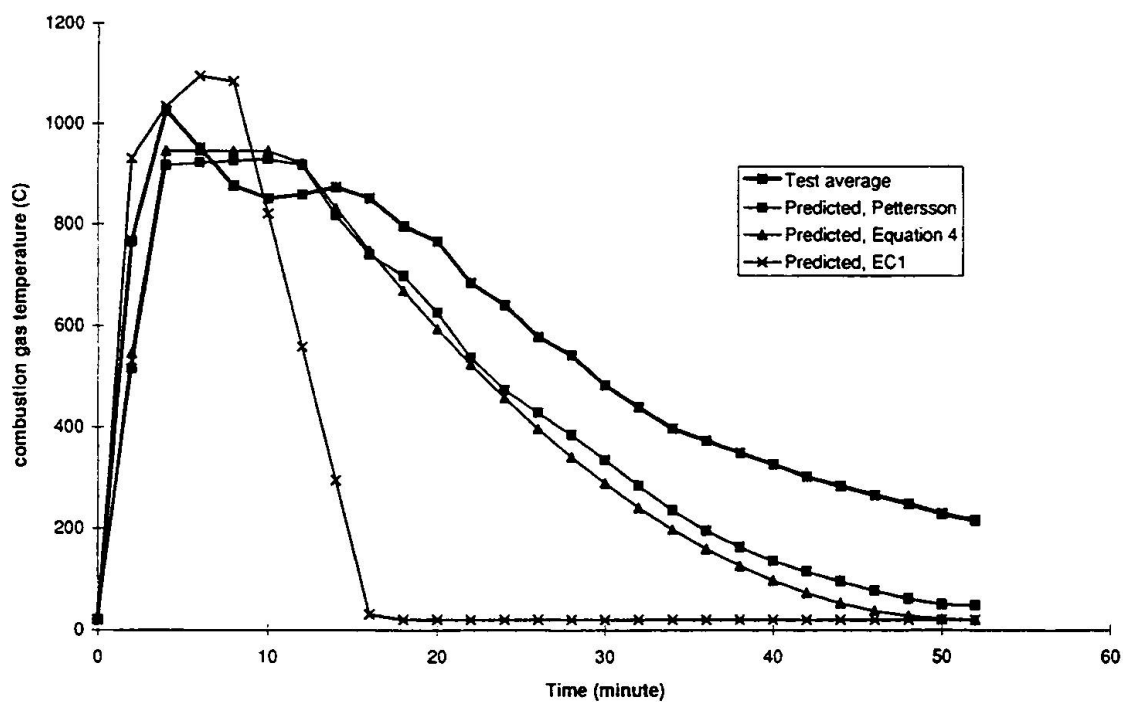Figure 5:   Combustion gas temperatures at three recording positions

Figure 6:   Measured and calculated steel temperatures, BRE/BST Test 2

Figure 1: Comparison of combustion gas temperatures, BRE/BST Test 1

Figure 2: Comparison of combustion gas temperatures for BRE/BST Test 5

Figure 3: Comparison of combustion gas temperatures for BRE/BST Test 6

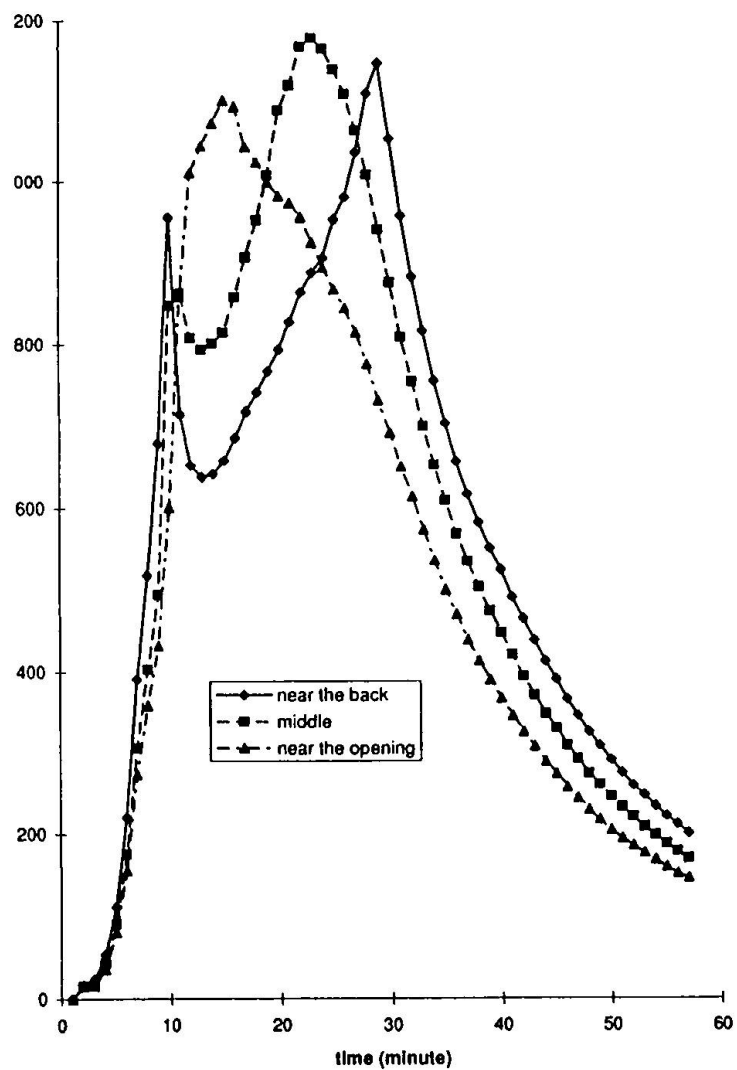Figure 4: Comparison of combustion gas temperatures for BRE corner test

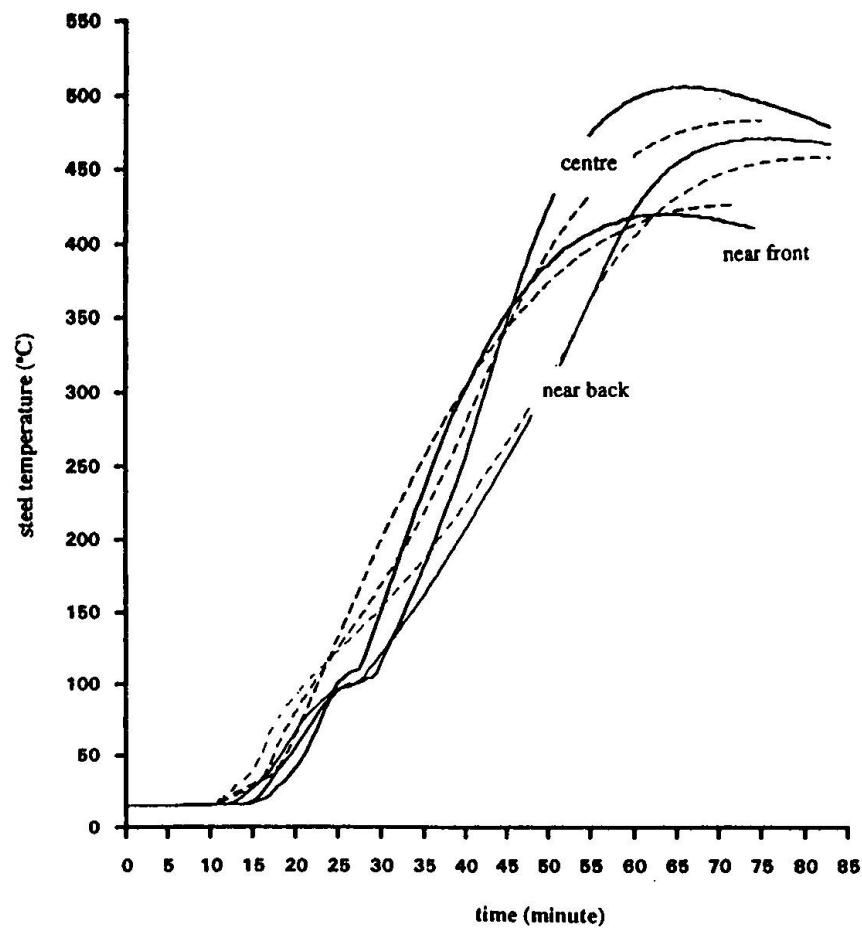Figure 5:   Combustion gas temperatures at three recording
positions

Figure 6:   Measured and calculated steel temperatures, BRE/BST Test 2

Leere Seite

Blank page

Page vide